Neural correlates of the processing of visually simulated self-motion

Neuronale Korrelate der Verarbeitung visuell simulierter Eigenbewegung

Dissertation

zur

Erlangung des Doktorgrades

der Naturwissenschaften

(Dr. rer. nat.)

dem Fachbereich Physik

der Philipps-Universität Marburg

vorgelegt von

Constanze Schmitt

aus Alsfeld

Marburg, 2019

Vom Fachbereich Physik der Philipps-Universität als Dissertation angenommen
am: 16.07.2019

Erstgutachter: Prof. Dr. Frank Bremmer (Universität Marburg, Fachbereich Physik)

Zweitgutachterin: Prof. Dr. Anna Schubö (Universität Marburg, Fachbereich Psychologie)

Tag der mündlichen Prüfung: 17.07.2019

Hochschulkennziffer: 1180

Contents

1 Summary

Successful interaction with our environment requires the perception of our surroundings. For coping with everyday challenges our own movements in this environment are important. In my thesis, I have investigated the neural correlates of visually simulated self-motion. More specifically, I have analyzed the processing of two key features of visual self-motion: the self-motion direction (heading) and the traveled distance (path integration) by means of electroencephalogram (EEG) measurements and transcranial magnetic stimulation (TMS). I have focused on investigating the role of prediction about the upcoming sensory event on the processing of these self-motion features. To this end, I applied the approach of the predictive coding theory. In this context, prediction errors induced by the mismatch between predictions and the actual sensory input are used to update the internal model responsible for creating the predictions. Additionally, I aimed to combine my findings with the results of previous studies on monkeys in order to further probe the role of the macaque monkey as an animal model for human sensorimotor processing.

In my first study, I investigated the processing of different self-motion directions using a classical oddball EEG measurement. The frequently presented self-motion stimuli to one direction were interspersed with a rarely presented different self-motion direction. The headings occurred with different probabilities which modified the prediction about the upcoming event and allowed for the formulation of an internal model. Unexpected self-motion directions created a prediction error. I could prove this in my data by detecting a specific EEG-component, the mismatch negativity (MMN). This MMN-component does not only reveal the influence of predictions on the processing of visually simulated self-motion directions according to the predictive coding theory, but is also known to indicate the preattentive processing of the analyzed feature, here the heading. EEG data from monkeys was recorded with identical equipment during the presentation of the previously described stimulus by colleagues from my lab in order to test for the similarities in monkey and human processing of visually simulated self-motion. Remarkably, data showing a MMN-component

similar to the human data was recorded. This led us to suggest that the underlying processes are comparable across human and non-human primates.

In my second study, the objective was to causally link the human functional equivalent of macaque medial superior temporal area (hMST) to the perception of self-motion directions. In previous studies this area has been shown to be important for the processing of self-motion. Applying TMS to right hemisphere area hMST resulted in an increase in variance when participants were asked to estimate heading to the left, i.e. to the direction contraversive to the stimulation site. The results of this study were used to test a model developed by colleagues of my lab. They used findings from single cell recordings in macaque monkeys to create it. Simulating the influence of lateralized TMS pulses on one hemisphere hMST this model hypothesized an increase in variance for estimation of headings contraversive to the TMS stimulated hemisphere. This is exactly what I observed in data of my TMS experiment. In this second study I verified the finding of previous studies that hMST is important for the processing of self-motion directions. In addition, I showed that a model based on recordings from macaque monkeys can predict the outcome of an experiment with human participants. This indicates the similarity of the processing of visually simulated self-motion in humans and macaque monkeys.

The third study focused on the representation of traveled distance using EEG recordings in human participants. The goal of this study was two-fold: First, I analyzed the influence of prediction on the processing of traveled distance. Second, I aimed to find a neural correlate of subjective traveled distance. Participants were asked to passively observe a forward self-motion. The movement onset and offset could not be predicted by them. In a next step participants reproduced double the distance of the previously observed self-motion. Since they actively modulated the movement to reach the desired distance, the resulting self-motion onset and offset could be predicted. Comparing the visually evoked potentials (VEPs) after self-motion onset and offsets of the predicted and unpredicted self-motion, I found differences supporting the predictive coding theory. Amplitudes for self-motion onset VEPs were larger in the passive condition. For self-motion offset, I found larger latencies for the

VEP-components in the passive condition. In addition to these results I searched for a neural correlate of the subjective estimation of the distance presented in the passive condition. During the active reproduction of double the distance obviously the single distance was passed. I assumed that half of the reproduced double distance would be the subjective estimation of the single distance. When passing this subjective single distance, an increase in the alpha band activity was detected in half of the participants. At this point in time prediction about the upcoming movement changed since participants started reproducing the single distance again. In context of the predictive coding theory these prediction changes are considered to be feedback processes. It has been shown in previous studies that these kinds of feedback processes are associated with alpha oscillations. With this study, I demonstrated the influence of prediction on self-motion onset and offset VEPs as well as on brain oscillations during a distance reproduction experiment.

In conclusion, with this thesis I analyzed the neural correlates of the processing of self-motion directions and traveled distance. The underlying neural mechanisms seem to be very similar in humans and macaque monkeys, which suggests the macaque monkey as an appropriate animal model for human sensorimotor processing. Lastly, I investigated the influence of prediction on EEG-components recorded during the processing of self-motion directions and traveled distances.

2 Zusammenfassung

Für eine erfolgreiche Interaktion mit unserem Umfeld ist die Wahrnehmung der Umgebung von großer Bedeutung. Besonders unsere eigene Bewegung innerhalb dieser Umgebung ist wichtig, um alltägliche Aufgaben meistern zu können. In meiner Arbeit habe ich die neuronalen Korrelate von durch optische Flussfelder visuell simulierter Eigenbewegung untersucht. In den unterschiedlichen Studien habe ich die Verarbeitung zweier elementarer Eigenschaften von Eigenbewegungen mit Hilfe von Elektroenzephalographie (EEG) Messungen und transkranieller Magnetstimulation (TMS) betrachtet: Die Verarbeitung sowohl der Bewegungsrichtung als auch die der zurückgelegten Distanz. Besonders der Einfluss von Vorhersagen über zukünftige Ereignisse war dabei von Interesse. Um diesen Zusammenhang genauer zu beschreiben, habe ich meine Ergebnisse im Kontext der *predictive coding theory* analysiert. Diese beschreibt interne Kreisläufe, in denen Vorhersagen über zukünftige Ereignisse mit den tatsächlich eintreffenden sensorischen Informationen verglichen werden. Vorhersagefehler (prediction errors), werden genutzt, um das interne Vorhersagemodel zu aktualisieren und an die neue Situation anzupassen. Ziel meiner Studien war es zusätzlich, die Vergleichbarkeit zwischen den Verarbeitungsprozessen in Menschen und Makaken zu untersuchen, um diese Primaten als geeignetes Tiermodel für sensomotorische Wahrnehmung in Menschen zu etablieren.

In meiner ersten Studie habe ich die Verarbeitung von Eigenbewegungsrichtungen mit Hilfe von EEG Messungen untersucht. Das Experimentdesign zielte darauf ab, die internen Vorhersagen über das kommende visuelle Ereignis zu beeinflussen, indem wiederholend die exakt gleiche Eigenbewegung, in genau die gleiche Richtung präsentiert wurde. Einzelne überraschend gezeigte Eigenbewegungen in eine andere Richtung sorgten somit zu einer Verletzung der Vorhersagen. Dies führte in den EEG Daten im Vergleich der erwarteten mit den unerwarteten Richtungen zu einer speziellen Komponente, der *mismatch negativity* (MMN). Diese zeigt nicht nur - angelehnt an die *predictive coding theory* - einen Einfluss der

Vorhersagen auf die Verarbeitung visuell simulierter Eigenbewegung, sondern ist auch eine Komponente, welche die präattentive Verarbeitung eines visuellen Ereignisses, hier der Bewegungsrichtung, anzeigt. Dieses interessante Ergebnis sollte nun auch an Makaken untersucht werden. Dazu wurde von Kollegen der AG Neurophysik das eben beschriebene Experiment an Makaken durchgeführt und EEG Daten wurden mit einem identischen Equipment gemessen. Bemerkenswerterweise zeigen die Daten einen ganz ähnlichen Verlauf und ebenfalls eine MMN-Komponente. Daraus lässt sich auf eine sehr ähnliche Verarbeitung von visuell simulierten Eigenbewegungsrichtungen in Menschen und Makaken schließen.

In meiner zweiten Studie habe ich diese Verarbeitung visuell simulierter Eigenbewegungsrichtungen mit Hilfe von TMS untersucht und konnte so einen kausalen Zusammenhang zu der stimulierten Gehirnregion hMST, dem menschlichen funktionalen Äquivalent der *medial superior temporal area* (MST) in Makaken, zeigen. Eine Stimulation dieses Gehirnareals in der rechten Hemisphäre führte zu einer vergrößerten Varianz in der Richtungseinschätzung für Eigenbewegungen nach links. Diese Ergebnisse wurden genutzt um ein Modell, das an Hand von Daten in Einzelzellableitungen an Makaken in der AG Neurophysik entwickelt wurde, zu testen. Dieses Modell sagt für ein TMS Experiment mit Stimulation von hMST in einer Hemisphäre eine erhöhte Varianz in der Einschätzung von der der stimulierten Hemisphäre gegenüberliegenden Bewegungsrichtung voraus. Dies ist genau das Ergebnis der Daten, die ich mit meinem TMS Experiment gemessen habe. Mit meiner zweiten Studie konnte ich somit zum einen replizieren, dass hMST für die Wahrnehmung von Eigenbewegungsrichtungen wichtig ist. Zum anderen konnte ein weiteres wichtiges Indiz für die gute Vergleichbarkeit von Verarbeitungsprozessen von visuell simulierter Eigenbewegung bei Makaken und Menschen gezeigt werden.

In meiner dritten Studie habe ich die Verarbeitung von durch Eigenbewegung zurückgelegten Distanzen analyziert. Zum einen habe ich den Einfluss von Vorhersagen darauf betrachtet und zum anderen nach einem neuronalen Korrelat für diese zurückgelegte Distanz gesucht. Die Versuchspersonen mussten in einer passiven Bedingung eine visuell simulierte

Eigenbewegung betrachten, deren Bewegungsanfang und –ende nicht vorhersehbar waren. In einem nächsten Schritt sollte durch aktives Steuern der Bewegung die doppelte Distanz der zuvor nur beobachteten Eigenbewegung reproduziert werden. Die gemessenen EEG Daten, im speziellen die visuell evozierten Potentiale (VEP) als Reaktion auf Bewegungsanfang und –ende, zeigten Unterschiede, die im Einklang mit der *predictive coding theory* stehen. Für unvorhersehbare visuelle Reize, also die passiv beobachtete Eigenbewegung, zeigten sich größere Amplituden in den EEG-Komponenten als Antwort auf den Bewegungsanfang und kürzere Latenzzeiten als Antwort auf das Bewegungsende im Vergleich mit Daten, die während der aktiven Steuerung der Bewegung gemessen wurden. In einem nächsten Schritt habe ich die subjektive Einschätzung der Distanzen untersucht. Während der aktiven Reproduktion der doppelten Distanz, wird die zuvor präsentierte einfache Distanz überschritten. Als subjektive Einschätzung für die einfache Distanz habe ich die Hälfte der gesteuerten doppelten Distanz angenommen. Bei Erreichen dieser Distanz, ist in den Daten von der Hälfte der Versuchspersonen ein Anstieg der Aktivität im Alpha-Band zu beobachten. Zu diesem Zeitpunkt wird die Vorhersage über die noch kommende Bewegung in Form eines Feedbackprozesses angepasst, da von nun an die einfache Distanz ein zweites Mal reproduziert werden muss. In früheren Studien wurde nachgewiesen, dass Alpha-Oszillationen für Feedback-Prozesse im Zusammenhang mit der *predictive coding theory* aktiviert werden. Mit meiner Studie konnte ich demnach nicht nur den Einfluss von Vorhersagen auf die Verarbeitung des visuellen Eigenbewegungsstarts und –endes zeigen, sondern auch einen Einfluss auf die Einschätzung der zurückgelegten Distanz.

Zusammenfassend habe ich in meiner Arbeit die neuronalen Korrelate der Verarbeitung von Eigenbewegungsrichtungen und zurückgelegten Distanzen untersucht. Die zugrunde liegenden neuronalen Mechanismen sind sehr ähnlich zwischen Menschen und Makaken, was Makaken als geeignetes Tiermodel für die sensomotorische Verarbeitung in Menschen empfiehlt. Zusätzlich konnte ich mit meinen Studien den Einfluss von Vorhersagen über die

kommenden sensorischen Ereignisse in Bezug auf die Verarbeitung von Eigenbewegungsrichtungen und zurückgelegten Distanzen nachweisen.

3 Introduction

3.1 General introduction

We live in a highly dynamic world and are required to interact with our environment. In everyday life estimating all movements surrounding us as accurately as possible is a key ability. Besides observing object motion or movements of people it is even more important to control our own motion e.g. in order to reach a desired location or to avoid obstacles. The judgement of the direction of our self-motion and also the traveled distance are features which have to be optimized in many situations even when paying attention to something else. Sensory input, like visual, vestibular, tactile and auditory information gets integrated to ensure adjustments to the existing conditions and provides the basis for successful navigation (e.g. Hlavacka et al., 1996; Angelaki et al., 2011; von Hopffgarten, 2011; Churan et al. 2017). These senses are of different importance for successful navigation. Primates rely particularly on visual and vestibular signals (Gu et al., 2006).

Since visual information is of great importance for self-motion perception, I used optic flow stimuli to simulate self-motion and analyzed the processing of the two key features, heading and traveled distance, respectively. The objective of the first study was to investigate if self-motion direction is processed preattentively, i.e. without paying attention to it, and if violations of the expected self-motion direction can be explained according to the theories of predictive coding (Friston, 2005). In the second study I could show the importance of the medial superior temporal brain area (MST) for heading discrimination and compared the study results to a model based on single cell recordings in macaque monkeys (Bremmer et al., 2017). Finally, in a third study I examined the ability to discriminate traveled distances in order to reproduce them based only on visual self-motion information. Specifically, I aimed to find differences for self-initiated self-motion compared to passively observed self-motion and tested for a neuronal correlate of traveled distance. For all studies human participants were invited to study the processing of visually induced self-motion.

3.2 Visual system and the visual motion processing pathway

The information provided by different senses about our environment is dominated by the visual system in primates (Gu et al., 2006). Visual information enters through the eyes and reaches the retina as a first processing step, before it gets transferred through two parallel and anatomically segregated visual pathways, the M- and P-pathway, to the primary visual cortex (V1) (Livingstone and Hubel, 1988; Nealey and Maunsell, 1994; Tobimatsu and Celesia, 2006; Yamasaki et al., 2011) (Figure I-1). Before reaching V1 the optic nerves pass two intermediate structures: the *chiasma opticum*, where information presented in the left and right visual fields is divided in a way that visual input from the left visual field reaches right hemisphere V1 and vice versa (Kidd, 2014), and the *lateral geniculate nucleus* (LGN). There, information carried by the M-pathway sensitive to stimulation with higher temporal and lower spatial frequencies is processed in two magnocellular layers. In contrast, the P-pathway is selective for color as well as high spatial and low temporal frequencies and is processed in four parvocellular layers of the LGN (Merigan and Maunsell, 1993). The further processing of the visual information follows also two pathways, which are less strictly separated than the M- and P-pathway, but instead share many connections (Felleman and Van Essen, 1991). They are referred to as the ventral and dorsal stream (Goodale and Milner, 1992) with the ventral stream receiving input mainly from the P-pathway and the dorsal stream mainly from the M-pathway (Ferrera et al., 1994) (Figure I-1). Since the ventral stream processes object shape and identity (Freud et al., 2016) it is also called the “what pathway”. It includes area V4 and the inferior temporal cortex (Yamasaki and Tobimatsu, 2011). The dorsal pathway is selective for object location as well as motion and visuomotor control (Freud et al., 2016) and is therefore also called the “how” or “where pathway”. The dorsal stream comprises V3a, V5/MT (middle temporal area), MST (medial superior temporal area), and areas of the parietal cortex, among them the ventral intraparietal area (VIP) (Yamasaki and Tobimatsu, 2011; Kandel et al., 2000).

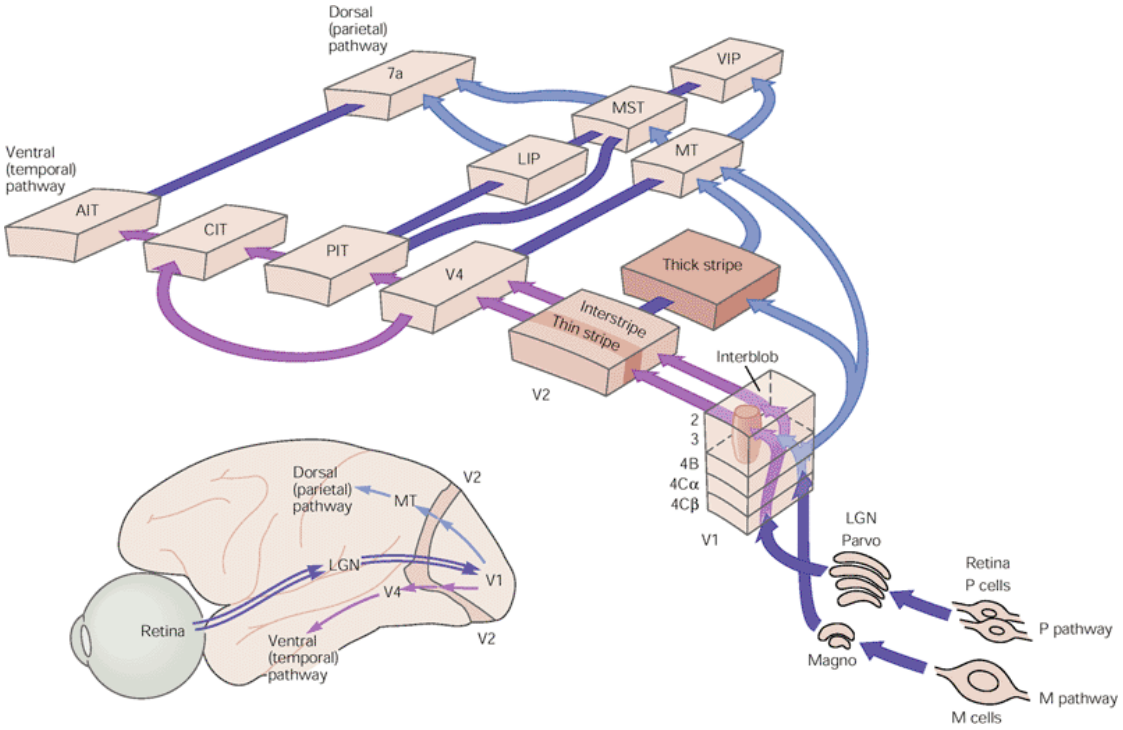

Figure I-1: The ventral and dorsal pathway. The two graphics depict how visual information is in a first step transferred through the magnocellular (M) and parvocellular (P) pathways from the retina through the lateral geniculate nucleus (LGN) to V1. Beginning in V1 information is processed in brain areas along the ventral (temporal) pathway or the dorsal (parietal) pathway. (Kandel et al., 2000)

In the dorsal stream local motion signals from V1 are integrated into global motion (Snowden et al., 1991) like radial optic flow which represents the visual information generated during self-motion. In the described cortical motion pathway area MST has been found in monkeys to be the first area with genuine optic flow selectivity (Saito et al., 1986; Duffy and Wurtz 1991; Lappe et al., 1996; Gu et al., 2006; Bremmer et al., 2010). The second cortical region being significantly involved in the encoding of self-motion information is area VIP (Bremmer et al. 2002; Schlack et al., 2002; Chen et al., 2011; Kaminiarz et al., 2014; Shao et al., 2018). Importantly, in humans, functional equivalents of both areas have been identified (hMST: Huk et al., 2002; VIP: Bremmer et al., 2001).

3.3 Visually simulated self-motion: optic flow

The accurate processing of visual information is essential for almost all our actions, such as for the orientation during movements. Although successful navigation requires the integration of different sensory signals (e.g. Hlavacka et al., 1996; Angelaki et al., 2011, von Hopffgarten, 2011; Churan et al. 2017) we mainly rely on the information provided by the visual system. This has been demonstrated in previous studies using simulations of visual self-motion not matched to real self-motion. One example for this was described in a study by Lee (Lee, 1980). Participants were standing on a stable floor and just the walls of the room surrounding them were moved. As a result, adults in unpracticed stances and toddlers were falling although the ground was not moving at all (Lee, 1980). In another study, a visual stimulus creating the illusion of moving through a tunnel or corridor was presented to adults walking on a treadmill. The stimulus caused an adjustment of their walking speed to the visual information (Prokop et al. 1997). In addition, numerous studies have revealed that the presentation of visual stimuli simulating self-motion to stationary participants induces the feeling of self-motion (e.g. Berthoz et al., 1975; Lee 1980).

While moving, the visual information we perceive is an optic flow field (Figure I-2). Objects within a short distance from the observer move faster than e.g. the landscape further away, resulting in a complex flow field with a velocity gradient (Gibson, 1950; Britten, 2008). In the case of no eye- or head-movements, all velocity vectors emanate from one point which forms a focus-of-expansion and indicates the current direction of self-motion. However, this field does not only contain information about our surrounding environment, but also about our self-motion and head or eye movements during the motion (eye motion: Royden et al. 1992; Kaminiarz et al. 2014; object motion: Dokka, et al., 2015).

Figure I-2: Optic flow field as created through forward self-motion. The yellow arrows depict the different velocities at different points in the image. These velocity vectors emanate from the black cross. It is the focus-of-expansion and shows, under certain conditions, the self-motion direction. (Britten, 2008)

In the animal model of human sensorimotor processing, the macaque monkey, but also in humans optic flow sensitive neurons have been revealed with neurophysiological studies mainly in two brain areas: the medial superior temporal area (area MST) (Saito et al., 1986; Duffy and Wurtz 1991; Lappe et al., 1996; Gu et al., 2006; Bremmer et al., 2010; human functional equivalent (hMST): Huk et al., 2002), and the ventral intraparietal area (area VIP) (Bremmer et al. 2002; Schlack et al., 2002; Chen et al., 2011; Kaminiarz et al., 2014; Shao et al., 2018; human functional equivalent: Bremmer et al., 2001). In addition, previous studies with human participants reported the involvement of these two areas in the encoding of self-motion information (e.g. Morrone et al., 2000; Wall and Smith, 2008).

3.4 Self-motion direction (heading)

There are several visual cues which can be used for heading discrimination and navigation (Cutting, 1996), but in this study I focused on the stimulation with optic flow fields and hence the resulting heading information. It has been shown before in experiments as well as theoretical studies that the visual flow field generated by our self-motion, the optic flow, provides enough information to estimate the direction of self-motion (e.g. Gibson, 1950; Warren and Hannon, 1988; Lappe et al. 1999; Lich & Bremmer, 2014). In static conditions, i.e. with fixed gaze during linear self-motion through a stationary scene, the flow field shows a singularity, the so-called focus-of-expansion. Its location indicates the direction of self-motion as has been already reported by Gibson (1950). This rather simple correlation between flow field and self-motion direction is usually more complicated under natural conditions. Eye as well as head movements and a non-static environment modify the optic flow (eye and head motion: e.g. Royden et al., 1992; Lappe & Rauschecker, 1995; Banks et al.1996; van den Berg and Beintema, 1997; Lappe et al. 1999; object motion: Dokka, et al., 2015). If restricted to static conditions small heading estimation errors of about 1–2 degrees of visual angle have been reported (Warren and Hannon, 1988; Foulkes et al., 2012). Accuracy in this range is required in order to control self-motion when avoiding obstacles (Cutting et al., 1992). The retinal eccentricity of the focus-of-expansion influences these values (Warren and Kurtz, 1992) with highest accuracy for a focus-of-expansion located near the fovea and small heading eccentricities (Crowell and Banks, 1993). Other studies with stimuli consisting of random dots inducing optic flow revealed that the accuracy of heading estimations does not mainly depend on the random dots' speed (Warren et al., 1991). In studies with macaque monkeys it has been shown that neurons in the areas MST and VIP are sensitive to heading (VIP: Schlack et al., 2002; Kaminiarz et al., 2014; MST: Lappe et al., 1996; Bremmer, 2010). A model based on the single neuron recordings in these areas has been developed to be used as predictor for heading estimations during eye movements (Bremmer et al. 2017). Previous studies using microstimulations in these areas could also

causally link them to heading judgments (Gu et al., 2012). Magnetic resonance imaging studies (MRI) with human participants have demonstrated the involvement of functionally equivalent areas in self-motion direction processing (MST: Cardin et al., 2012; VIP: Furlan et al., 2014).

3.5 Self-motion distance (path integration)

Successful navigation does not only require an accurate estimation of self-motion direction, but knowledge about traveled distance is essential, too. Under natural conditions information from different senses is available and is used to optimize navigation (for a review see Britten, 2008), like the vestibular system (e.g. Fetsch et al., 2009; Gu et al., 2006; Cullen, 2012, Churan et al., 2017) or the auditory system (von Hopffgarten and Bremmer, 2011; for a review see Väljamäe 2009). However, traveled distance can be estimated and reproduced also when input only from a single sensory modality is available. It could be shown that only vestibular or somatosensory signals, e.g. with blindfolded participants, provided enough information to reproduce a passive linear displacement (Berthoz et al. 1995; Israël et al., 1997). Interestingly, similar to heading discrimination solely based on visual information optic flow contains enough information to estimate a traveled distance quite accurately or even to reproduce a seen distance (Gibson, 1950; Bremmer and Lappe, 1999; Harris et al., 2000; Redlick et al., 2001; Frenz et al., 2007; von Hopffgarten and Bremmer, 2011; Churan et al., 2017). Bremmer and Lappe (1999) could show that participants' accuracy in discriminating distances showed an error less than 3%, independent of the displacement being forward or backward. However, it has to be considered that optic flow as observed in linear self-motion cannot give absolute information about ego-motion if the distances of the visual objects to the observer, or more general the depth layout of the stimulus are unknown (Lee, 1980). The limitation to retinal image velocities solely allows the extraction of combined information about distance and velocity which can only be judged up to a scaling factor. Comparing two

distances is less problematic if it is assumed that both movements have the same depth structure. This is the case in many distance reproduction tasks. When asked to reproduce a previously seen passive movement an overshoot of small displacements and an undershoot of large displacements has been reported (Berthoz et al., 1995; Bremmer and Lappe, 1999; Glasauer et al., 2007; von Hopffgarten and Bremmer, 2011; Churan et al., 2017). In the most self-motion reproduction experiments participants were explicitly asked to reproduce a passively observed distance, but they relied heavily on the velocity profile of the observed movement and tended to reproduce it in their own active motion (Bremmer and Lappe, 1999; von Hopffgarten and Bremmer, 2011). This strategy does not allow answering the question if an internal representation of the traveled distance is built up. Frenz and Lappe (Frenz and Lappe, 2005) were investigating this question and could show that in addition to a representation of the velocity profile an abstract distance measure is essential for accurate distance discrimination. In their study only the reference distance was presented as optic flow stimulus and different modalities were used for the responses: active walking without visual information or adjustment of a static interval as distance indicator. In both cases participants were able to reproduce the previously observed distance. Additionally, also in a discrimination study with optic flow stimuli, Frenz and colleagues (Frenz et al., 2003) revealed very accurate distance discrimination. They could show the robustness of these results by varying experimental modalities. Neither variations in observers' velocities nor different environments in the reference and test distance, nor the visibility range or the viewing angle led to a significant impairment of distance discrimination. In addition, by varying the simulated height of the observer above the presented stimulus, they asked if the accurate distance estimations are affected by changes in the optic flow and not by the observers' speed. Participants were able to compensate for these changes. With their studies Frenz and colleagues give strong evidence for the idea that human observers do not use image velocities directly to estimate distances, but rather a combination of self-motion speed with respect to the environment.

3.6 Predictive coding

Our perceptual systems provide us with all necessary information to survive in a dynamically changing environment including the demanding task of self-motion. Internal models about the incoming sensory information help with a fast processing of actual input and make a preselection of appropriate reactions possible before an event is realized. In recent years some studies used the concept of predictive coding to explain how these models could be formed and kept updated with regard to our changing environment (Rao and Ballard, 1999; Schütz-Bosbach and Prinz, 2007). The principle of free energy minimization (Friston, 2005, 2010) is a basic concept in these studies. In predictive coding theories the priority of our perceptual system is to keep the differences between our environment and the resulting sensory inputs on the one hand, and the predictions formed by internal generative models about upcoming events on the other hand as small as possible. Especially repeated events showing some kind of regularity lead to a representation of the invariant feature and the building of predictions (Stefanics et al., 2014).

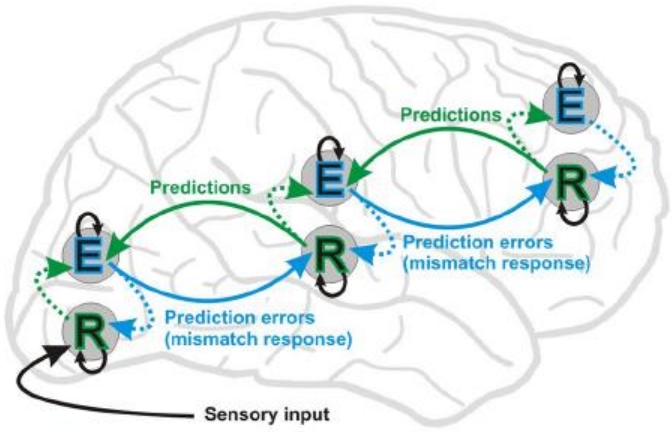

Figure I-3: Simplified model of the hierarchical predictive coding framework based on Friston (2005, 2010). The transporting of messages between two neuronal populations, the error unit (E) and the representation unit (R) is depicted. Bottom-up forward connections which represent prediction errors or mismatch responses and top-down backward connections which carry predictions build loops between the error and representation units. Representation units are considered coding the causes of sensory inputs and receive input from error coding units from superficial layers in the same level (dotted lines) as well as from lower hierarchical levels. (Stefanics et al., 2014)

The underlying model of the predictive coding theory is hierarchically structured (Figure I-3). There is a top-down flow of predictions from each level which get tested with data emerging from the next lower level. If differences occur, these prediction errors are passed upwards in the hierarchy in a bottom-up flow. This is an important process because especially unpredicted events can provide us with information being essential for surviving. The prediction error is used to modify the predictions on this higher level and adjust them to better match the sensory input and our environment. The continuous interaction between these top-down and bottom-up information flows keeps our internal system and the predictive models up-to-date.

One method to show and measure an indicator for this updating process is using electroencephalography (EEG) recordings. A special event related potential (ERP) component, the visual mismatch negativity (vMMN) is considered as a signal being involved in the updating process of the perceptual system (for reviews see Winkler and Czigler, 2012; Stefanics et al., 2014). In the predictive coding theories this component has the important role of carrying the prediction error elicited by the mismatch of a sensory event with the predictions (Friston, 2005; Winkler and Czigler, 2012; Stefanics et al., 2014).

3.7 Electroencephalography (EEG)

Already in 1929 Berger (Berger, 1929) demonstrated that it is possible to record the electric activity, the Electroencephalogram (EEG), of human brains by placing electrodes on the scalp. The amplified signal showed the voltage changes over time. In the raw form EEG signals represent the activity of a variety of neural sources, but it is possible to extract the responses to specific sensory, cognitive or motor events. The so-called event-related potentials (ERPs) show the electrical potentials associated with specific events (Luck, 2005). Simple averaging over EEG data aligned to the same sensory event extracts ERPs from the continuous EEG data. Compared to other techniques EEG measurements have a very good temporal resolution (typically 1 ms), but the spatial resolution is poor due to an infinite

number of ERP generator configurations which are possible to elicit the resulting pattern of ERP data.

The source of the potentials measured on the scalp, the EEG data, originates in the single neurons as described by Luck (Luck, 2005). Due to the timing and physical arrangement of cell bodies, dendrites and axons, surface electrodes cannot detect action potentials, but instead measure postsynaptic potentials. These potentials usually sum up instead of canceling each other and their duration of between tens to hundreds of milliseconds makes it possible to measure them at relatively large distances, like the scalp.

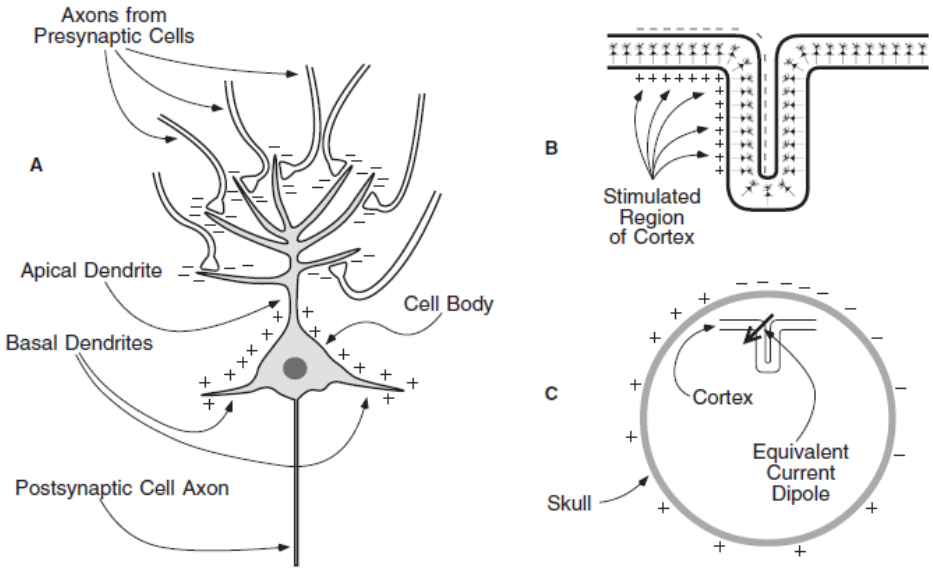

Figure I-4: Basic principles of event related potential (ERP) generation. A) A schematic picture of a pyramidal cell is presented. The presynaptic terminals release an excitatory neurotransmitter which results in positive ions flowing into the postsynaptic neuron. This causes a net negative extracellular voltage around the apical dendrites and a positive voltage around the basal dendrites, yielding a small dipole. **B**) Many pyramidal cells in a folded sheet of cortex. The stimulation of a region of cortex leads to dipoles from individual neurons which summate. **C**) A single equivalent current dipole (arrow) can be used to approximate the summated dipoles of individual neurons. The positive and negative voltages and their distribution measured by surface EEG electrodes are determined by the position and orientation of this single dipole. (Luck, 2005)

Each single neuron creates a small dipole (Figure I-4 A). The negative part of this dipole is located outside of the neuron around the apical dendrite. Due to the release of an excitatory

neurotransmitter at the apical dendrite of a cortical pyramidal cell, current flows from the extracellular space into the cell. In addition, current flows out of the cell body at basal dendrites which leads to a positivity, the positive part of the dipole, in this area. A single neuron's dipole would be too small to be recorded, but they add up to a larger dipole which is detected by electrodes on the surface of the scalp (Figure I-4 C). This is possible when the single neurons' dipoles occur in a large number of spatially aligned neurons at around the same time, most likely due to similar input (excitatory or inhibitory neurotransmitters).

In order to avoid cancelation, the spatial alignment of the cells is important, too. The cells are usually oriented perpendicular to the cortical surface, but the folding of the cortex itself can lead to cancelations or interactions (Figure I-4 B). Data recorded with surface electrodes can have its origin in a distant part of the brain. Before the dipole can be detected with electrodes on the scalp surface the electric field has to pass several layers of tissue, i.e. the brain itself, the scull and the scalp. The ERPs spread out as they travel and in addition with the fact that electricity chooses the path of least resistance it leads to a blurring of the voltage.

3.8 Visual evoked potentials (VEPs)

A special form of ERPs is the visual evoked potential (VEP) which is recorded in response to the onset of a visual stimulus (Odom et al., 2016). A typical VEP waveform is presented in Figure I-5 A. The different positive and negative VEP-components get labeled according to their polarity (positive: P, or negative: N) and their position within the waveform. The first components elicited by a visual event are described in the following based on work by Luck (Luck, 2005). The first visual, the C1-component (in some studies e.g. Odom et al., 2016 named N1-component) has its source most likely in the primary visual cortex (V1), which is folded into the calcarine fissure in humans. Depending on the location of the visual stimulus, this component is positive (stimulation in the lower visual field) or negative (stimulation in the upper visual field). The C1-component starts between 40 and 60 ms after stimulus onset, peaks at around 80-100 ms and is largest at posterior midline electrodes. The component

immediately following is the P1-component. Its latency varies depending on the stimulus contrast, but typically the onset is about 60-90 ms after stimulation onset and it peaks between 100 and 130 ms, being largest at lateral occipital electrode sites. The most likely source location for the early part of this component is the extrastriate visual cortex and the fusiform gyrus for the later part. This component is sensitive to different stimulus parameters and also the direction of spatial attention as well as the state of the participants' arousal has an influence on this component (Luck, 2005). The next component, the N2-component, with a peak around 150 ms to 200 ms over occipital and occipito-temporal electrodes is the dominant component in motion-onset VEPs (Heinrich, 2007; Kuba, 2007) (Figure I-5 B). The following P2-component peaks around 240 ms over parietal to central electrodes. This component's value increases with more complex visual moving stimuli (Kuba, 2007) and is larger if the stimulus contains target features (Luck, 2005).

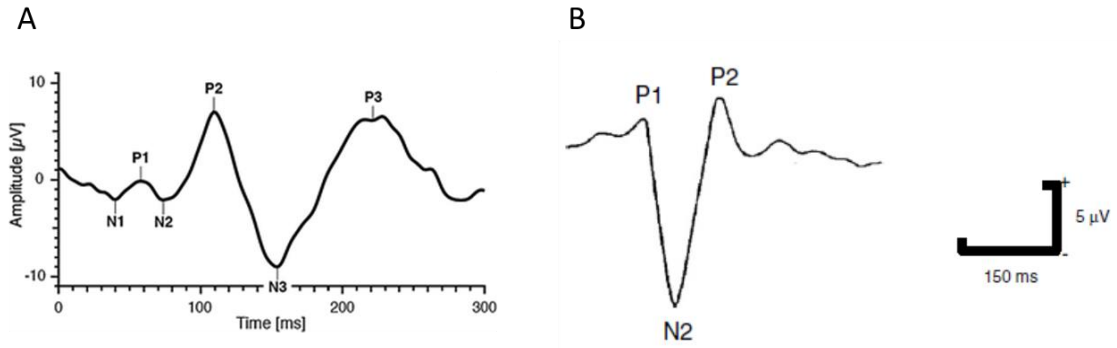

Figure I-5: A typical flash visual evoked potential (VEP) and a typical motion-onset VEP. Both VEPs show a series of characteristic positive and negative components. **A**) The VEP recorded after the flash of a visual stimulus at t=0 ms is presented. **B**) The VEP recorded after visual motion-onset at t=0 ms is depicted. Compared to the flash-VEP in **A** the P1-N2-P2 complex is most prominent with a large N2-component. (A: Odom et al., 2016; B: Kuba et al., 2007, modified)

3.9 Mismatch negativity (MMN)

The mismatch negativity (MMN) is a specific ERP-component elicited by an unexpected stimulus appearing among the frequent presentation of another, frequent stimulus and therefore violating a statistical regularity. The MMN can be used to test for two interesting stimulus processing concepts. On the one hand, it shows the automatic registration of unattended changes in the environment and is considered to reveal preattentive processing of stimulus features (Berti, 2011; Schmitt et al., 2018). On the other hand, this component can also be determined in the context of predictive coding (Friston, 2005, 2010) and is a correlate for model updating processes carrying the prediction error signal (Stefanics et al., 2014).

MMN-components were first found in the auditory domain (Näätänen et al., 1978; Winkler and Czigler, 2012) and for many years research focused solely on auditory stimuli. It was not clear if other sensory modalities could also show a MMN. A visual MMN (vMMN) has been observed in the recent years by different groups (Amenedo et al., 2007; Kimura et al., 2010; Müller et al., 2010; Schmitt et al., 2018) for many different visual stimulus features. Some of these features are orientation (Czigler and Pató, 2009; Kimura et al., 2010; Sulykos and Czigler, 2011), direction of motion (Urban et al., 2008; Kuldkepp et al., 2013), duration (Khodanovich et al., 2010), color (Thierry et al., 2009; Stefanics et al., 2011; Müller et al., 2012), numerosity (Hesse et al., 2017), but also higher cognitive features such as object structure (Müller et al., 2013) and facial emotions (Stefanics et al., 2012; Wang et al., 2016) were used as stimuli to test for vMMNs. Typically, the MMN is shown in oddball experiments. The difference between ERPs elicited by frequently presented standard stimuli and the ERPs elicited by the interspersed deviant stimuli is defined as MMN (Kimura, 2012). In particular the N2-component has more negative values after deviant compared to standard stimulation (Pazo-Álvarez, et al., 2004; Schmitt et al., 2018) (Figure I-6). This leads to the MMN, i.e. a negative component in the ERP-difference (deviant – standard).

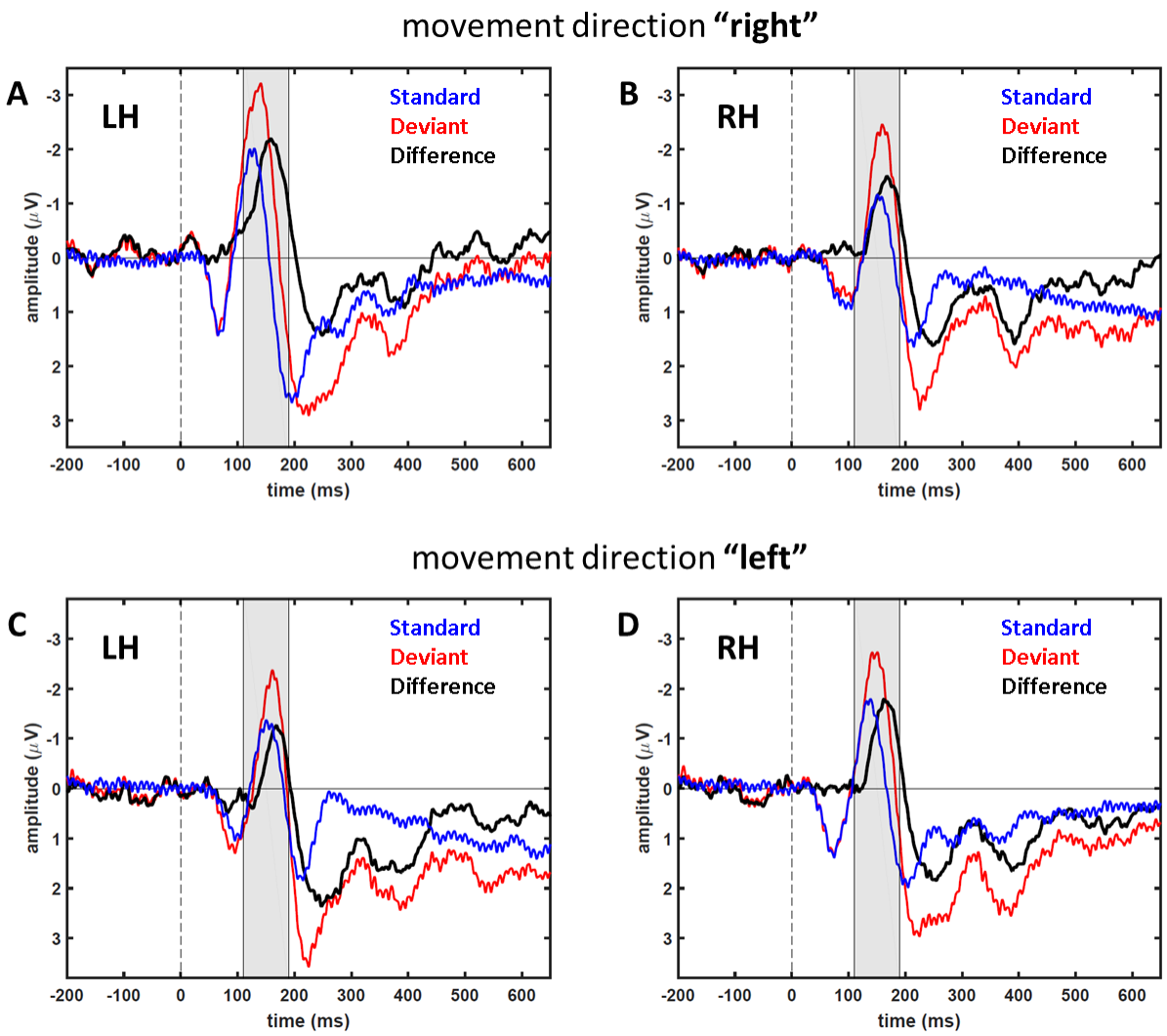

Figure I-6: Time course of a visual mismatch negativity (vMMN) component. The EEG data was recorded in an oddball experiment showing a target moving from left to right (movement direction "right") or right to left (movement direction "left") on a monitor while participants fixated the center of the screen. The central part of the screen represented an occluder masking the target trajectory in this area. The EEG data presented was aligned (t=0 ms) to the reappearance of the moving visual target. In deviant trials the target's trajectory changed in the occluded phase, while no change happened in standard trials. The time course of data recorded after standard (blue) and deviant (red) stimuli as well as the difference between these two (deviant – standard; black) showing the vMMN-component around 150 ms is depicted for the two movement directions. LH represents a left hemisphere electrode cluster (P3, P7 and PO3) and RH the average over the respective electrodes over the right hemisphere (P4, P8 and PO4). (Schmitt et al., 2018, modified)

The MMN-component peaks in a time window between 100 and 400 ms after the sensory event (Kimura, 2012; Czigler, 2014) with a posterior scalp distribution (Kimura, 2012) (Figure I-7). A main characteristic of the MMN is that it has been shown to be an automatic

signal which represents the preattentive processing of a sensory signal (Maekawa et al., 2005; Czigler, 2007; Müller et al., 2013; Yu et al., 2017). This characteristic was demonstrated in experiments finding a MMN-component although a demanding task was introduced to capture the participants' attention (Pazo-Àlvarez et al., 2004; Stefanics, et al., 2012; Li et al., 2012; Kuldkepp et al., 2013). Importantly, these tasks were unrelated to the stimulus feature which was tested for a MMN-component. Nevertheless, standard and deviant stimuli were processed differently. In order to recognize the deviant stimuli as being different from the standard stimuli, our brain needs to extract an abstract sequential rule from the presented stimulus.

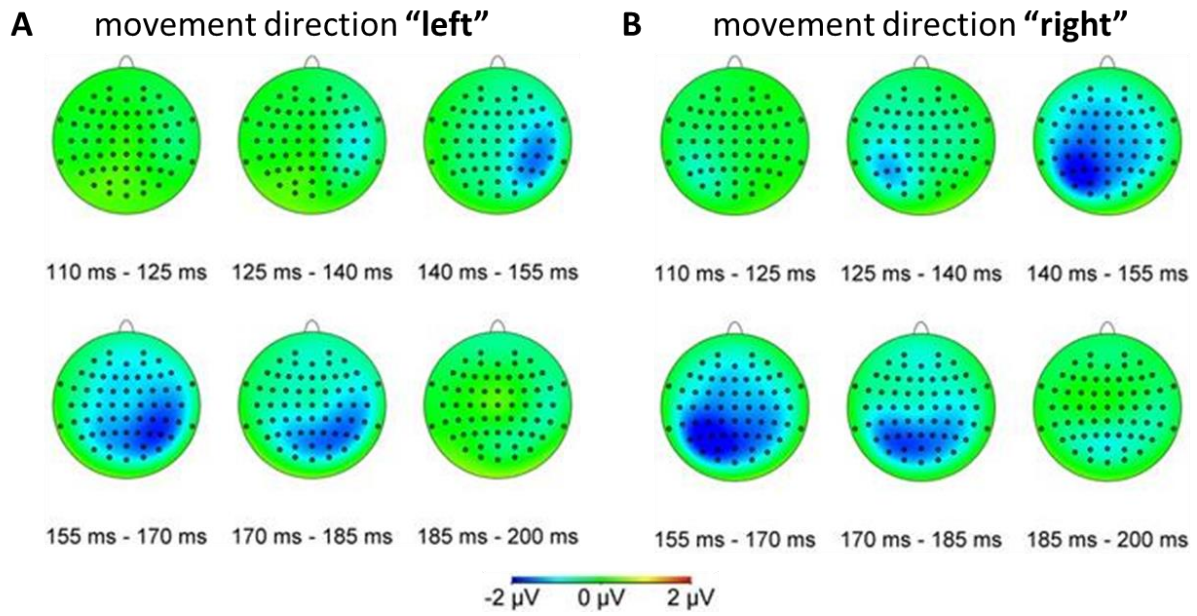

Figure I-7: Topographic maps of a visual mismatch negativity (vMMN) component. The data presented in this Figure was collected in the same experiment described in the caption of Figure I-6. The topographic maps show the data of all electrodes for the difference (deviant – standard) for the two different movement directions. In blue the negative vMMN-component is visible around 150 ms, lateralized to the hemisphere contralateral to the target reappearance. (Schmitt et al., 2018, modified)

This can be explained in the context of the predictive coding framework (Friston, 2005, 2010). In order to optimize our perception, predictions about the environment and the events most likely to happen in the future are formed. In an oddball paradigm, it is statistically more

likely that a standard stimulus is presented and therefore in these experiments participants form a representation of the standard stimuli's feature (Stefanics et al., 2014). With the presentation of each trial the sensory input is compared to this prediction and in case of a deviant stimulus a mismatch is detected which is correlated with the appearance of a MMN-component. The MMN is interpreted as a prediction error signal send feedforward to keep the predictions of our internal model about the environment up-to-date (for reviews see Winkler and Czigler, 2012; Stefanics et al., 2014). In the predictive coding theories this information flow is structured in hierarchical loops with prediction errors flowing bottom up to adjust predictions at a higher level whereas top-down connections sending these predictions have the objective to reduce prediction errors (Czigler and Winkler, 2012; Stefanics et al., 2014).

Taken together the MMN-component is an EEG signal showing our capability to automatically extract statistical regularities of the environment and identifying events violating the prediction about a continuation of these regularities.

3.10 EEG oscillations

In addition to the ERP signals, the EEG data contains regular oscillations which provide additional information (for a review see e.g. Herrmann et al., 2016) and are thought to facilitate communication between neural populations (Clayton et al., 2015). They are grouped into a small number of characteristic frequencies (Cohen, 2017) and provide insights in the neural computations linked to perception, cognition and action. In 1929 Berger already reported the detection of continuous and periodic fluctuations in the potentials he recorded in his first EEG publication (Berger, 1929). The frequencies are grouped into five well-established frequency bands (Wang, 2010; Herrmann et al., 2016): delta (0–3.5 Hz), theta (4–8 Hz), alpha (8–14 Hz), beta (15–30 Hz) and gamma (30–80 Hz), see Figure I-8.

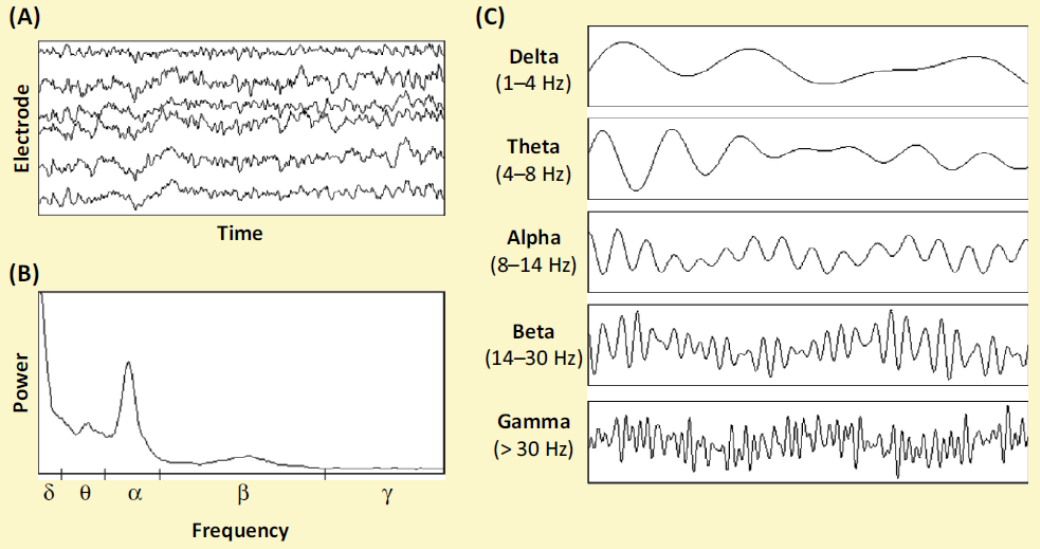

Figure I-8: Illustration of cortical oscillations recorded with EEG. A) The EEG data recorded from six different electrodes is presented. **B**) The power of specific oscillatory frequencies in EEG data in a resting state EEG measurement with eyes-closed participants is plotted. **C**) EEG data band-pass filtered to represent the well-established five frequency bands: delta, theta, alpha, beta and gamma. (Clayton et al., 2015)

Each of these five frequency bands has been associated with different cognitive processes. **Delta** oscillations are mainly correlated with the detection of targets within a group of non-targets. This leads to a focus of attention on a stimulus or a location and is also represented by a P300 ERP-component (Başar-Eroglu et al., 1992). This focus of attention on a limited aspect of the stimulus can be achieved by inhibiting other unrelated stimuli or locations. The sources found for delta oscillations in the frontal and cingulate cortex span a wide region of possibly inhibitory neural networks (Harmony, 2013). Cortical **theta** oscillations are closely linked with memory processes (Klimesch, 1999) and activity in the hippocampus, a brain region serving memory functions (Mitchell et al., 2008). **Alpha** oscillations are modulated by sensory stimulations (Schürmann and Başar, 2001) as well as attentional processes (Hanslmayr, et al., 2011). They seem to inhibit task-irrelevant cortical structures (Jensen and Mazaheri, 2010) being inverse correlated with cognitive performance. There are recent studies suggesting that this inhibition of neural networks is at least partly coordinated by alpha oscillations (Klimesch et al. 2007; Jensen et al., 2014, Cohen, 2017). Many

independent alpha generators exist in the brain. This idea is based on the finding that the amplitude, time course and peak frequency of alpha oscillations can be modified by varying cognitive task, cortical region and cortical layer (Haegens et al. 2014; Haegens et al. 2015). Recent studies have described alpha oscillations to represent feedback processes (Bastos et al., 2015; Jensen et al., 2015). In combination with gamma oscillations reflecting bottom-up processes (Michalareas et al., 2016) these feedback processes associated with alpha band activity (for a review see Clayton et al., 2018) build the loops important in the predictive coding theory (Friston, 2005, 2010) reflecting the top-down flow of predictions to the next lower level in order to be compared to incoming sensory information (Stefanics et al., 2014). **Beta** oscillations are linked to motor task performances (Neuper and Pfurtscheller, 2001), but are also modulated during cognitive tasks which require sensorimotor interactions (Kilavik et al., 2013). A study combining these two factors proposed that beta activity indicates an expectation of the current sensorimotor state to remain stable and not to change (Engel and Fries, 2010). The high frequency **gamma** oscillations are shown to be an indicator of cortical activation (Merker, 2013), linked to attentive processing of information (Fries et al., 2001), active maintenance of memory contents (Herrmann et al., 2004) and conscious perception (Singer, 2001).

3.11 Functional magnetic resonance imaging (fMRI)

In addition to a variety of clinical applications like functional characterization of disease states (Matthews et al., 2006; Bullmore, 2012) and monitoring the plasticity in studies of drug development (Wise and Preston, 2010), functional magnetic resonance imaging (fMRI) is a technique widely used in neuroscience research due to its noninvasive nature and the high spatial resolution (typical voxel size (minimal spatial resolution): 2,8 mm to 3,5 mm edge length at 3 T (Soares et al., 2016)). Appropriate fMRI analysis can show the whole network of the brain being engaged in a specific task (Logothetis, 2008). The basic concept of fMRI is the connection between an increase of local neuronal activity and the resulting higher energy

consumption and increased blood flow. Typically, a statistical map showing the regional activity is presented as a result following complex workflows of analyses (for a review see e.g.: Soares et al., 2016), for an example see Figure I-9.

fMRI measurements use the magnetic properties of nuclei, including the hydrogen nuclei in water and lipids contained in most biological materials (Amaro and Baker, 2006). Due to their spin they have a magnetic moment and in the strong and homogeneous magnetic field of the MRI system a specific number of them are aligned with the main magnetic field vector (Lange, 1996). These aligned spins produce a bulk magnetization with a precession movement around the direction of the magnetic field, executed with a specific frequency (the Larmor frequency) which depends on the magnitude of the magnetic field. During a measurement, radiofrequency pulses are applied forcing the spins to change their orientation till they are perpendicular to the main magnetic field. This orientation in the field induces a voltage which can be measured, usually by a coil placed around the region of interest, before the spins slowly return to their original orientation. The measured radiofrequency signal can be assigned to a specific position due to magnetic field gradients which lead to varying magnetic field strengths and therefore corresponding different resonance frequencies at different positions. The amount of water or other hydrogen containing material at any point in the body can be determined by the strength of the signal which depends on the number of spins involved. The decaying rate of the signal, or the relaxation time, describes the interaction of the spins with the surrounding material.

Most often the BOLD (blood oxygenation level dependent) contrast imaging method is used to gain information about brain activity. The oxygenation level of hemoglobin during e.g. visual stimulation as compared to rest leads to different magnetic properties which are detected and depicted in the resulting images with higher signals for a higher concentration of oxyhemoglobin. Increased neuronal activity in a specific area could be shown to be the cause of a spatially localized increase in the BOLD contrast (Logothetis et al., 2001). The increase of oxyhemoglobin concentration in specific activated areas of the brain results from

an increased blood flow. The hemodynamic response function represents the complex signal of oxygen transport in a particular area over time. Importantly, it is a dynamically changing function showing a delay of the peak BOLD effect of about 5 s after the stimulation leading to a relatively low temporal resolution (Amaro and Baker, 2006). Usually, images covering the whole brain are acquired every 1–2 s revealing the dynamic changes during the experiment. The fMRI technique can therefore be used for the localization of activated brain areas based on the comparison between different conditions leading to different localized BOLD responses.

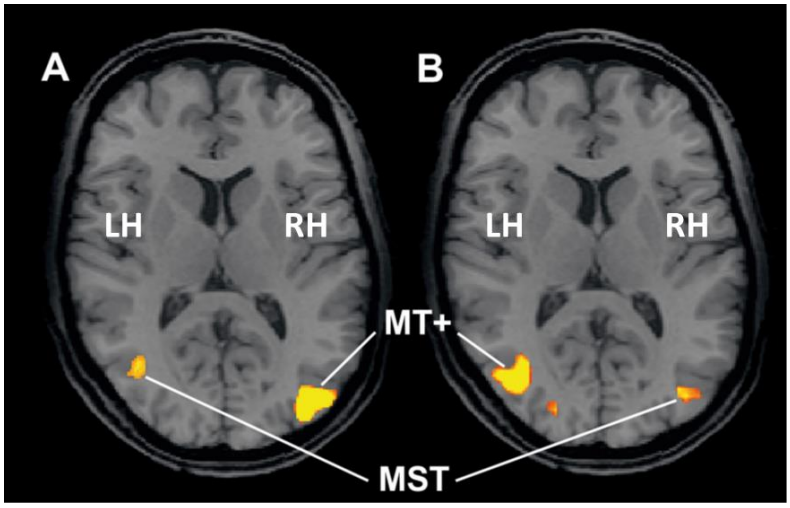

Figure I-9: Results of the analysis of fMRI responses to a mapping stimulus for localizing areas MT and MST. An expanding dot stimulus was presented in the left visual field (**A**) or the right visual field (**B**). The significant activation related to these stimuli is presented as colorful clusters on the anatomical scan which shows the brain structure without information about activation. LH marks the left hemisphere and RH the right hemisphere of the participant. (Wall et al., 2008, modified)

3.12 Transcranial magnetic stimulation (TMS)

Transcranial magnetic stimulation (TMS) is a noninvasive method to test for causal interactions between brain areas and behavior by modulating the excitability level of localized cortical regions.

In the first half of the 19th century Faraday proposed the magnetic induction principles which have been discovered the first time by Baker and colleagues (Baker et al., 1985) as a method to stimulate the brain using an external magnetic field. A device consisting of a loop of conducting wire has to be placed close to the scalp above the desired brain area (Valero-Cabré et al., 2017). The brief and rapidly changing high intensity electrical current in the wire results in a powerful magnetic field orthogonal to the coil's surface. This in return can induce an electric current in excitable brain tissue. The intensity of the induced electric current is proportional to the original coil current but is attenuated depending on the distance to the coil and the material the magnetic field has to transit, like bone, air and tissue (Wagner et al., 2009). Therefore, it is crucial to accurately place the center of the coil on the scalp over the stimulation area to provide a tangential profile for the magnetic field and thus the shortest path to the stimulated brain area. The coil is connected to capacitors which can rapidly, in around 100 µs, transfer the stored energy to the stimulating coil (Nollet et al., 2003). The current in the coil with values about 5 kA induces the required time varying magnetic field with peak values usually ranging from 1 to 4 Tesla (Wagner et al., 2007). The stimulation depth depends on many factors like the coil size and the orientation of the neuronal cell bodies and fibers with respect to the flow of the induced current (Walsch and Cowey, 2000). In general, the magnetic field decays logarithmically with distance to the coil which leads to a maximal depth of 2 to 3 cm of brain tissue directly affected by standard TMS (Sack and Linden, 2003). A small cortical region is usually in the peak of the field, but broader regions are affected in a range of around 100 mm^2 to 200 mm^2, whereas the focality of TMS is highly influenced by the specific coil and relative position (Wagner et al., 2009).

In cortical areas the induced current depolarizes nearby located neuron assemblies (Valero-Cabré et al., 2017), which leads to the initiation of action potentials. In addition, the level of neural excitability can be altered as well as the membrane resting potentials. Furthermore, thresholds and channel properties can be influenced (Wagner et al., 2009). TMS experiments can be employed to learn more about higher cognitive functions with TMS pulses being able to interfere with normal processing and communicating of interconnected regions by disrupting firing encoding rhythms (e.g. Coslett and Monsul, 1994; Mottaghy et al., 2000; Dessing et al., 2013). Importantly, previous studies have shown that TMS stimulations do not only show effects locally but effects distant to the stimulation site are possible due to the connectivity of different regions of the same cerebral circuit (e.g. Chouinard, et al., 2003).

Since many stimulation factors depend on the stimulated area and used equipment, an adjustment of the stimulation's intensity to the specific experiment and participants is required. A commonly used method is measuring the intensity acquired to induce visible muscle activation (Rossini et al., 1994). Relative to the result the stimulation intensity is adjusted during the experiment individually for each participant. Another possibility to influence the intensity of the stimulation effect is the modification of the experimental design. TMS pulses can be delivered as single pulses which should be separated by time intervals of at least 4 s (Valero-Cabré et al., 2017) to give the depolarized neurons enough time to recover after the refractory period and avoid a summation of the single TMS effects. TMS pulses can also be delivered as double or paired pulses consisting of a test stimulus followed by a conditioning stimulus to analyze the presence or absence of connectivity between the two stimulated areas (Valero-Cabré et al., 2017). The third possibility of TMS experimental design is the use of repetitive TMS (rTMS). This means more than two pulses are delivered within 2 s or less during the stimulus (online), before the stimulus (offline) or during the stimulus, but only at specific times as short bursts of TMS pulses (chronometric). This approach leads to three different outcome effects. For the online effect, a repeated depolarization caused by the TMS pulses leads to a direct and measurable interference with

ongoing neuronal activity. The offline effect (or after-effect) is a longer lasting modification on cerebral processes and shows an impact of TMS pulses delivered before the stimulus. Depending on the frequency cortical activity remains modified (Romero et al., 2002; Allen et al., 2007) and this effect can last 30 minutes post stimulation (Thut and Pascual-Leone, 2010) or more (Schindler et al., 2008). In general, the neuromodulatory effects decay over time and have a limited lifetime, i.e. in the motor cortex around half the time of the rTMS stimulation duration. However, long-term effects can be obtained by a periodic repetition of stimulation sessions (Maeda et al., 2000; Bäumer et al., 2003), which makes TMS also important for therapeutic applications.

3.13 References

Allen, E. A., Pasley, B. N., Duong, T., Freeman, R. D. Transcranial magnetic stimulation elicits coupled neural and hemodynamic consequences. *Science*, **217**, 1918-1921 (2007).

Amaro Jr., E., Barker, G. J. Study design in fMRI: Basic principles. *Brain and Cognition*, **60**, 220-232 (2006).

Amenedo, E., Pazo-Alvarez, P., Cadaveira, F. Vertical asymmetries in pre-attentive detection of changes in motion direction. *International Journal of Psychophysiology*, **64(2)**, 184-189 (2007).

Angelaki, D. E., Gu, Y., DeAngelis, G. C. Visual and vestibular cue integration for heading perception in extrastriate visual cortex. *J Physiol*, **589.4**, 825-833 (2011).

Baker, A. T., Jalinous, R., Freeston, I. L. Non-invasive magnetic stimulation of human motor cortex. The Lancet, 325 (8437), 1106-1107 (1985).

Banks, M. S., Ehrlich, S. M., Backus, B. T., Crowell, J. A. Heading During Real and Simulated Eye Movements. *Vision Res*, **36:3**, 431-443 (1996).

Başar-Eroglu, C., Başar, E., Demiralp, T., Schürmann, M. P300-response: possible psychophysiological correlates in delta and theta frequency channels. A review. *International Journal of Psychophysiology*, **13**, 161-179 (1992).

Bastos, A. M., Vezoli, J., Bosman, C. A., Schoffelen, J.-M., Oostenveld, R., Dowdall, J. R., De Weerd, P., Kennedy, H., Fries, P. Visual areas exert feedforward and feedback influences through distinct frequency channels. *Neuron*, **85**, 390-401 (2015).

Bäumer, T., Lange, R., Liepert, J., Weiller, C., Siebner, H. R., Rothwell, J. C., Münchau, A. Repeated premotor rTMS leads to cumulative plastic changes of motor cortex excitability in humans. *NeuroImage*, **20**, 550-560 (2003).

Berger, H. Über das Elektrenkephalogramm des Menschen. *Arch. Psychiatr. Nervenkr*. **87**, 527-570 (1929).

Berthoz, A., Pavard, B., Young, L. R. Perception of Linear Horizontal Self-Motion Induced by Peripheral Vision (Linearvection) Basic Characteristics and Visual-Vestibular Interactions. *Exp. Brain Res.*, **23**, 471-489 (1975).

Berthoz, A., Israel, I., Georges-Francois, P., Grasso, R. and Tsuzuku, T. Spatial memory of body linear displacement: what is being stored? *Science,* **269**, 95–98 (1995).

Berti, S. The attentional blink demonstrates automatic deviance processing in vision. *NeuroReport*, **22(13)**, 664-667 (2011).

Bremmer, F., Lappe, M. The use of optical velocities for distance discrimination and reproduction during visually simulated self motion. *Exp Brain Res*, **127**, 33-42 (1999).

Bremmer, F., Schlack, A., Shah, N. J., Zafiris, O., Kubischik, M., Hoffmann, K., Zilles, K., Fink, G.R. Polymodal motion processing in posterior parietal and premotor cortex: a human fMRI study strongly implies equivalencies between humans and monkeys. *Neuron*. **29(1)**, 287-96 (2001).

Bremmer, F., Klam, F., Duhamel, J.-R., Hamed, S. B., Graf, W. Visual-vestibular interactive responses in the macaque ventral intraparietal area (VIP). *European Journal of Neuroscience*, **16**, 1569-1586 (2002).

Bremmer, F., Kubischik, M., Pekel, M., Hoffmann, K.-P-, Lappe, M. Visual selectivity for heading in monkey area MST. *Exp. Brain Res.*, **200**, 51-60 (2010).

Bremmer, F., Churan, J., Lappe, M. Heading representations in primates are compressed by saccades. *Nature Communications*, **8:920,** (2017).

Britten, K. H. Mechanisms of self-motion perception. *Annu. Rev. Neurosci.*, **31**, 389–410 (2008).

Bullmore, E., The future of functional MRI in clinical medicine. *NeuroImage*, **62**, 1267-1271 (2012).

Cardin, V., Hemsworth, L., Smith, A. T. Adaptation to heading direction dissociates the roles of human MST and V6 in the processing of optic flow. *J Neurophysiol*, **108**, 794–801 (2012).

Chen, A., DeAngelis, G. C., Angelaki, D. E. Representation of Vestibular and Visual Cues to Self-Motion in Ventral Intraparietal Cortex. *The Journal of Neuroscience*, **31(33)**, 12036-12052 (2011).

Chouinard, P. A., Van Der Werf, Y. D., Leonard, G., Paus, T. Modulating neural networks with transcranial magnetic stimulation applied over the dorsal premotor and primary motor cortices. *J Neurophysiol*, **90**, 1071.1083 (2003).

Churan, J., Paul, J., Klingenhoefer, S., Bremmer, F. Integration of visual and tactile information in reproduction of traveled distance. *J Neurophysiol*, **118**, 1650-1663 (2017).

Clayton, M. S., Yeung, N., Kadosh, R. C. The roles of cortical oscillations in sustained attention. *Trends in Cognitive Sciences*, **19(4)**, 188-195 (2015).

Cohen, M. X. Where does EEG come from and what does it mean? *Trends in Neurosciences*, **40(4)**, 208-218 (2017).

Coslett, H. B., Monsul, N. Reading with the right hemisphere: evidence from transcranial magnetic stimulation. *Brain And Language*, **46**, 198-211 (1994).

Crowell, J. A., Banks, M. S. Perceiving heading with different retinal regions and types of optic flow. *Perception and Psychophysics*, **53(3)**, 325-337 (1993).

Cullen, K. E. The vestibular system: multimodal integration and encoding of self-motion for motor control. Trends in Neurosciences, 35(3), 185-196 (2012).

Cutting, J. E., Braren, P. A., Johnson, S. H., Springer, K. Wayfinding on foot from information in retinal, not optical, flow. *Journal of Experimental Psychology: General*, **121(1)**, 41-72 (1992).

Cutting, J. E. Wayfinding from multiple sources of local information in retinal flow. *Journal of Experimental Psychology: Human Perception and Performance*, **22(5)**, 1299-1313 (1996).

Czigler, I. Visual mismatch negativity: violation of nonattended environmental regularities. *Journal of Psychophysiology*, **21**, 224–230 (2007).

Czigler, I., Pató, L. Unnoticed regularity violation elicits change-related brain activity. *Biological Psychology*, **80(3)**, 339-347 (2009).

Czigler, I. Visual mismatch negativity and categorization. *Brain Topogr*, **27**, 590-598 (2014).

Dessing, J. C., Vesia, M., Crawford, J. D. The role of areas MT+/V5 and SPOC in spatial and temporal control of manual interception: an rTMS study. *Frontiers in Behavioral Neuroscience*, **7(15)** (2013).

Dokka, K., DeAngelis, G. C., Angelaki, D. E. Multisensory Integration of Visual and Vestibular Signals Improves Heading Discrimination in the Presence of a Moving Object. *The Journal of Neuroscience*, **35(40)**, 113599-13607 (2015)

Duffy, C., Wurtz, R. H. Sensitivity of MST Neurons to Optic Flow Stimuli. I. A Continuum of Response Selectivity to Large-Field Stimuli. *Journal of Neurophysiology*, **65:6** (1991).

Engel, A. K., Fries, P. Beta-band oscillations – signaling the status quo? *Current Opinion in Neurobiology*, **20**, 156-165 (2010).

Fellman, D. J., Van Essen, D. C. Distributed hierarchical processing in the primate cerebral cortex. *Cerebral Cortex*, **1**, 1-47 (1991).

Ferrera, V. P., Nealey, T. A., Manusell, J. H. R. Responses in macaque visual V4 following inactivation of the parvocellular and magnocellular LGN pathways. *The Journal of Neuroscience*, **14(4)**, 2018-2088 (1994).

Fetsch, C. R., Turner, A. H., DeAngelis, G. C., Angelaki, D. E. Dynamic reweighting of visual and vestibular cues during self-motion perception. *The Journal of Neuroscience*, **29(49)**, 15601-15612 (2009).

Foulkes, A. J., Rushton, S. K., Warren, P. A. Heading recovery from optic flow: comparing performance of humans and computational models. *Frontiers in Behavioral Neuroscience*, **7(53)** (2013).

Frenz, H., Bremmer, F., Lappe, M., Discrimination of travel distances from 'situated' optic flow. *Vision Research*, **43**, 2173-2183 (2003).

Frenz, H., Lappe, M., Absolute travel distance from optic flow. *Vision Research*, **45**, 1679-1692 (2005).

Frenz, H., Lappe, M., Kolesnik, M., Bührmann, T. Estimation of travel distance from visual motion in virtual environments. *ACM Trans. Appl. Percpt*., **4(1)**, Article 3 (2007).

Freud, E., Plaut, D. C., Behrmann, M. 'What' is happening in the dorsal visual pathway. *Trends in Cognitive Sciences*, **20(10)**, 773-784 (2016).

Fries, P., Reynolds, J. H., Rorie, A. E., Desimone, R. Modulation of oscillatory neuronal synchronization by selective visual attention. *Science*, **291**, 1560-1563 (2001).

Friston, K. A theory of cortical responses. *Philosophical Transactions of the Royal Society B*, **360(1456)**, 815-836 (2005).

Friston, K. The free-energy principle: a unified brain theory? *Nat Rev Neurosci.*, **11(2)**, 127-38 (2010).

Furlan, M., Wann, J. P., Smith, A. T. A representation of changing heading direction in human cortical areas pVIP and CSv. *Cerebral Cortex*, **24**, 2848-2858 (2014).

Glasauer, S., Schneider, E., Grasso, R., Ivanenko, Y. P. Space–Time Relativity in Self-Motion Reproduction. *J Neurophysiol*, **97**, 451-461 (2007).

Gibson, J. J. The perception of the visual world. *The Riverside Press*, Cambridge, Massachusetts (1950).

Goodale, M. A., Milner, A. D. Separate visual pathways for perception and action. *TINS*, **15(1)**, 20-25 (1992).

Gu, Y., Watkins, P. V., Angelaki, D. E., DeAngelis, G. C. Visual and Nonvisual Contributions to Three-Dimensional Heading Selectivity in the Medial Superior Temporal Area. *The Journal of Neuroscience*, **26(1)**, 73-85 (2006).

Gu, Y., DeAngelis, G. C., Angelaki, D. E. Causal Links between Dorsal Medial Superior Temporal Area Neurons and Multisensory Heading Perception. *The Journal of Neuroscience*, **32(7)**, 2299-2313 (2012)

Haegens, S., Cousijn, H., Wallis, G., Harrison, P. J., Nobre, A. C. Inter- and intra-individual variability in alpha peak frequency. *NeuroImage*, **92**, 46-55 (2014).

Haegens, S., Barczak, A., Musacchia, G., Lipton, M. L., Mehta, A. D., Lakatos, P., Schoeder, C. E. Laminar profile and physiology of the α rhythm in primary visual, auditory, and somatosensory regions of neocortex. *The Journal of Neuroscience*, **35(42)**, 14341-14352 (2015).

Harmony, T. The functional significance of delta oscillations in cognitive processing. *Frontiers in Integrative Neuroscience*, **7(83)** (2013).

Harris, L. R., Jenkin, M., Zikovitz, D. C. Visual and non-visual cues in the perception of linear self motion. *Exp Brain Res*, **135**, 12–21 (2000).

Hanslmayr, S., Gross, J., Klimesch, W., Shapiro, K. L. The role of alpha oscillations in temporal attention. *Brain Research Reviews*, **67**, 331-343 (2011).

Heinrich, S. P. A primer on motion visual evoked potentials. *Doc Ophthalmol*, **114**, 83-105 (2007).

Herrmann, C. S., Munk, M. H. J., Engel, A. K. Cognitive functions of gamma-band activity: memory match and utilization. *Trends in Cognitive Sciences*, **8(8)**, 347-355 (2004).

Herrmann, C. S., Strüber, D., Helfrich, R. F., Engel, A. K. EEG oscillations: From correlation to causality. *International Journal of Psychophysiology*, **103**, 12-21 (2016).

Hesse, P. N., Schmitt, C., Klingenhoefer, S., Bremmer, F. Preattentive processing of numerical visual information. *Frontiers in human neuroscience*, **11**, 70 (2017).

Hlavacka, F., Mergner, T., Bolha, B. Human self-motion perception during translatory vestibular and proprioceptive stimulation. *Neuroscience Letters*, **210**, 83-86 (1996).

Huk, A. C., Dougherty, R. F., Heeger, D. J. Retinotopy and functional subdivision of human areas MT and MST. *J Neurosci*. 22(16), 7195-205 (2002).

Israël, I., Grasso, R., Georges-François, P., Tsuzuku, T., Berthoz, A. Spatial memory and path integration studied by self-driven passive linear displacement. I. Basic properties. *J Neurophysiol.,* **77(6)**, 3180-92 (1997).

Jensen, O., Mazaheri, A. Shaping functional architecture by oscillatory alpha activity: gating by inhibition. *Frontiers in Human Neuroscience*, **4(186)** (2010).

Jensen, O., Gips, B., Bergmann, T. O., Bonnefond, M. Temporal coding organized by coupled alpha and gamma oscillations prioritize visual processing. *Trends in Neurosciences*, **37(7)**, 357-369 (2014).

Jensen, O., Bonnefond, M., Marshall, T. R., Tiesinga. P. Oscillatory mechanisms of feedforward and feedback visual processing. *Trends in Neurosciences*, **38(4)**, 192-194 (2015).

Kaminiarz, A., Schlack, A., Hoffmann, K.-P., Bremmer, F. Visual selectivity for heading in the macaque ventral intraparietal area. *J Neurophysiol*, **112**, 2470-2480 (2014).

Kandel, E. R., Schwartz, J. H., Jessell, T. M. Principles of neural science 4th Ed. (2000).

Khodanovich, M. Y., Esipenko, E. A., Svetlik, M. V., Krutenkova, E. P. A Visual Analog of Mismatch Negativity When Stimuli Differ in Duration. *Neuroscience and Behavioral Physiology*, **40(6)**, 653-661 (2010).

Kidd, D. The optic chiasm. *Clinical anatomy*, **27**, 1149-1158 (2014).

Kilavik, B. E., Zaepffel, M., Brovelli, A., MacKay, W. A., Riehle, A. *Experimental Neurology*, **245**, 15-26 (2013).

Kimura, M., Schröger, E., Czigler, I., Ohira. H. Human Visual System Automatically Encodes Sequential Regularities of Discrete Events. *Journal of Cognitive Neuroscience*, **22(6)**, 1124-1139 (2010).

Kimura, M. Visual mismatch negativity and unintentional temporal-context-based prediction in vision. *International Journal of Psychophysiology*, **83(2)**, 144-155 (2012).

Klimesch, W. EEG alpha and theta oscillations reflect cognitive and memory performance: a review and analysis. *Brain Res Rev.*, **29(2-3)**, 169-195 (1999).

Klimesch, W., Sauseng, P., Hanslmayr, S. EEG alpha oscillations: The inhibition-timing hypothesis. *Brain Research Reviews*, **53**, 63-88 (2007).

Kuba, M., Kubová, Z., Kremlácek, J., Langrová, J. Motion-onset VEPs: characteristics, methods, and diagnostic use. *Vision Research*, **47(2)**, 189-202 (2007).

Kuldkepp, N., Kreegipuu, K., Raidvee, A., Näätänen, R., Allik, J. Unattended and attended visual change detection of motion as indexed by event-related potentials and its behavioral correlates. *Frontiers in Human Neuroscience*, **7**, 476 (2013).

Lange, N., Tutorial in biostatistics. Statistical approaches to human brain mapping by functional magnetic resonance imaging. *Statistics in Medicine*, **15**, 389-428 (1996).

Lappe, M., Rauschecker, J. P. An illusory transformation in a model of potic flow processing. *Vision Res*. **35:11**, 1619-1631 (1995).

Lappe, M., Bremmer, F., Pekel, M., Thiele, A., Hoffmann, K.-P. Optic Flow Processing in Monkey STS: A Theoretical and Experimental Approach. *The Journal of Neuroscience*, **16(19)**, 6265–6285 (1996).

Lappe, M., Bremmer, F., van den Berg, A.V. Perception of self-motion from visual flow. *Trends in Cognitive Sciences*, **3:9** (1999).

Lee, D. N. The optic flow field: the foundation of vision. *Philos Trans R Soc Lond (Biol)*, **290**, 169-179 (1980).

Li, X., Lu, Y., Sun, G., Gao, L., Zhao, L. Visual mismatch negativity elicited by facial expressions: new evidence from the equiprobable paradigm. *Behavioral and Brain Functions*, **8**, 7 (2012).

Lich, M., Bremmer, F. Self-motion perception in the elderly. *Frontiers in Human Neuroscience*, **8:681** (2014).

Livingstone, M., Hubel, D. Segregation of form, color, movement, and depth: Anatomy, physiology, and perception. *Science*, **240**, 740-749 (1988).

Logothetis, N. K., Pauls, J., Augath, A., Trinath, T., Oeltermann, A. Neurophysiological investigation of the basis of the fMRI signal. *Nature*, **412**, 150-157 (2001).

Logothetis, N. K. What we can do and what we cannot do with fMRI. *Nature*, **453**, 869-878 (2008).

Luck, S. J. An Introduction to the Event-Related Potential Technique. 1st Edition, *MIT Press Cambridge, Massachusetts*; London, England, 1-50 (2005).

Maeda, F., Keenan, J. P., Tormos, J. M., Topka, H., Pascual-Leone, A. Modulation of corticospinal excitability by repetitive transcranial magnetic stimulation. *Clinical Neurophysiology*, **111**, 800-805 (2000).

Maekawa, T. et al. Functional characterization of mismatch negativity to a visual stimulus. *Clinical Neurophysiology*, **116(10)**, 2392-2402 (2005).

Matthews, P. M., Honey, G. D., Bullmore, E. T. Applications of fMRI in translational medicine and clinical practice. *Nat Rev Neurosci*., **7**, 732-744 (2006).

Merigan, W. H., Manusell, J. H. R. How parallel are the primate visual pathways? *Annu. Rev. Neurosci.* **16**, 369-402 (1993).

Merker, B. Cortical gamma oscillations: the functional key is activation, not cognition. *Neuroscience and Biobehavioral Reviews*, **37**, 401-417 (2013).

Michalareas, G., Vezoli, J., van Pelt, S., Schoffelen, J.-M., Kennedy, H., Fries, P. Alpha-beta and gamma rhythms subserve feedback and feedforward influences among human visual cortical areas. *Neuron*, **89**, 384-397 (2016).

Mitchell, D. J., McNaughton, N., Flanagan, D., Kirk, I. J. Frontal-midline theta from the perspective of hippocampal “theta”. *Progress in Neurobiology*, **86**, 156-185 (2008).

Morrone, M. C., Tosetti, M., Montanaro, D., Fiorentini, A., Cioni, G., Burr, D. C. A cortical area that responds specifically to optic flow, revealed by fMRI. *Nat Neurosci*, **3(12)**, 1322-8 (2000).

Mottaghy, F. M., Krause, B. J., Kemna, L. J., Töpper, R., Tellmann, L., Beu, M., Pascual-Leone, A., Müller-Gärtner, H.-W. Modulation of the neuronal circuitry subserving working memory in healthy human subjects by repetitive transcranial magnetic stimulation. *Neuroscience Letters*, **280**, 167-170 (2000).

Müller, D. et al. Visual Object Representations Can Be Formed outside the Focus of Voluntary Attention: Evidence from Event-related Brain Potentials. *Journal of Cognitive Neuroscience*, **22(6)**, 1179-1188 (2010).

Müller, D., et al. Impact of lower- vs. upper-hemifield presentation on automatic colour-deviance detection: a visual mismatch negativity study. *Brain Research*, **1472**, 89-98 (2012).

Müller, D., Widmann, A., Schröger, E. Object-related regularities are processed automatically: evidence from the visual mismatch negativity. *Frontier in Human Neuroscience*, **7**, 259 (2013).

Näätänen, R., Gaillard, A. W. K., Mäntysalo, S. Early selective-attention effect on evoked potential reinterpreted. *Acta Psychologica*, **42(4)**, 313-329 (1978).

Nealey, F. A., Manusell, J. H. R. Magnocellular and parvocellular contributions to the responses of neurons in macaque striate cortex. *The Journal of Neuroscience*, **14(4)**, 2069-2079 (1994).

Neuper, C., Pfurtscheller, G. Event-related dynamics of cortical rhythms: frequency-specific features and functional correlates. *International Journal of Psychophysiology*, **43**, 41-58 (2001).

Nollet, H., Van Ham. L., Deprez, P., Vanderstraeten, G. Transcranial magnetic stimulation: review of the technique, basic principles and applications. *The Veterinary Journal*, **166**, 28-42 (2003).

Odom, J. V., Bach, M., Brigell, M., Holder, G. E., McCulloch, D. L. Mizota, A., Tormene, A. P., International Society for Clinical Electrophysiology of Vision. ISCEV standard for clinical visual evoked potentials: (2016 update). *Doc Ophthalmol*, **133**, 1-9 (2016).

Pazo-Álvarez, P., Amenedo, E., Lorenzo-López, L., Cadaveira, F. Effects of stimulus location on automatic detection of changes in motion direction in the human brain. *Neuroscience Letters*, **371(2-3)**, 111-116 (2004).

Prokop, T., Schubert, M., Berger, W. Visual influence on human locomotion. Modulation to changes in the optic flow. *Exp Brain Res*, **114**, 63-70 (1997).

Rao, R. P. N., Ballard, D. H. Predictive coding in the visual cortex: a functional interpretation of some extra-classical receptive-field effects. *Nature Neuroscience*, **2(1)**, 79-87 (1999).

Redlick, F. P., Jenkin, M., Harris, L. R. Humans can use optic flow to estimate distance of travel. *Vision Research*, **41**, 213-219 (2001).

Romero, J. R., Anschel, D., Sparing, R., Gangitano, M., Pascual-Leone, A. Subthreshold low frequency repetitive transcranial magnetic stimulation selectively decreases facilitation in the motor cortex. *Clinical Neurophysiology*, **113**, 101-107 (2002).

Rossini, P. M., Baker, A. T., Berardelli, A., Caramia, M. D., Caruso, G., Cracco, R. Q., Dimitrijevid, M. R., Hallett, M., Katayama, Y., Lücking C. H., Maertens de Noordhout, A. L., Marsden, C. D., Murray, N. M. F., Rothwell, J. D., Swash, M., Tomberg, C. Non-invasive electrical and magnetic stimulation of the brain, spinal cord and roots: basic principles and procedures for routine clinical application. Report of an IFCN committee. *Electroencephalography and clinical Neurophysiology*, **91**, 79-92 (1994).

Royden, C. S., Banks, M. S., Crowell, J. A. The perception of heading during eye movements. *Nature*, **360** (1992).

Sack, A. T., Linden, D. E. J. Combining transcranial magnetic stimulation and functional imaging in cognitive brain research: possibilities and limitations. *Brain Research Reviews*, **43**, 41-56 (2003).

Saito, H., Yukie, M., Tanaka, K., Hikosaka, K., Fukada, Y., Iwai, E. Integration of direction signals of image motion in the superior temporal sulcus of the macaque monkey. *The Journal of Neuroscience*, **6(1)**, 145-157 (1986).

Schindler, K., Nyffeler, T., Wiest, R., Hauf, M., Mathis, J., Hess, Ch. W., Müri, R. Theta burst transcranial magnetic stimulation is associated with increased EEG synchronization in the stimulated relative to unstimulated cerebral hemisphere. *Neuroscience Letters*, **436**, 31-34 (2008).

Schlack, A., Hoffmann, K.-P., Bremmer, F. Interaction of linear vestibular and visual stimulation in the macaque ventral intraparietal area (VIP). *European Journal of Neuroscience*, **16**, 1877-1886 (2002).

Schmitt, C., Klingenhoefer, S., Bremmer, F. Preattentive and predictive processing of visual motion. *Sci Rep.*, **8(1)**:12399 (2018).

Schürmann, M., Başar, E. Functional aspects of alpha oscillations in the EEG. *International Journal of Psychophysiology*, **39**, 151-158 (2001).

Schütz-Bosbach, S., Prinz, W. Prospective coding in event representation. *Cogn Process*, **8**, 93-102 (2007).

Shao, M., DeAngelis, G. C., Angelaki, D. E., Chen, A. Clustering of heading selectivity and perception-related activity in the ventral intraparietal area. *J Neurophysiol*, **119**, 1113-1126 (2018).

Singer, W. Consciousness and the binding problem. *Ann N Y Acad Sci*., **929**, 123-146 (2001).

Snowden, R. J., Treue, S., Erickson, R. G., Andersen, R. A. The response of area MT and V1 neurons to transparent motion. *The Journal of Neuroscience*, **11(9)**, 2768-2785 (1991).

Soares, J. M., Magalhães, R., Moreira, P. S., Sousa, A., Ganz, E., Sampaio, A., Alves, V., Marques, P., Sousa, N. A hitchhiker's guide to functional magnetic resonance imaging. *Frontiers in Neuroscience*, **10(515)** (2016).

Sulykos, I., Czigler, I. One plus one is less than two: Visual features elicit non-additive mismatch-related brain activity. *Brain Research*, **1398**, 64-71 (2011).

Stefanics, G., Kimura, M., Czigler, I. Visual mismatch negativity reveals automatic detection of sequential regularity violation. *Frontiers in Human Neuroscience*, **5**, 46 (2011).

Stefanics, G., Csukly, G., Komlósi, S., Czobor, P., Czigler, I. Processing of unattended facial emotions: A visual mismatch negativity study. *NeuroImage*, **59(3)**, 3042-3049 (2012).

Stefanics, G., Kremlácek, J., Czigler, I. Visual mismatch negativity: a predictive coding view. *Frontiers in Human Neuroscience*, **8**, 666 (2014).

Stippich, C. Clinical functional MRI. Presurgical functional neuroimaging. 2nd Edition. Tobimatsu, S., Celesia, G. G. Studies of human visual pathophysiology with visual evoked potentials. *Clinical Neurophysiology*, **117**, 1414-1433 (2006).

Thierry, G., Athanasopoulos, P., Wiggett, A., Dering, B., Kuipers, J-R. Unconscious effects of language-specific terminology on preattentive color perception. *PNAS*, **106(11)**, 4567-4570 (2009).

Thut, G., Pascual-Leone, A. A review of combined TMS-EEG studies to characterize lasting effects of repetitive TMS and assess their usefulness in cognitive and clinical neuroscience. *Brain Topogr*, **22**, 219-232 (2010).

Urban, A., Kremlácek, J., Masopust, J., Libiger, J. Visual mismatch negativity among patients with schizophrenia. *Schizophrenia Research*, **102(1-3)**, 320-328 (2008).

Valero-Cabré, A., Amengual, J. L., Stengel, C., Pascual-Leone, A., Coubard, O. A. Transcranial magnetic stimulation in basic and clinical neuroscience: A comprehensive review of fundamental principles and novel insights. *Neuroscience and Biobehavioral Reviews*, **83**, 381-404 (2017).

Väljamäe, A. Auditory-induced illusory self-motion: A review. *Brain Research Reviews*, **61**, 240-255 (2009).

Van den Berg, A. V., Beintema, J. A. Motion templates with eye velocity gain fields for transformation of retinal to head centric flow. *NeuroReport*, **8**, 835-840 (1997).

von Hopffgarten, A., Bremmer, F. Self-motion reproduction can be affected by associated auditory cues. *Seeing Perceiving*, **24(3)**, 203-22 (2011).

Wagner, T., Valero-Cabre, A., Pascual-Leone, A. Noninvasive human brain stimulation. *Annu. Rev. Biomed. Eng.*, **9**, 527-65 (2007).

Wagner, T., Rushmore, J., Eden, U., Valero-Cabre, A. Biophysical foundations underlying TMS: Setting the stage for an effective use of neurostimulation in the cognitive neurosciences. *Cortex*, **45**, 1025-1034 (2009).

Wall, M. B., Smith, A. T. The Representation of Egomotion in the Human Brain. *Current Biology*, **18**, 191–194 (2008).

Walsh, V., Cowey, A. Transcranial magnetic stimulation and cognitive neuroscience. *Nat Rev Neurosci.*, **1**, 73-79 (2000).

Wang, X.-J. Neurophysiological and computational principles of cortical rhythms in cognition. *Physiol Rev*, **90**, 1195-1268 (2010).

Wang, S. et al. ERP comparison study of face gender and expression processing in unattended condition. *Neuroscience Letters*, **618**, 39-44 (2016).

Warren, W. H., Hannon, D. J. Direction of self-motion is perceived from optical flow. *Nature*, **336** (1988).

Warren, W. H., Blackwell, A. W., Kurtz, K. J., Hatsopoulos, N. G., Kalish, M. L. On the sufficiency of the velocity field for perception of heading. *Biol. Cybern*., **65**, 311-320 (1991).

Warren, W. H., Kurtz, K. J. The role of central and peripheral vision in perceiving the direction of self-motion. *Perception and Psychophysics*, **51(5)**, 443-454 (1992).

Winkler, I., Czigler, I. Evidence from auditory and visual event-related potential (ERP) studies of deviance detection (MMN and vMMN) linking predictive coding theories and perceptual object representations. *International Journal of Psychophysiology,* **83**, 132-143 (2012).

Wise, R. G., Preston, C. What is the value of human fMRI in CNS drug development? *Drug Discovery Today*, **15(21/22)**, 973-980 (2010).

Yamasaki, T., Tobimatsu, S. Motion perception in healthy humans and cognitive disorders. In: Early detection and rehabilitation technologies for dementia: Neuroscience and biomedical applications, Wu J, ed. IGI Global, Hershey, Pennsylvania, 156-161 (2011).

Yamasaki, T., Fujita, T., Kamio, Y., Tobimatsu, S. Motion perception in autism spectrum disorder. *Advances in Psychology Research*, **82**, 197-211 (2011).

Yu, M., Mo, C., Zeng, T., Zhao, S., Mo, L. Short-term trained lexical categories affect preattentive shape perception: Evidence from vMMN. *Psychophysiology*, **54(3)**, 462-468 (2017).

4 Studies

4.1 Overview of included studies

Study I:

Predictive and preattentive processing of visually simulated self-motion

Constanze Schmitt and Frank Bremmer

In preparation

Study II:

TMS-induced disturbance of self-motion perception in humans

Constanze Schmitt, Bianca R. Baltaretu, J. Douglas Crawford and Frank Bremmer

In preparation

Study III:

A neural correlate of the subjective encoding of distance

Constanze Schmitt, Milosz Krala and Frank Bremmer

In preparation

4.2 Motivation and scope of the studies

In my thesis I have investigated the perception of visually simulated self-motion. I conducted three studies to learn more about the underlying processes. In the first two studies I examined the perception of self-motion direction (heading) and in the third study the perception of traveled distance.

The aim of the first study was two-fold. First, while recording EEG data I conducted an oddball experiment with human participants presenting visually simulated forward self-motion. The difference between deviant and standard stimuli was the self-motion direction. The heading was either forward to the left (10° to the left) or forward to the right (10° to the right). With this study design, I aimed to show a MMN-component elicited after the presentation of deviant stimuli. This result would be indicative of a preattentive processing of self-motion direction as well as a predictive error signal, thereby supporting prediction error theories (e.g. Friston, 2005, Winkler and Czigler, 2012; Stefanics et al., 2014). In a second step, we repeated the experiment with macaque monkeys as participants to learn more about the comparability of sensorimotor processing in monkeys and humans. This approach is also an important first step of our group to record EEG data simultaneously with single cell activation.

In the second study we presented visually simulated forward self-motion into three different directions (straight forward and 30° to the left and right, each). The scope of the second study was to show the importance of the medial superior temporal brain area (MST) for the accurate perception of self-motion direction. In order to causally link this area to the heading estimation performance we used TMS stimulating this area in human participants to temporary disturb self-motion processing. A model based on single cell recordings in macaque monkeys (Bremmer et al., 2017) predicted a decline of performance. Similar to the first study in this thesis we aimed to provide further evidence for the macaque monkey as animal model for human sensorimotor processing.

In the third study I presented a visually simulated self-motion and measured EEG-activity in human participants. The objective was to find an indicator for traveled distance estimation. Participants were asked to reproduce twice the distance of a previously observed forward self-motion. This study design enabled me to analyze the time point of the individual and subjective estimation of the observed distance and to identify neural correlates of path integration. In addition, this approach allowed for a comparison of the processing of externally- and self-induced self-motion information in the context of the predictive coding theories.

Study I:

Predictive and preattentive processing of visually simulated self-motion

Constanze Schmitt and Frank Bremmer

In preparation

4.3 Study I: Predictive and preattentive processing of visually simulated self-motion

4.3.1 Abstract

The control of self-motion through an environment is a challenging task, amongst others requiring immediate adjustments to keep on track. Accordingly, it would appear advantageous if the processing of self-motion was predictive, thereby facilitating the encoding of prediction errors, and independent from attentional load. Here, we set out to test for such an encoding of self-motion direction (heading).

Participants viewed a random dot pattern that simulated self-motion across a ground plane in an oddball EEG paradigm. Trials differed only in their simulated heading direction (forward-left vs. forward-right). Event-related potentials (ERPs) as observed in response to standard and deviant stimuli were compared in order to test for the occurrence of a visual mismatch negativity (vMMN), a component that reflects preattentive processing of sensory stimuli. The participant's attention was drawn off the self-motion stimuli by one of two different unrelated secondary tasks. Analysis of the evoked ERPs revealed a MMN between 100 ms and 180 ms after self-motion onset. This component was slightly lateralized over parietal and occipital areas, i.e. contralateral with respect to the simulated heading direction. We consider our results strong evidence for a predictive and preattentive processing of visually simulated self-motion direction.

4.3.2 Introduction

Navigation through an environment is a challenging task. Signals from different sensory modalities have to be combined and motor output has to be adjusted e.g. to keep track of one's direction of self-motion (heading), to aim for a target or to avoid collision with obstacles. From a theoretical point of view, it would appear advantageous if this processing was predictive and independent from attentional load. Predictive coding is suggested to facilitate sensory processing by attenuating responses to predictable sensory information and enhancing responses to unpredicted events like unexpected changes in heading (Rao and Ballard, 1999; Friston, 2005). Along the same vein, a preattentive processing of self-motion direction could facilitate successful navigation irrespective of cognitive load. Such processing of heading would be different to path integration whose accuracy has been shown before to be modulated by a secondary task (Glasauer et al., 2009).

Electroencephalography (EEG) recordings allow determining such predictive and preattentive processing of stimulus features. A specific EEG-component, the so-called visual mismatch negativity (vMMN) has been shown to be indicative of predictive coding and preattentive processing of sensory stimuli (Berti, 2011; Stefanics et al., 2018). The MMN is computed as the difference between two event-related potentials (ERPs) recorded after stimulation of two different types of trials, usually recorded in an oddball experiment (Kimura, 2012; Stefanics, et al., 2014). The deviant stimuli elicit more negative N2 ERP-components than the frequently presented standard stimulations (Luck, 2005). This leads to the negative MMN-component when comparing the responses (deviant-standard). The MMN typically peaks in a time window between 100 and 400 ms after stimulus onset on parietal electrodes (Kimura, 2012; Czigler, 2014). In the predictive coding theories this component has the important role of carrying the prediction error elicited by the mismatch of a sensory event with the predictions formed by prior experience (Friston, 2005; Winkler and Czigler, 2012; Stefanics et al., 2014). A generative model representation of the standard stimuli is formed based on the detection of the regularities in their presentation. This leads to predictions

about the upcoming events which are compared to the actual sensory input. The principle of free energy minimization (Friston, 2005, 2010) proposed that differences arising from theses comparisons have to be kept as small as possible to optimize perception. Deviant stimuli do not match the prediction formed by the regularity of standard stimuli and produce a mismatch. The resulting prediction error is forwarded to the next hierarchical level to be used for updating the predictive model.

Originally the MMN was only analyzed in the auditory domain (Näätänen, et al., 1978; Winkler and Czigler, 2012). For many years it was unclear whether a MMN-component can also be shown in other sensory domains, like e.g. vision. In recent years several studies reported a visual mismatch negativity (vMMN) component (Amenedo et al., 2007; Kimura et al. 2010; Müller, et al., 2010; Hesse, et al., 2017; Schmitt et al., 2018; Czigler, et al., 2019). The MMN has now been shown among others for the orientation of visual stimuli (Kimura et al., 2010; Czigler and Pató, 2009; Sulykos and Czigler, 2011; Durant et al., 2017; Yan et al., 2017), the direction of motion (Urban et al., 2008; Kuldkepp et al., 2013), color (Thierry, et al., 2009; Stefanics, et al., 2011; Müller et al., 2012), numerosity (Hesse et al., 2017) and also higher cognitive features such as object structure (Müller et al., 2013) and facial emotions (Stefanics et al., 2012; Wang et al., 2016). Previous studies introduced secondary tasks to distract participants' attention from the MMN inducing stimulus and capture their attention on properties unrelated to the stimulus feature (Pazo-Álvarez et al., 2004; Stefanics et al., 2012; Li et al, 2012; Kuldkepp et al., 2013; Hesse et al., 2017; Schmitt et al., 2018). Nevertheless, MMN-components have been shown also under such experimental conditions. This led to the conclusion that the MMN is indicative of predictive and preattentive processing of sensory signals (Maekawa, 2005; Czigler, 2007; Müller et al., 2013; Yu, et al., 2017; Stefanics et al., 2018).

Here, we aimed to investigate if heading is processed preattentively and unexpected headings lead to a prediction error signal. We presented two self-motion directions (forward to the left and right) in an oddball experiment alternately as standard and deviant stimulus. This approach allowed us to compare the EEG response to two physically identical stimuli. In

all cases, the participants' attention was drawn off the different headings by an unrelated discrimination task. We then analyzed the resulting EEG data for the existence of a vMMN-component.

4.3.3 Materials and Methods

4.3.3.1 Participants

Twelve volunteers (8 female, aged between 21 and 31, mean 25 years) with normal or corrected to normal vision participated in our study. The participants were naïve about the objective of our study. Prior to the experiment they provided written informed consent. Our study was in accordance with the Declaration of Helsinki and was approved by the local Ethics Committee. All participants finished data collection on four different days. They were compensated with 8 € per hour.

4.3.3.2 Setup

Participants were sitting in a darkened, sound attenuated and electrically shielded room. The stimuli were presented on a computer monitor (*VPixx Technologies Inc.*, Saint-Bruno, QC, Canada) 68 cm in front of them at eye level. The participants' heads were stabilized by a chin rest. The display was 42° wide and 24° high and was set to 1920 × 1080 pixels at a refresh rate of 100 Hz. Eye movements were recorded using an EyeLink 1000 system (*SR Research*, ON, Canada). Trials containing blinks and other movement artefacts were excluded from further offline data analysis (see below).

4.3.3.3 Stimulus

We presented an optic flow stimulus to our participants which simulated self-motion across a ground plane (white dots with a lifetime of 1 s on a dark background) with heading directed either forward and 10° to the left or 10° to the right (Figure S1-1). In addition, a central white

fixation dot with a radius of 3 pixels was displayed throughout the whole experiment. In the first phase of each trial the dots were shown stationary for 800 (+/-200) ms. In the second phase self-motion across the ground plane was simulated by movement of the dots for 400 (+/-50) ms. One of the movement directions was shown as the standard stimulus (80% occurrence), the other one as deviant stimulus (20% occurrence). Across sessions, deviant and standard directions were counterbalanced. For further analysis, all data were aligned to self-motion onset.

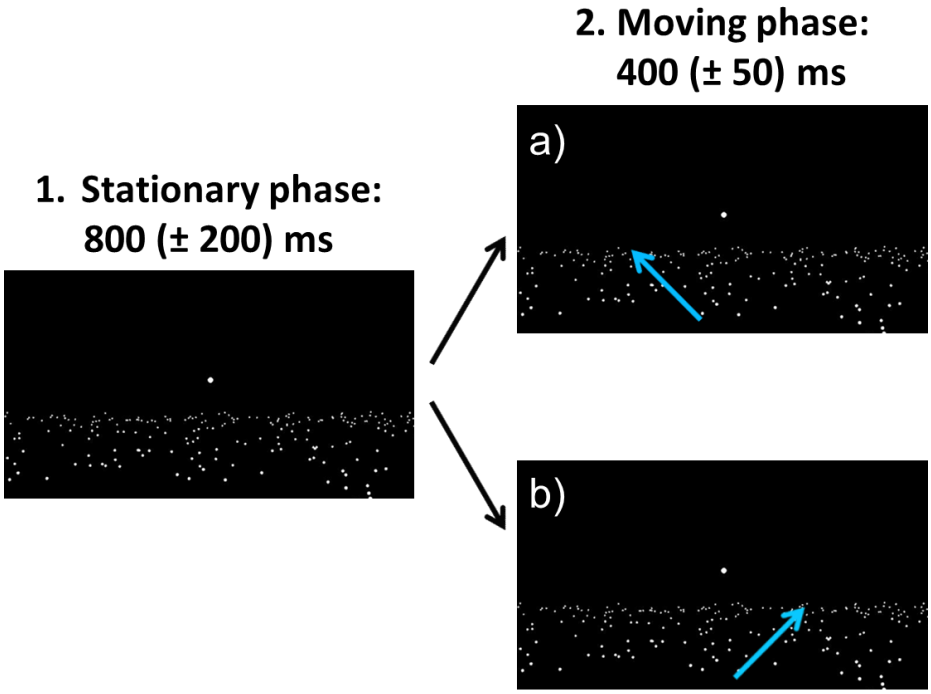

Figure S1-1: Self-motion stimulus for the two headings forward to the left and to the right. Each trial consisted first of a stationary ground plane formed by random white dots which was presented to the participants for 800 (±200) ms. In a following second phase the ground plane moved for 400 (±50) ms to induce visual self-motion to one of two headings: forward and 10° to the left (a)) or forward and 10° to the right (b)). Throughout the whole trial a fixation target was displayed in the center of the screen.

4.3.3.4 Task

The main task of the participants was to fixate the central target. An additional secondary task was introduced to control the participants' focus of attention. They had to report a color change within the visual scene by a button press. The task consisted of two different

attention conditions. The color change could affect either the fixation target, “attention towards the fixation target”, (10% of all trials) or the dots of the ground plane, “attention towards the ground plane” (10% of all trials). In the “attention towards the fixation target” condition a small black dot (radius 2 pixels) appeared in the middle of the white fixation target. In the “attention towards the ground plane” condition all the white dots of the ground plane changed to grey. These changes appeared randomly in a time window from self-motion start to 100 ms before self-motion end and stayed throughout the rest of the trial. As soon as the participants got aware of the change they were asked to press the key “5” on the numerical pad of a normal computer keyboard which was lying in comfortable reaching distance on a table in front of them. Trials which showed a color change were excluded from further offline data analysis. Due to the smaller number of deviant trials the attention task only appeared in standard trials. On each day of data collection we presented only one attention condition. Participants got informed before the start of the experiment which condition would be presented.

4.3.3.5 Procedure

On each day we collected data from eight sessions: four of them with heading to the left as the oddball stimulus and four sessions with heading to the right as the oddball stimulus. The sequence of movement directions of the oddball stimulus was pseudorandomized across blocks and participants. Each session was subdivided into 10 blocks of 20 trials. This leads to a total number of 6400 trials per participant. On the first two days of data collection we presented the attention condition “attention towards the fixation target” and on the other two days the attention condition “attention towards the ground plane”.

4.3.3.6 EEG recordings

We used an actiCHamp module (*Brain Products GmbH*, Gilching, Germany) and the software Brain Vision PyCorder (*Brain Vision LLC*, Morisville, NC, USA) to record the

electroencephalogram (EEG) continuously throughout the whole experiment. The continuously recorded EEG signal was digitized at a sampling rate of 1000 Hz at each electrode. We used 64 active Ag/AgCl electrodes positioned according to the extended international 10-20 system. Principally the impedances of all electrodes were kept below 5 kΩ during the whole experiment.

4.3.3.7 Analysis

For the offline analysis of our EEG data we used the software Brain Vision Analyzer (*Brain Products*, Gilching, Germany). In a first step we redefined the average signal of the two mastoid electrodes TP9 and TP10 as our new reference signal. Per default during data collection electrode Cz was used as reference signal. We applied a Notch filter at 50 Hz and a low pass filter with a cut-off frequency of 70 Hz to our data. In a next step we excluded all trials with blinks or eye movements as well as all trials which showed one of the two attention tasks (10% each) from further analysis because motor responses were induced in these trials. Based on these exclusion criteria, approximately 25% of all trials were removed.

All remaining data were aligned to the onset of the self-motion phase and epochs with a length of 550 ms (50 ms before motion onset to 500 ms after motion onset) were extracted from the continuous data stream. Each epoch was baseline corrected (centered) using the average signal from -50 ms to 0 ms relative to motion onset. In a last step all the epochs were averaged for subjects and conditions separately.

To calculate the MMN-component we compared data for a given heading direction collected in oddball trials with data for the same heading direction collected in standard trials (deviant-standard). As stated already above, in half of the sessions this given self-motion direction served as standard stimulus, while in the other half it served as deviant.

For our statistical analysis we compared ERPs in a fixed temporal window from 100 ms to 180 ms after self-motion onset. We wanted to cover the full time course of the MMN-

component and based the decision for this time window on the peak time of the MMN and its maximum width.

The datasets generated and analyzed during the current study are available from the corresponding author on reasonable request.

4.3.4 Results

In order to draw the subjects' attention away from the visual feature under study, i.e. heading direction, we employed them in a secondary task, i.e. a color change detection task of either the central fixation target or the moving ground plane stimulus. This task was intended to be rather difficult to capture our participants' attention. Our results show a correct response rate between 43% and 64% (mean: 52%) for attention directed towards the fixation target. This corresponds to 65 to 195 true positives per subject, while we only recorded 8 false positives together for all subjects, i.e. on average one false positive per subject. For attention directed towards the color-change of the ground plane stimulus we found between 35% and 56% (mean 45%) correct performance. This corresponds to 77 to 178 true positives per subject, with only 0 to 8 false positives per subject, except for one subject who had 29 false positives, but also 144 true positives.

4.3.4.1 Timeline of electrode Pz

In a first step we analyzed the activity recorded by electrode Pz averaged across all participants (Figure S1-2). Data was aligned to movement onset. In all cases (standard and deviant trials) the onset of visually simulated self-motion induced a clear visual evoked potential (VEP) (Luck, 2005): a positive peak (P1) at around 85 ms, a negative peak (N2) around 150 ms and a positive peak (P2) around 220 ms after self-motion onset. The four panels (A—D) depict data from four different experimental conditions. A: heading to the left and attention towards the fixation target; B: heading to the right and attention towards the

fixation target; C: heading to the left and attention towards the ground plane; D: heading to the right and attention towards the ground plane.

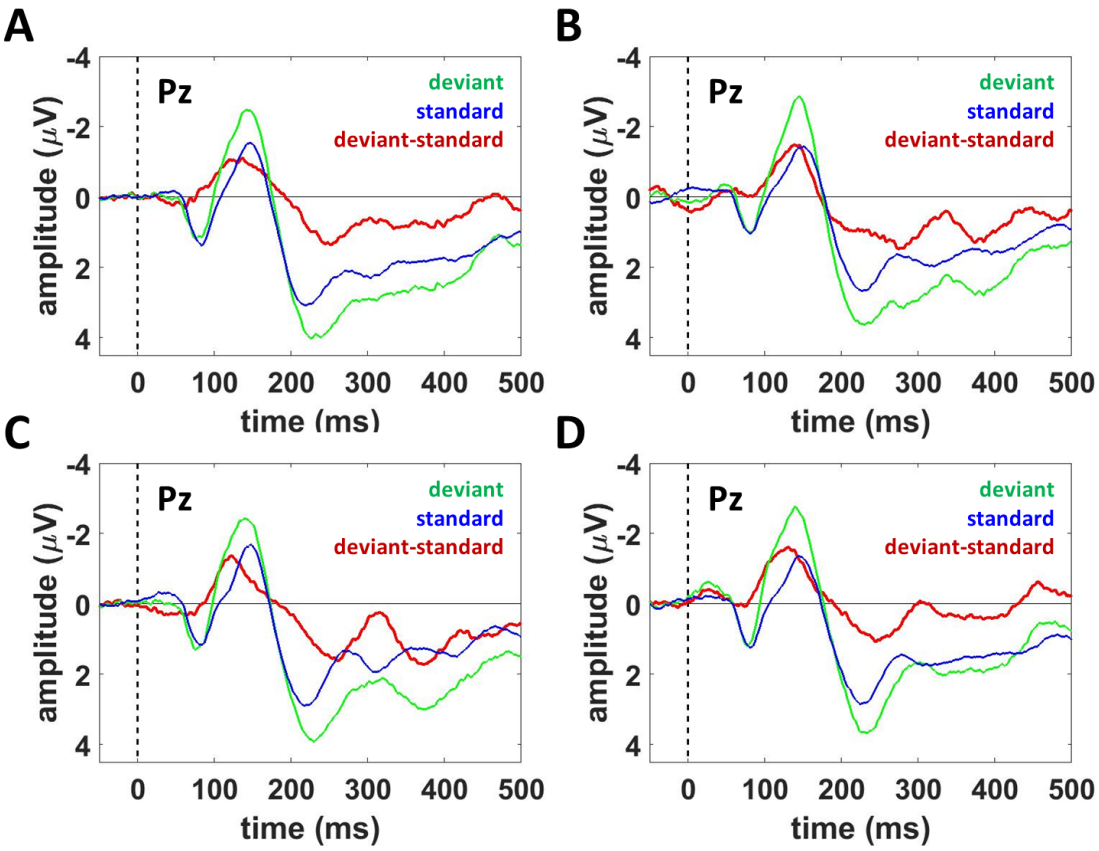

Figure S1-2: Grand-Average data of electrode Pz for the two different headings and attention conditions. In all the four graphs the time course of data collected on electrode Pz is plotted from 50 ms before self-motion onset till 500 ms after self-motion onset. In green data from deviant trials, in blue data from standard trials and in red the difference between deviant and standard trial data is visualized. In **A** and **C** data collected after presentation of self-motion to the left and in **B** and **D** data collected after presentation of self-motion to the right is shown. **A** and **B** show data from the condition "attention towards the fixation target" and **C** and **D** from the condition "attention towards the ground plane".

In all four conditions, the N2-peak was more negative for data collected in deviant trials compared to standard trials. This is clearly visible by the red data curve in each panel, which depicts the VEP-difference between deviant and standard trials (deviant - standard). The resulting visual Mismatch-Negativity peaked at around 140 ms after self-motion onset. In all

four conditions, the VEP-difference, i.e. the vMMN, in a time window ranging from 100 ms to 180 ms after self-motion onset was significant (Figure S1-2): (One-sided t-test. A: $t(10)=-3.49$, $p=0.0029$; B: $t(10)=-3.31$, $p=0.0039$; C: $t(10)=-2.29$, $p=0.023$; and D: $t(10)=-4.36$, $p=0.00071$).

Previous studies have argued that the vMMN is indicative of predictive and preattentive processing of sensory stimuli (preattentive: e.g. Maekawa et al., 2005; predictive: Stefanics et al., 2018). To provide further evidence for this finding, our subjects had to solve a secondary task, which was not related to the direction of self-motion, i.e. the sensory feature under study. More specifically, subjects had to respond to a change in color of either the central fixation target or the ground plane stimulus, as described above. The vMMN-components for the two attention conditions did not reveal a significant difference (heading to the left: $t(10)=0.23$, $p=0.82$; heading to the right: $t(10)=-1.1$, $p=0.29$).

4.3.4.2 Lateralization of the processing of self-motion information

A recent study combining neurophysiology in the macaque monkey, i.e. the animal model of human sensorimotor processing, with behavior in humans and modeling (Bremmer et al., 2017) suggested that the processing of self-motion information in primates is lateralized, i.e. processing of leftward self-motion occurs predominantly in the right cortical hemisphere and vice versa. This hypothesis has been corroborated by a recent TMS study from our group (Schmitt et al., 2017) showing that TMS over right visual cortex modulates predominantly perception of self-motion to the left. The experimental approach of our current study allowed for further investigating such lateralization in self-motion processing. We determined the VEP-difference (deviant - standard) at all electrodes and show the group data in a topographic plot for the condition “attention towards the fixation target” (Figure S1-3).

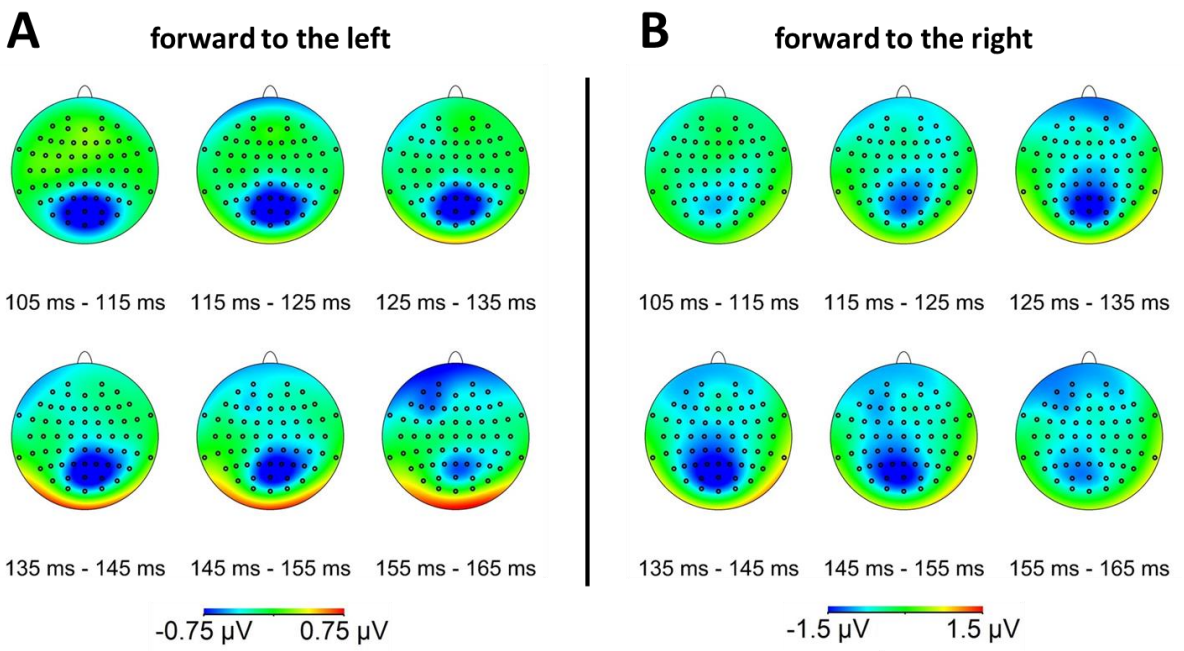

Figure S1-3: Topographic analysis of the MMN-component of the attention towards the fixation target condition for the two different headings averaged over all participants. In **A** data collected in trials with simulated self-motion forward to the left and in **B** data collected in trials with simulated self-motion forward to the right is presented. For both headings a time window from 101 ms to 179 ms after self-motion onset is displayed. Each topographic map shows the average over 13 ms. For better visibility of the vMMN-component different voltage scales are chosen: ±0.75 µV for heading to the left and ±1.5 µV for heading to the right.

Negative VEP values are displayed in blue. For both headings, forward to the left and right, respectively, a vMMN-component could be observed over parietal and occipital electrodes. The vMMN was indeed slightly lateralized, i.e. shifted towards electrodes in the hemisphere contralateral to the simulated self-motion direction. This can be easily seen in Figure S1-4. In order to compare the vMMNs of the two self-motion directions we normalized the data to the maximum value of the MMN-component for each condition.

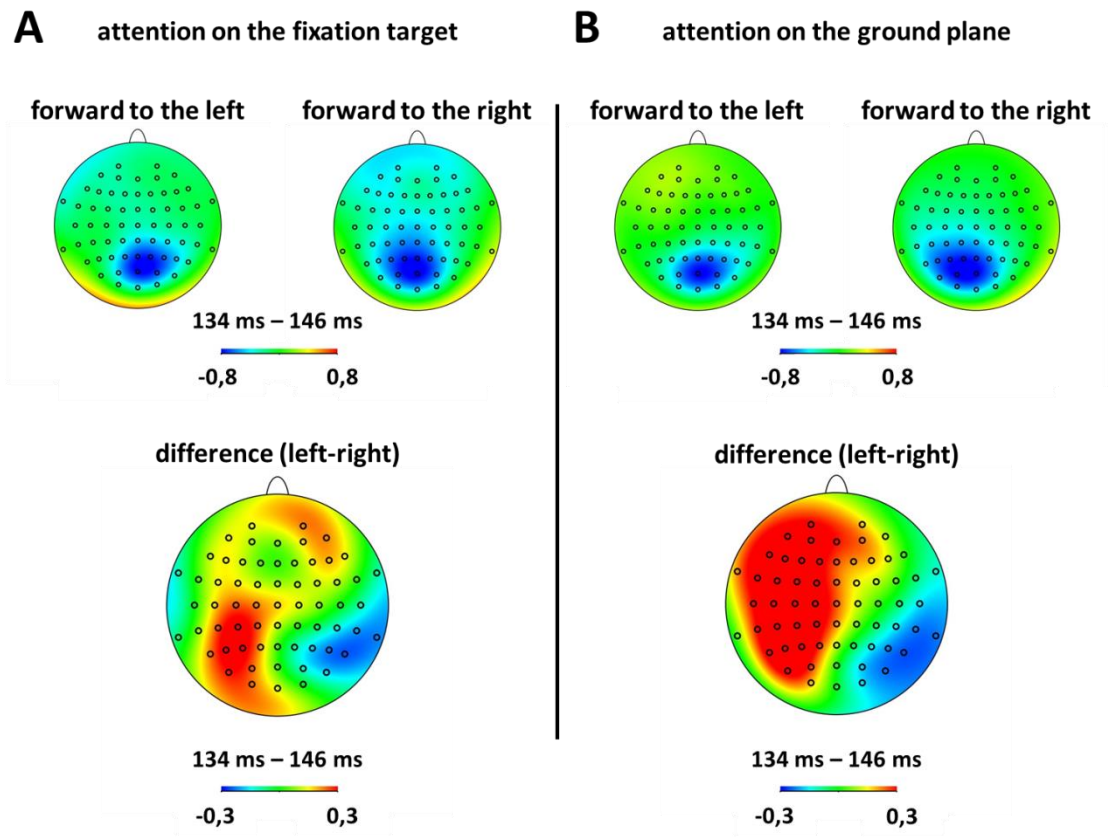

Figure S1-4: Topographic analysis of the difference between MMN-components for the two different headings averaged over all participants. In **A** data collected in trials with "attention towards the fixation target" and in **B** with "attention towards the ground plane" are presented. For both attention conditions time windows from 134 ms to 146 ms after self-motion onset around the peak of the MMNs are displayed. Each topographic map shows the average over 12 ms. The four topographic maps at the top show the MMN-components normalized to the maximum value of each MMN-component. The two topographic maps at the bottom present the differences (heading to the left – heading to the right) between these data sets for each attention condition.

Panels in the upper row show the normalized topographic maps for headings to the left and right in the two attention conditions. Panels in the bottom row show the difference between the maps for a given attention condition. Both different maps show a bi-phasic topography: positive values in the left hemisphere and negative values in the right hemisphere. This bi-phasic pattern is indicative of a lateralized vMMN.

In order to quantify this effect of a stronger contralateral vMMN-component we pooled data from three electrodes each in the left and right hemispheres: electrodes P1, P3 and PO3 over the left hemisphere and electrodes P2, P4 and PO4 over the right hemisphere. We

collapsed data from both hemispheres to obtain two time courses of the vMMN: one for contra- and one for ipsiversive self-motion. This data is presented for the two attention conditions separately. Figure S1-5 A shows data for attention directed towards the fixation target and Figure S1-5 B for attention directed towards the ground plane. In both cases the vMMN-component for contraversive self-motion was significantly more negative than for ipsiversive self-motion (Paired t-tests for VEPs in a time window ranging from 100 ms to 180 ms after motion onset. Attention directed towards the fixation target: $t(10)=-1.83$, $p=0.049$; attention directed towards the ground plane: $t(10)=-5.2$, $p=0.0002$).

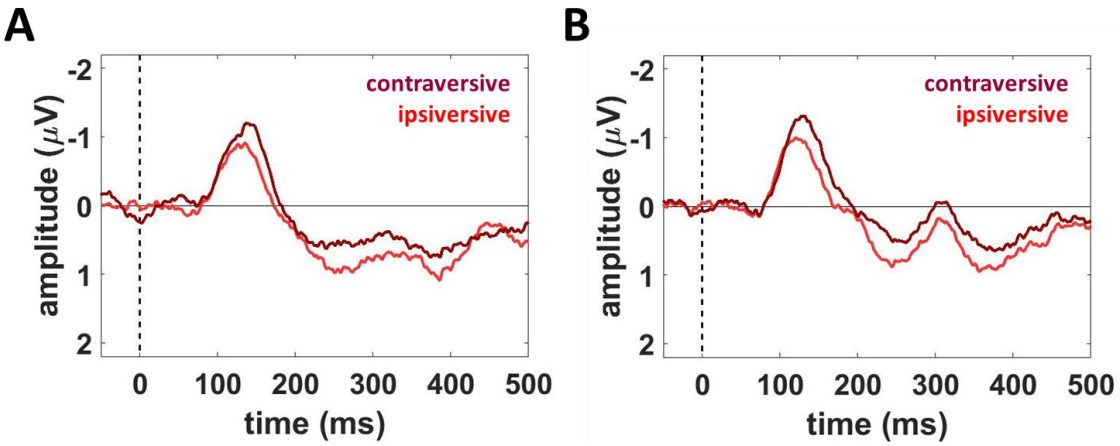

Figure S1-5: Comparison of vMMN-components for contra- and ipsiversive self-motion direction for all participants. In both graphs a time window of 50 ms before to 500 ms after self-motion onset is plotted. In dark red the difference between deviants and standards (deviant-standard) on electrodes contraversive to the self-motion direction is presented and in light red on electrodes ipsiversive to the self-motion direction. Electrodes pooled for a signal on the left hemisphere are P1, P3 and PO3 and for the right hemisphere P2, P4 and PO4. **A** shows data of the condition "attention towards the fixation target" and **B** "attention towards the ground plane".

4.3.5 Discussion

In this study we aimed to determine if the processing of self-motion direction (heading) is in line with the predictive coding framework (Friston, 2018). We recorded human EEG data to test for a visual MMN-component with stimuli simulating forward self-motion. Unlike self-motion processing under natural conditions involving different sensory modalities (e.g. Hlavacka et al., 1996; Angelaki et al., 2011, von Hopffgarten, 2011; Churan et al. 2018),

here, we focused only on visual information (optic flow) typically induced by self-motion. Importantly, the pure visual information during self-motion (optic flow) is sufficient to determine heading (Gibson, 1950; Warren and Hannon, 1988; Lappe et al. 1999; Lich & Bremmer, 2014).

We aligned our data to self-motion onset and investigated the first 500 ms of the resulting event-related potentials (ERPs). Since a stationary ground plane was presented to the participants in each trial before the moving phase, we found the expected visual motion onset stimulus response (Kuba et al., 2007). Of critical importance for our further analysis was the N2-component around 150 ms after self-motion onset. Our results revealed a more negative N2-component for data collected in deviant trials compared with standard trials. Importantly, we only compared data collected after the presentation of physically identical visual stimuli. This was possible because a given heading direction was presented as deviant in half of the trials and as standard in the other trials. The peak time of the MMN as found in our study was at about 140 ms after self-motion onset and hence approximately in the time range of 100 ms to 400 ms as reported earlier (e.g. Kimura, 2012; Czigler, 2014).

There is still an ongoing discussion about the neural basis for this MMN-component. A widely accepted hypothesis suggests the MMN-component and the differences in processing of standard and deviant trials to be based on a prediction error account (Kimura, 2012). A prediction about the upcoming stimulus presentation is formed by extracting a sequential rule from the repeatedly presented standard stimulus. This prediction is compared to the actual appearing stimulus and can have two different outcomes in an oddball experiment. Most likely a standard stimulus (typically and as chosen in our current study, standard stimuli are presented in 80% of the trials, deviants in 20% of the trials) is presented and there is a match between prediction and the actual sensory information. In the less likely case of an unexpected deviant stimulus presentation the prediction is violated and in line with the concept of predictive coding a MMN-component is created as a perceptual prediction error signal (Stefanics, et al., 2014; Friston, 2005). The observed mismatch negativity (MMN) is

indicative of such a sensory prediction error signal (Kimura, 2012; Wacongne, et al., 2012, Qian, et al., 2014; Hesse et al., 2017; Schmitt et al., 2018).

Our study design employed two different attention conditions to further test for the preattentive nature of the MMN (Czigler, 2007). Subjects' attention was either directed towards the fixation target or the ground plane stimulus in order to detect a luminance change. In both cases the task was not related to the feature under study, i.e. the self-motion direction. In 10% of all trials per attention condition the change was displayed and in about half the cases detected. The correct response rates of 52% for "attention towards the fixation target" and 45% for "attention towards the ground plane" reflect the difficulty of the task and thus required focused attention throughout the experiment. These values correspond to a total of 1827 and 1631 true positives in the two attention tasks. The very small number of false-positives (in total 8 for "attention towards the fixation target" and 57 for "attention towards the ground plane") supports this view. The slight difference in correct response rates between the two attention conditions most likely reflect slightly different behavioral task loads, which are not expected to influence the MMN-components. It has been demonstrated before that vMMN is not modulated by task load (Pazo-Álvarez et al., 2004; Kremláček, et al., 2013). We conclude from our data that the exact location of the spatial attention (fixation target vs. ground plane cloud of dots) also does not have an influence on the preattentive and predictive processing of self-motion information.

We could not only find vMMN-components for both attention conditions, but also for the two different heading directions, forward to the left and forward to the right. Topographic analysis of the vMMN-components revealed an occipital-posterior scalp distribution which is in line with previous studies (Kimura, 2012; Qian, et al., 2014). The scalp distribution revealed differences between the two headings. For self-motion to the left the vMMN-component was located more over the right hemisphere and vice versa. Previous studies have reported a larger N2-component over contralateral hemispheres (Pazo-Álvarez, et al., 2004). Yet, while these previous studies employed visual stimuli presented only in one part of the visual field (contralateral or ipsilateral with respect to the EEG electrodes), our stimuli always covered

bilaterally a large part of the visual field (the central 42 degrees) regardless of the self-motion direction. Comparing the vMMN-components pooled over electrodes on either hemisphere resulted in more negative vMMNs for the contraversive self-motion as compared to the ipsiversive. This result of a lateralization of the processing of self-motion direction is fully in line with recent results combining neurophysiology in the monkey with a behavioral study in humans and modeling (Bremmer et al., 2017) as well as with a result employing TMS in humans (Schmitt et al., 2017). In their multi-method study, Bremmer and colleagues could show that saccadic eye movements induce a misperception of heading directions: persisaccadically, heading perception is compressed towards the line of sight. The authors were able to predict this behavioral result in humans based on modeling the processing of self-motion information. This model was based on results from previous cell recordings in two key areas of the monkey visual cortical system, the medial superior temporal area (MST; Bremmer et al., 2010) and the ventral intraparietal area (VIP; Kaminiarz et al., 2014)). The involvement of both areas in the processing of self-motion information has been documented in monkeys (MST: Duffy & Wurtz, 1991; Lappe et al., 1996; Sasaki, et al., 2019; VIP: Bremmer et al., 2002; Shao et al., 2018; for review, see e.g. Britten, 2008) and humans (MST: Huk et al., 2002; VIP: Bremmer et al., 2001). The results from their monkey recordings had shown for the first time that a majority of cells in the right hemisphere of the macaque responded most strongly for self-motion to the left and vice versa (Bremmer et al., 2010; Kaminiarz et al., 2014). Further support for a lateralized processing of self-motion information comes from a recent TMS study in humans (Schmitt et al., 2017). Here, TMS over right cortical area MST in humans induced an impairment (an increase of response variance) of heading perception, but only for leftward heading. This result was, again, predicted from an extended version of the model from Bremmer and colleagues (2017).

Finally, a most recent study from our group employing surface EEG on an awake macaque monkey provides further and additional strong support for preattentive and predictive self-motion processing (Schütz et al., 2018). In this study, stimulus features were chosen as in our current study, but other than in our study, no secondary task was presented. Due to

space limitations on the monkey's head only seven electrodes were positioned on the skin of the monkey, mainly over parietal areas. Similar to the data presented in this study, data collected in oddball trials compared to standard trials revealed a more negative component around 100 ms after self-motion onset, i.e. a vMMN-component. Such difference in latencies of the ERP-components for humans and for nun human primates (NHP), i.e. about 140 ms after stimulus onset vs. 100 ms after stimulus onset, has been reported in previous studies (e.g. Reinhart et al., 2012, Woodman, 2012). Latencies of homologous ERP-components are often about 25% shorter in monkeys than in humans.

Taken together, these previous and our current results strongly suggest that the processing of self-motion information in the primate brain not only is in line with the framework of predictive coding, as indicated by the vMMN, but also lateralized with respect to the heading direction.

4.3.6 References

Amenedo, E., Pazo-Alvarez, P., Cadaveira, F. Vertical asymmetries in pre-attentive detection of changes in motion direction. *International Journal of Psychophysiology*, **64(2)**, 184-189 (2007).

Angelaki, D. E., Gu, Y., DeAngelis, G. C. Visual and vestibular cue integration for heading perception in extrastriate visual cortex. *J Physiol*, **589.4**, 825-833 (2011).

Berti, S. The attentional blink demonstrates automatic deviance processing in vision. *NeuroReport*, **22(13)**, 664-667 (2011).

Bremmer, F., Schlack, A., Shah, N. J., Zafiris, O., Kubischik, M., Hoffmann, K., Zilles, K., Fink, G.R. Polymodal motion processing in posterior parietal and premotor cortex: a human fMRI study strongly implies equivalencies between humans and monkeys. Neuron. **29(1)**, 287-96 (2001).

Bremmer, F., Klam, F., Duhamel, J.-R., Hamed, S. B., Graf, W. Visual-vestibular interactive responses in the macaque ventral intraparietal area (VIP). *European Journal of Neuroscience*, **16**, 1569-1586 (2002).

Bremmer, F., Kubischik, M., Pekel, M., Hoffmann, K.-P., Lappe, M. Visual selectivity for heading in monkey area MST. *Exp. Brain Res.*, **200**, 51-60 (2010).

Bremmer, F., Churan, J., Lappe, M. Heading representations in primates are compressed by saccades. *Nature Communications*, **8:920,** (2017).

Britten, K. H. Mechanisms of self-motion perception. *Annu. Rev. Neurosci.*, **31**, 389–410 (2008).

Churan, J., von Hopffgarten, A., Bremmer, F. Eye movements during path integration. *Physiol Rep*, **6(22)**, e13921 (2018).

Czigler, I. Visual mismatch negativity: violation of nonattended environmental regularities. *Journal of Psychophysiology*, **21**, 224–230 (2007).

Czigler, I., Pató, L. Unnoticed regularity violation elicits change-related brain activity. *Biological Psychology*, **80(3)**, 339-347 (2009).

Czigler, I. Visual mismatch negativity and categorization. *Brain Topogr*, **27**, 590-598 (2014).

Czigler, I., Sulykos, I., File, D., Kojouharova, P., Gaál, Z. A. Visual mismatch negativity to disappearing parts of objects and textures. *PLoSONE,* **14(2)**: e0209130 (2019).

Dokka, K., DeAngelis, G. C., Angelaki, D. E. Multisensory Integration of Visual and Vestibular Signals Improves Heading Discrimination in the Presence of a Moving Object. *The Journal of Neuroscience*, **35(40)**, 113599-13607 (2015).

Duffy, C., Wurtz, R. H., Sensitivity of MST Neurons to Optic Flow Stimuli. I. A Continuum of Response Selectivity to Large-Field Stimuli. *Journal of Neurophysiology*, **65:6** (1991).

Durant, S., Sulykos, I., Czigler, I. Automatic detection of orientation variance. *Neuroscience Letters*, **658**, 43-47 (2017).

Friston, K. A theory of cortical responses. *Philosophical Transactions of the Royal Society B*, **360(1456)**, 815-836 (2005).

Friston, K. Does predictive coding have a future? *Nature Neuroscience*, **21**, 1019-1021 (2018).

Gibson, J. J. The perception of the visual world. *The Riverside Press*, Cambridge, Massachusetts (1950).

Glasauer, S., Stein, A., Günther, A. L., Flanagin, V. L., Jahn, K., Brandt, T. The effect of dual tasks in locomotor path integration. *Ann N Y Acad Sci.*, **1164**, 201-5 (2009).

Hesse, P. N., Schmitt, C., Klingenhoefer, S., Bremmer, F. Preattentive processing of numerical visual information. *Frontiers in human neuroscience*, **11**, 70 (2017).

Hlavacka, F., Mergner, T., Bolha, B. Human self-motion perception during translatory vestibular and proprioceptive stimulation. *Neuroscience Letters*, **210**, 83-86 (1996).

von Hopffgarten, A., Bremmer, F. Self-motion reproduction can be affected by associated auditory cues. *Seeing Perceiving*, **24(3)**, 203-22 (2011).

Huk, A. C., Dougherty, R. F., Heeger, D. J. Retinotopy and functional subdivision of human areas MT and MST. *J Neurosci*. 22(16), 7195-205 (2002).

Kaminiarz, A., Schlack, A., Hoffmann, K.-P., Bremmer, F. Visual selectivity for heading in the macaque ventral intraparietal area. *J Neurophysiol*, **112**, 2470-2480 (2014).

Kimura, M., Schröger, E., Czigler, I., Ohira. H. Human Visual System Automatically Encodes Sequential Regularities of Discrete Events. *Journal of Cognitive Neuroscience*, **22(6)**, 1124-1139 (2010).

Kimura, M. Visual mismatch negativity and unintentional temporal-context-based prediction in vision. *International Journal of Psychophysiology*, **83(2)**, 144-155 (2012).

Kremláček, J., Kuba, M., Kubová, Z., Langrová, J., Szanyi, J., Vít, F., Bednář, M. Visual mismatch negativity in the dorsal stream is independent of concurrent visual task difficulty. *Front. Hum. Neurosci.*, **7:411** (2013).

Kuba, M., Kubová, Z., Kremlácek, J., Langrová, J. Motion-onset VEPs: characteristics, methods, and diagnostic use. *Vision Research*, **47(2)**, 189-202 (2007).

Kuldkepp, N., Kreegipuu, K., Raidvee, A., Näätänen, R., Allik, J. Unattended and attended visual change detection of motion as indexed by event-related potentials and its behavioral correlates. *Frontiers in Human Neuroscience*, **7**, 476 (2013).

Lappe, M., Rauschecker, J. P. An illusory transformation in a model of potic flow processing. *Vision Res*. **35:11**, 1619-1631 (1995).

Lappe, M., Bremmer, F., Pekel, M., Thiele, A., Hoffmann, K.-P. Optic Flow Processing in Monkey STS: A Theoretical and Experimental Approach. *The Journal of Neuroscience*, **16(19)**, 6265–6285 (1996).

Lappe, M., Bremmer, F., van den Berg, A.V. Perception of self-motion from visual flow. *Trends in Cognitive Sciences*, **3:9** (1999).

Li, X., Lu, Y., Sun, G., Gao, L., Zhao, L. Visual mismatch negativity elicited by facial expressions: new evidence from the equiprobable paradigm. *Behavioral and Brain Functions*, **8**, 7 (2012).

Lich, M., Bremmer, F. Self-motion perception in the elderly. *Frontiers in Human Neuroscience*, **8:681** (2014).

Luck, S. J. An Introduction to the Event-Related Potential Technique. 1st Edition, *MIT Press Cambridge, Massachusetts*; London, England, 1-50 (2005).

Maekawa, T., Goto, Y., Kinukawa, N., Taniwaki, T., Kanba, S., Tobimatsu, S. Functional characterization of mismatch negativity to a visual stimulus. *Clinical Neurophysiology*, **116(10)**, 2392-2402 (2005).

Müller, D. et al. Visual Object Representations Can Be Formed outside the Focus of Voluntary Attention: Evidence from Event-related Brain Potentials. *Journal of Cognitive Neuroscience*, **22(6)**, 1179-1188 (2010).

Müller, D., et al. Impact of lower- vs. upper-hemifield presentation on automatic colour-deviance detection: a visual mismatch negativity study. *Brain Research*, **1472**, 89-98 (2012).

Müller, D., Widmann, A., Schröger, E. Object-related regularities are processed automatically: evidence from the visual mismatch negativity. *Frontier in Human Neuroscience*, **7**, 259 (2013).

Näätänen, R., Gaillard, A. W. K., Mäntysalo, S. Early selective-attention effect on evoked potential reinterpreted. *Acta Psychologica*, **42(4)**, 313-329 (1978).

Pazo-Álvarez, P., Amenedo, E., Lorenzo-López, L., Cadaveira, F. Effects of stimulus location on automatic detection of changes in motion direction in the human brain. *Neuroscience Letters*, **371(2-3)**, 111-116 (2004).

Qian, X. et al. The visual mismatch negativity (vMMN): Toward the optimal paradigm. *International Journal of Psychophysiology*, **93(3)**, 311-315 (2014)

Rao R. P., Ballard D. H. (1999): Predictive coding in the visual cortex: A functional interpretation of some extra-classical receptive-field effects. *Nat Neurosci.,* **2**, 79–87 (1999).

Reinhart, R. M. G., Heitz, R. P., Purcell, B. A., Weigand, P. K., Schall, J. D., Woodman, G. F. Homologous mechanisms of visuospatial working memory maintenance in macaque and human: Properties and sources. *J Neurosci.*, **32(22)**, 7711-7722 (2012).

Royden, C. S., Banks, M. S., Crowell, J. A. The perception of heading during eye movements. *Nature*, **360** (1992).

Sasaki, R., Angelaki, D. E., DeAngelis, G. C. Processing of object motion and self-motion in the lateral subdivision of the medial superior temporal area in macaques. *Journal of Neurophysiology,* **121**, 1207-1221 (2019)

Schmitt, C., Klingenhoefer, S., Bremmer, F. Preattentive and predictive processing of visual motion. *Sci Rep.*, **8(1)**:12399 (2018).

Schmitt, C., Baltaretu, B. R., Crawford, J. D., Bremmer, F. TMS-induced disturbance of self-motion perception in humans. Program No. 685.09. 2017 Neuroscience Meeting Planner. Washington, DC: Society for Neuroscience, 2017. Online.

Schütz, A., Schwenk, J., Schmitt, C., Kaminiarz, A., Werner, B.-O., Churan, J., Bremmer, F. Preattentive processing of visually simulated self-motion in humans and monkeys. Program No. 220.01. 2018 Neuroscience Meeting Planner. San Diego, CA: Society for Neuroscience, 2018. Online.

Shao, M., DeAngelis, G. C., Angelaki, D. E., Chen, A. Clustering of heading selectivity and perception-related activity in the ventral intraparietal area. *J Neurophysiol*, **119**, 1113-1126 (2018).

Stefanics, G., Kimura, M., Czigler, I. Visual mismatch negativity reveals automatic detection of sequential regularity violation. *Frontiers in Human Neuroscience*, **5**, 46 (2011).

Stefanics, G., Csukly, G., Komlósi, S., Czobor, P., Czigler, I. Processing of unattended facial emotions: A visual mismatch negativity study. *NeuroImage*, **59(3)**, 3042-3049 (2012).

Stefanics, G., Kremlácek, J., Czigler, I. Visual mismatch negativity: a predictive coding view. *Frontiers in Human Neuroscience*, **8**, 666 (2014).

Stefanics, G., Heinzle, J., Horváth, A. A., Stephan, K. E. Visual mismatch and predictive coding: a computational single-trial ERP study. *J. Neurosci.*, **38(16)**, 4020-4030 (2018).

Sulykos, I., Czigler, I. One plus one is less than two: Visual features elicit non-additive mismatch-related brain activity. *Brain Research*, **1398**, 64-71 (2011).

Thierry, G., Athanasopoulos, P., Wiggett, A., Dering, B., Kuipers, J-R. Unconscious effects of language-specific terminology on preattentive color perception. *PNAS*, **106(11)**, 4567-4570 (2009).

Urban, A., Kremlácek, J., Masopust, J., Libiger, J. Visual mismatch negativity among patients with schizophrenia. *Schizophrenia Research*, **102(1-3)**, 320-328 (2008).

Van den Berg, A. V., Beintema, J. A. Motion templates with eye velocity gain fields for transformation of retinal to head centric flow. *NeuroReport*, **8**, 835-840 (1997).

Wacongne, C., Changeux, J.-P., Dehaene, S. A neuronal model of predictive coding accounting for the mismatch negativity. *Journal of Neuroscience*, **32(11)**, 3665-3678 (2012).

Wall, M. B., Smith, A. T. The Representation of Egomotion in the Human Brain. *Current Biology*, **18**, 191–194 (2008).

Wang, S. et al. ERP comparison study of face gender and expression processing in unattended condition. *Neuroscience Letters*, **618**, 39-44 (2016).

Warren, W. H., Hannon, D. J. Direction of self-motion is perceived from optical flow. *Nature*, **336** (1988).

Winkler, I., Czigler, I. Evidence from auditory and visual event-related potential (ERP) studies of deviance detection (MMN and vMMN) linking predictive coding theories and perceptual object representations. *International Journal of Psychophysiology,* **83**, 132-143 (2012).

Woodman, G. F. in The Oxford handbook of event-related potential components, Homologues of human event-related potential components in nonhuman primates, eds Luck, S. J., Kappenman, E. (Oxford UP, New York), 611-625 (2012).

Yan, T., Feng, Y., Liu, T., Wang, L., Mu, N., Dong, X., Liu, Z., Qin, T., Tang, X., Zhao, L. Theta Oscillations Related to Orientation Recognition in Unattended Condition: A vMMN Study. *Front. Behav. Neurosci.,* **11:166** (2017).

Yu, M., Mo, C., Zeng, T., Zhao, S., Mo, L. Short-term trained lexical categories affect preattentive shape perception: Evidence from vMMN. *Psychophysiology*, **54(3)**, 462-468 (2017).

Study II:

TMS-induced disturbance of self-motion perception in humans

Constanze Schmitt, Bianca R. Baltaretu, J. Douglas Crawford and Frank Bremmer

In preparation

4.4 Study II: TMS-induced disturbance of self-motion perception in humans

4.4.1 Abstract

Accurate perception of one's direction of self-motion is of utmost importance during everyday life. Previous neurophysiological studies in the animal model (macaque monkey) and human imaging studies have provided clear evidence for an involvement of cortical regions in the primate brain in the encoding of self-motion, one of them the macaque medial-superior temporal area (MST) and its human functional equivalent, hMST. In a recent study (Bremmer et al., 2017) combining monkey neurophysiology, human psychophysics and computational modeling we showed that saccadic eye movements modulate heading representations. Using those computational modeling results, we predict here a direction-specific increase of response variance in heading perception for transcranial magnetic stimulation (TMS) upon area hMST.

We presented eight human participants with an optic flow stimulus simulating forward self-motion across a ground plane in one of three directions. Participants had to indicate perceived heading direction. In 57% of the trials TMS pulses were applied, centered on self-motion onset. TMS stimulation site was either right-hemisphere hMST, which we identified using an fMRI localizer, or a control area located 1.5 cm posterior to hMST.

TMS over area hMST increased response variance of perceived heading. As predicted by our model, this result was strongest for simulated self-motion to the left (contraversive). This contraversive specificity was absent from TMS over the control area. Our results provide further strong evidence for a critical role of primate area MST for visually-guided navigation.

4.4.2 Introduction

Successful navigation through an environment is based on the integration of visual, vestibular, tactile and auditory information (e.g. Hlavacka et al., 1996; Angelaki et al., 2011, von Hopffgarten, 2011; Churan et al. 2018). Numerous experimental and theoretical studies have shown that the visual optic flow resulting from self-motion can be used to determine the direction of one's self-motion (heading. e.g. Gibson, 1950; Warren and Hannon, 1988; Lappe et al. 1999; Lich & Bremmer, 2014). As pointed out already by Gibson (1950), the direction of self-motion is indicated by the so-called focus-of-expansion, the singularity of the optic flow field. Yet, this is only true under static conditions, i.e. with fixed gaze during linear translation. Under natural conditions, however, head and eye movements as well as object motion in the environment impose changes to the optic flow field (eye and head motion: e.g. Royden et al. 1992; Lappe & Rauschecker, 1995; Banks et al.1996; van den Berg and Beintema, 1997; Lappe et al. 1999, object motion: Dokka, et al., 2015).

Over the last three decades, neurophysiological studies in the animal model of human sensorimotor processing, the macaque monkey, have revealed mainly two cortical regions being significantly involved in the encoding of self-motion information: the medial superior temporal area (area **MST**) (Saito et al., 1986; Duffy and Wurtz 1991; Lappe et al., 1996; Gu et al., 2006; Bremmer et al., 2010) and the ventral intraparietal area (area **VIP**) (Bremmer et al. 2002; Schlack et al., 2002; Chen et al., 2011; Kaminiarz et al., 2014; Shao et al., 2018). Functional equivalents of both areas have been identified in humans (hMST: Huk et al., 2002; VIP: Bremmer et al., 2001) and their involvement in the encoding of self-motion information in humans has been documented (e.g. Morrone et al., 2000; Wall and Smith, 2008).

In systems neuroscience, recordings of neural activity typically reveal correlations between activation patterns in certain brain areas and sensory stimulation. Yet, they do not allow testing for a causal involvement of these brain regions for an observable behavior. As a noninvasive technique, transcranial magnetic stimulation (TMS) has been used to provide

evidence for such a causal relationship (e.g. Taylor & Thut, 2012 for review). TMS can transiently disturb the activity in specific brain regions (Rossi et al., 2009) and a TMS-induced modulation of behavioral performance is typically considered evidence for a critical involvement of the brain region under study for that behavior.

Bremmer and colleagues recently provided evidence for a strong modulation of heading representations due to saccadic eye movements (Bremmer et al., 2017). Saccades are known to disturb visual processing (for review see e.g. Ross et al., 2001; Binda & Morrone, 2018). In their study, Bremmer and colleagues had recorded neural activity from monkey areas MST and VIP during presentation of self-motion stimuli and concurrent reflexive slow and fast eye movements (saccades). A network model trained to decode heading from neuronal discharges, performed veridical during slow eye-movements. Yet, it erroneously reported compression of heading towards straight-ahead across saccades. This result from neurophysiological recordings in the monkey and a computational approach led Bremmer and colleagues hypothesize an as yet unknown visual illusion, i.e. a saccade-induced compression of perceived heading, which was confirmed in a follow-up experiment in humans. The cross-link between neurophysiology in monkeys and observable behavior in humans via a neural network model allowed an in-depth analysis of the underlying neural processes. The analysis revealed that the compression of perceived heading could not be due to a global effect of saccadic suppression, a well-known phenomenon shown behaviorally (Burr et al., 1994) and at the neural level (Bremmer et al., 2009). Instead, compression was most likely to occur due to a balanced suppression of highly active neurons and a slightly delayed release-from-inhibition from another sub-population of neurons. Response properties of primate areas MST and VIP were found to be consistent with being the substrate of this newly described visual illusion.

On-line TMS (delivered during behavior), like saccades, induces a phasic perturbation of neural activity. Here, based on an extension of the above described heading model, we hypothesized that TMS should lead to a disturbance, i.e. greater variance in the perception of heading. Importantly and due to an overrepresentation of contraversive heading in

(macaque) areas, MST and VIP, respectively, this greater perceptual variance should only occur for headings contraversive with respect to the site of TMS stimulation. We employed structural and functional magnetic resonance imaging (fMRI)-guided TMS to stimulate the human functional equivalent of macaque area MST (hMST) and a control area about 1.5 cm posterior of area hMST. We hypothesized a TMS-induced diminished heading performance for stimulation over hMST but not over the control area and for a no-stimulation condition.

4.4.3 Materials and Methods

4.4.3.1 Participants

Eight subjects participated in our study (6 female, 2 male, mean age: 22 years, ranging from 20 to 31). The participants had normal or corrected to normal vision. fMRI data was collected on a single day. TMS data was collected on one, two or four days depending on the individual availability of our participants. Participants were compensated with 25 Canadian dollar per hour for the fMRI experiment and 20 Canadian dollar per hour for the TMS experiment. Our study was in line with the Declaration of Helsinki and approved by York University Human Participants Review Committee within the context of the York Senate Policy on Research Ethics. Prior to each part of the experiment, participants provided written informed consent. The participants did not report any side effects attributed to the TMS besides the feeling of some discomfort during the stimulation.

4.4.3.2 Functional localizer

We aimed to stimulate area hMST because of its potential role for the processing of self-motion information (Gu et al., 2010; Bremmer et al., 2017). Therefore, we aimed to determine the exact location of area hMST as well as an appropriate control area on a subject-by-subject level. Based on the results of the study by Dessing and colleagues (Dessing et al., 2013) we chose a control area spatially close to area hMST. By doing so, participants were not able to distinguish between the two TMS stimulation sites, i.e. area hMST and the control

site, based on the tingling skin sensation induced by TMS. We analyzed the fMRI data in two steps. First we aimed to identify areas sensitive to visual motion. These include area hMST, but also other areas like area hMT (Wall and Smith, 2008) and the functional equivalent of macaque area VIP (Bremmer et al., 2001). In order to narrow down our region of interest to area hMST, we determined in a second step the part of the human MT/MST complex that responded not only to visual stimulation in the contralateral part of the visual field (hMT), but also to stimulation in the ipsilateral part of the visual field (hMST) (Dukelow et al., 2001; Smith et al., 2006).

4.4.3.3 Setup

Once participants felt comfortable with the requirements of the localizer task, they were asked to lie flat on the MRI table. They were then fit with a 20-channel head coil. A head-mounted apparatus containing a mirror was then placed above the coil in order to reflect images from the screen in the MRI bore, along with a head-mounted eye tracker (to track right eye movement). Head motion and eye movement were inspected offline.

4.4.3.4 Localizer Stimulus

To identify our regions-of-interest (ROIs), we presented a stimulus based on previous studies to identify motion specific areas (Dukelow et al., 2001). The localizer stimulus consisted of a central fixation target and random white dots in a circular field with a radius of 8° diameter either on the left or the right of the fixation target on a black background (Figure S2-1 A). Every trial consisted first of a moving and second of a stationary phase which lasted for 16 s each. In the moving phase a 100% coherent expansion and contraction movement of all the dots was presented with expansion and contraction alternating every second. In the stationary phase the dots were stationary within the circular aperture. We presented 8 trials per block and 2 blocks per participant. In one block the dots were on the left side of the fixation target, in the other block they were on the right side of the fixation target.

The main task of the participants was to fixate the central target: a bullseye with a white surrounding circle, a black inner circle and a dot in the middle that changed contrast every 0.5 s. We added a counting task to keep participants interested in the stimulus. The inner dot of the fixation target changed randomly between three different grey values, black and white throughout the experiment. Participants had to count how often the fixation target was white. It happened between 5 and 15 times per block. After each block they reported this number verbally.

4.4.3.5 Imaging

We collected imaging data at York University (Toronto, ON, Canada), using the 3.0 Tesla MRI scanner (Siemens Magnetom TIM Trio, Erlangen, Germany). We acquired functional data using an echo-planar imaging sequence (repetition time [TR] = 2000 ms; echo time [TE] = 30 ms; flip angle [FA] = 90°; field of view [FOV] = 240 mm, matrix size: 80 x 80 with an in-slice resolution of 3 mm x 3 mm; slice thickness= 3.5 mm, no gap). These parameters were the same for each of the two blocks per participant. Data were collected in an interleaved and ascending order. Thirty-three slices were obtained for each volume; 210 volumes were collected in total. In each experimental session, a T1-weighted anatomical reference volume was obtained using an MPRAGE sequence (TR = 2300 ms; FA = 9°; voxel size = 1 x 1 x 1 mm^3). For each volume of anatomical data, 192 slices were collected.

4.4.3.6 Analysis

Preprocessing

In a first step, we screened the functional data for head movements that would produce artifacts. To do this, slice scan time correction (cubic spline), temporal filtering (to remove frequencies <2 cycles/run), and 3D motion correction (trilinear/sinc) were applied to the data (BrainVoyager QX 2.8, Brain Innovation). Volumes that showed (abrupt) movements greater than 2 mm were removed from our data set as confound predictors. Data that remained after

preprocessing was then coregistered via gradient-based affine alignment (translation, rotation, and scale affine transformation) to the raw anatomical data. We, then, applied spatial smoothing using an FWHM of 8 mm to the data.

fMRI analysis

For each participant's data, we used a general linear model (GLM) with 5 predictors. There was a predictor for each of our four conditions ("movement_right", "stationary_right," "movement_left", "stationary_left"). Each of these predictors had a duration of 16 s or 8 volumes. The fifth predictor was a baseline predictor at the beginning of each block. It lasted for 10 s or 5 volumes. A standard hemodynamic response function (HRF; Brain Voyager QX's default double-gamma HRF) was convolved with the predictor variables using a rectangular wave function. GLMs were modified to ensure that confound predictors were included for trials in which there was excessive head motion. If more than 50% of the trials in a single run were modeled by a confound predictor, then that entire run was excluded from further analysis.

4.4.3.7 Control condition (C1)

Our selection of the control area was based on two boundary conditions. First, the control area must not have been activated by the visual stimulus. This argued for an area remote from the stimulation site. Second, based on findings reported by Dessing and colleagues (Dessing et al., 2013), the control area should be located close to the stimulation site. Their conclusion was drawn from the fact that subjects experience tactile sensations from TMS stimulation. If target and control areas are located closely enough, the tactile sensations induced by the TMS pulses in the two stimulation conditions (target vs. control) do not differ and, hence, should not differently affect the TMS-induced modulation of visual processing. Based on these two boundary conditions, we decided to stimulate a location about 1.5 cm posterior to the area we identified as hMST.

4.4.4 Behavioral/TMS

4.4.4.1 Setup

Participants sat on a chair in a darkened room. We used individually formed bite bars for each participant made of dental compound to stabilize the head in front of the center of the screen (Heuer et al., 2016). Self-motion stimuli were back projected on the screen (185 cm wide and 140 cm high) 54 cm away from the participant's eyes. The refresh rate of the projector was set to 60 Hz and the resolution to 1280 x 960 pixels. Participants used the number pad of a normal computer keyboard to type in their responses (for the exact task: see below).

An Eyelink 2 system (SR Research, ON, Canada) was used to control for the participant's eye movements. The Eyelink data was analyzed online and trials in which participants did not maintain fixation on the central target were aborted and repeated later in the experiment.

4.4.4.2 Neuronavigation

During the experiment we constantly controlled the position of the TMS coil so we could stimulate the regions of interest as accurately as possible. We used the Brainsight TMS software (Brainsight TMS, Rogue Research Inc, Montreal, Canada).

Prior to a TMS session, first, we loaded the anatomical fMRI scans we collected in the localizer stimulus session and determined the axis from the anterior to the posterior commissure (AC-PC). Next, the skin was reconstructed and we set landmarks (the tip of the nose, the nasion and the left and right ear) for the calibration of our tracking system. The predefined locations for the areas we wanted to stimulate (Table S2-1) were marked in the program.

Before the start of each TMS session we calibrated the location of the TMS coil and the landmarks on the participant's head using the Brainsight motion tracker system.

S1	hMST (41,-69,4)	Control (33,-79,4)
S2	hMST (49,-62,-2)	Control (38,-73,-2)
S3	hMST (48,-60,1)	Control (39,-71,1)
S4	hMST (39,-63,7)	Control (29,-80,10)
S5	hMST (42,-61,4)	Control (36,-78,4)
S6	hMST (42,-67,-3)	Control (29,-82,-3)
S7	hMST (42,-67,6)	Control (31,-85,4)
S8	hMST (43,-56,-2)	Control (33,-76,-2)
Mean (SD)	hMST (43(3),-63(4),2(4))	Control (34(4),-78(5),2(4))

Table S2-1: Talairach coordinates of area hMST and the control area (for control condition C1) for each participant as identified by the localizer stimulus.

Visual feedback was provided to the experimenter during the whole experiment which showed the 3D distance between a vector through the center of the figure of eight coil and the regions of interest. This image could only be seen by the experimenter on a dimly lit monitor. The TMS coil was connected to an adjustable holding device to reduce the weight. During the experiment the coil was positioned and held manually by the experimenter above the head of the participant to stimulate the regions of interest as accurately as possible.

4.4.4.3 Experimental Stimulus

In the behavioral and TMS part of our study we presented a stimulus simulating self-motion across a ground plane made of white random dots in otherwise darkness. The location of the fixation target was on the vertical meridian, slightly above the horizon. Each trial consisted of three phases. The first lasted between 1200 ms and 2000 ms and showed the stationary ground plane. The immediately following second phase (50 ms) simulated a forward self-motion into one of three directions (Figure S2-1 B): 30° to the left, straight-ahead, or 30° to the right. In the third phase, right after the movement, we presented a ruler with random numbers which was used to identify the perceived heading (Kaminiarz et al., 2007).

Later we defined as individual baselines for the different participants the mean values of the single trial responses separately for the three different headings and subtracted the single trial data from these values (per participant and per self-motion direction). In 57% of all trials, three TMS pulses (300 ms, 10 Hz) were delivered. We stimulated in half of the TMS trials over right-hemisphere hMST (targetTMS (T)), in the other half of the TMS trials over the control site (first control condition, C1), also over the right hemisphere. The TMS pulses were centered in time on self-motion onset and all three equally spaced by dt=100 ms. The first pulse was always aligned to 100 ms before self-motion onset.

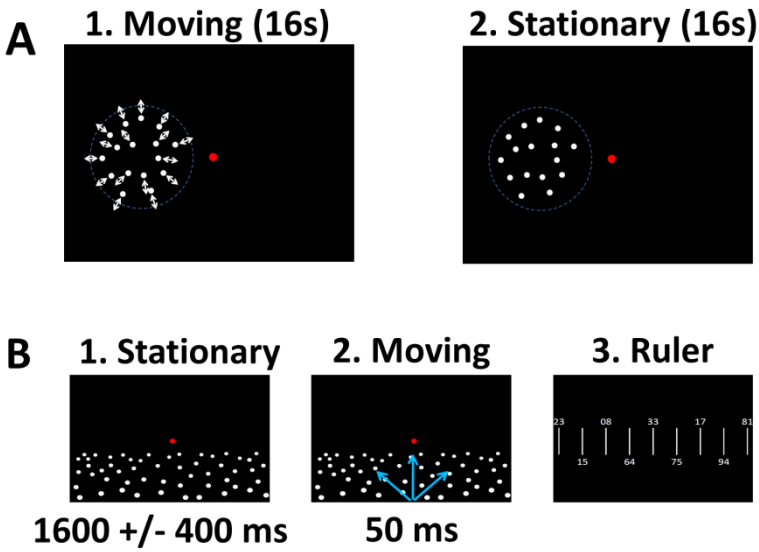

Figure S2-1: Functional localizer and behavioral/TMS stimulus. In **A** the stimulus for the functional localizer is plotted. It consisted of two phases. First, in a moving phase white dots were moving radially in and outwards (1 s for each movement direction) for 16 s on a black background. In the second, the stationary phase, the dots were just displayed without movement for 16 s. There was always a fixation target displayed in the middle of the screen, which changed between three different grey levels, black and white. Here we potted only the case for visual stimulation left of the fixation target, but in a second block the same stimulus was presented with the dots right of the fixation target. In **B** we present the stimulus for the behavioral and TMS part or this study. In a first stationary phase a ground plane consisting of white random dots was displayed on a black background. In the second, the moving phase, self-motion (blue arrows) to one of three headings (30° to the left, straight forward, 30° to the right) was simulated by moving the dots for 50 ms. In the third phase a ruler stimulus was presented to respond the perceived self-motion direction. It showed lines which were one degree apart and random numbers alternating above and below each line.

We collected data from 12 blocks and presented 21 trials in each block. In each block we presented pseudorandomized 12 TMS trials and 9 control trials without TMS, our second control condition, C2. In a given block, only one area was stimulated using the TMS coil. In the no-TMS trials the TMS coil remained over the area that was stimulated in the same block, but no pulse was delivered.

4.4.4.5 Experimental Task

During the trials, participants were asked to fixate the central target. Trials with eye movements or blinks were not included in our analysis.

In the third phase of each trial, i.e. after the movement phase, participants had to report the number on the ruler stimulus that was closest to their perceived heading by using a regular keyboard. The numbers of the ruler stimulus were one degree apart and shown in different random order in each trial.

4.4.4.6 TMS Session Protocol

For our experiment we used a Magstim Rapid^2 (Magstim, UK) figure-of-eight coil for the TMS part. The motor threshold was identified for each participant before the experiment (mean for all eight participants: 65% of the maximum stimulator output) by stimulating over the hand motor area. The resting motor threshold was defined as smallest output value that still induced a visible finger movement in 3 out of 6 cases (Rossini et al., 1994). In the experiment we stimulated with 110% of each participant's threshold. All our stimulation parameters were within the safety limits (Rossi et al., 2009). Some participants reported a slight discomfort during the TMS stimulation, which might have occurred because we also stimulated nerves or neck muscles. Throughout the experiment the participants as well as the experimenter wore earplugs to dampen the discharging noise of the TMS coil.

4.4.4 Results

4.4.4.1 fMRI localizer data

In order to be as precise as possible in delivering the TMS pulses over the human functional equivalent of macaque area MST (hMST, Huk et al., 2002), participants took part in a functional magnetic resonance imaging (fMRI) localizer task. We chose the TMS stimulation sites based on individual fMRI scans. Figure S2-2 shows the functional data of one representative participant. In color we marked the areas which were activated by the self-motion stimulus ($p<0.05$). Different colors indicate data from the two different presentation conditions, i.e. visual motion only in the left (activation shown in blue) or right (activation shown in yellow) part of the visual field. We identified area hMST in each participant as part of the human motion complex activated not only by contra-, but also ipsilateral stimulation (Dukelow et al., 2001).

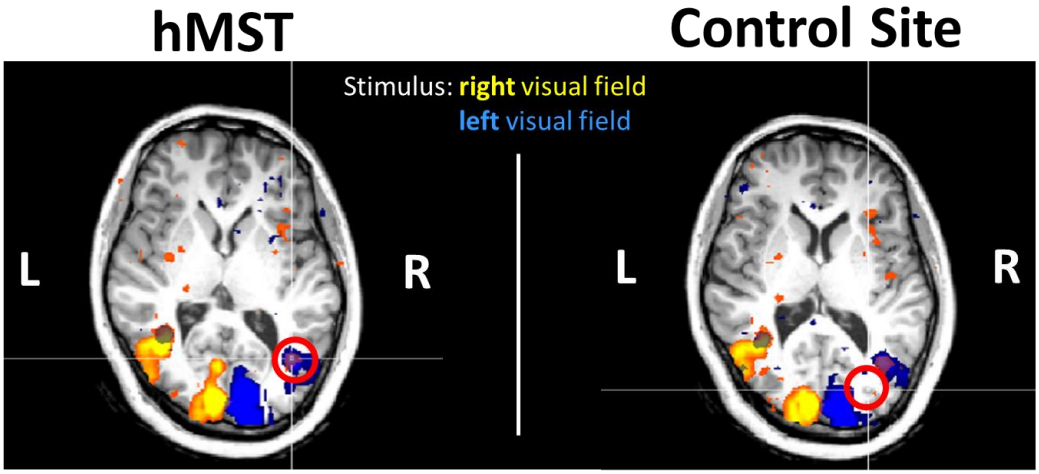

Figure S2-2: Functional localizer data of one representative participant. Two axial plane slices of a functional scan of one participant are plotted. In the left slice we marked area hMST with a red circle and in the left slice the control site. Both TMS stimulation sites are in the right hemisphere. We colored the voxels which show a significant difference between the two phases “moving” and “stationary”. In yellow data collected in sessions with stimulus presentation on the right half of the monitor and in blue data from stimulus presentation on the left side of the monitor are presented.

The exact Talairach coordinates for all the participants can be found in Table S2-1. Values were in line with previous studies identifying human area MST (Dukelow et al., 2001; Cardin et al., 2012). Table S2-1 also reports the exact coordinates of each participant's control area, which we stimulated in our first control condition (C1).

4.4.4.2 Model-based hypothesis

Here we present the predictions of a model proposed by Bremmer et al., (2017) based on their study of the influence of saccades on the representation of headings in primates. A linear-decoder model predicted a compression of perceived heading, which could be confirmed in a follow-up behavioral study in humans. An in-depth analysis of the decoder, which was designed after neurophysiological data recorded from the monkey (Bremmer et al., 2010; Kaminiarz et al., 2014), revealed that this perceptual compression was most likely due to a saccade-induced modulation of neuronal firing rates: cells responding strongly for the self-motion stimulus (preferred direction) were peri-saccadically suppressed. On the other hand, cells which were inhibited by the self-motion stimulus (non-preferred direction) revealed a (delayed) release-from-inhibition. Importantly, the neurophysiological data showed a strong overrepresentation of neurons from a given cortical hemisphere with preference for contraversive heading (Greenlee et al., 2016). In our current work, we extended this model and simulated TMS as a disturbance of neural activity. More specifically, with TMS to be applied over only one hemisphere, we assumed to influence mostly neurons being responsive for contraversive heading. We modeled the influence of TMS as inducing noise, i.e. as inducing suppression and enhancement of neural activity at an equal proportion of neurons (Hallett, 2007).

We implemented a neural network model of 1000 neurons with biologically plausible activity profiles (Bremmer et al., 2017). The effect of TMS was modeled to occur at t=0 ms. Decoded heading was close to veridical for all three simulated self-motion directions and did not reveal a TMS-induced modulation (Figure S2-3A). Likewise, the relative compression, defined as

the normalized standard deviation of the three decoded headings, was invariant across the whole time-course of simulated activity (Figure S2-3B). The temporal profile of the simulated suppression and enhancement is shown in Figure S2-3C. The profile of suppression was modeled after neurophysiological data (Bremmer et al., 2017).

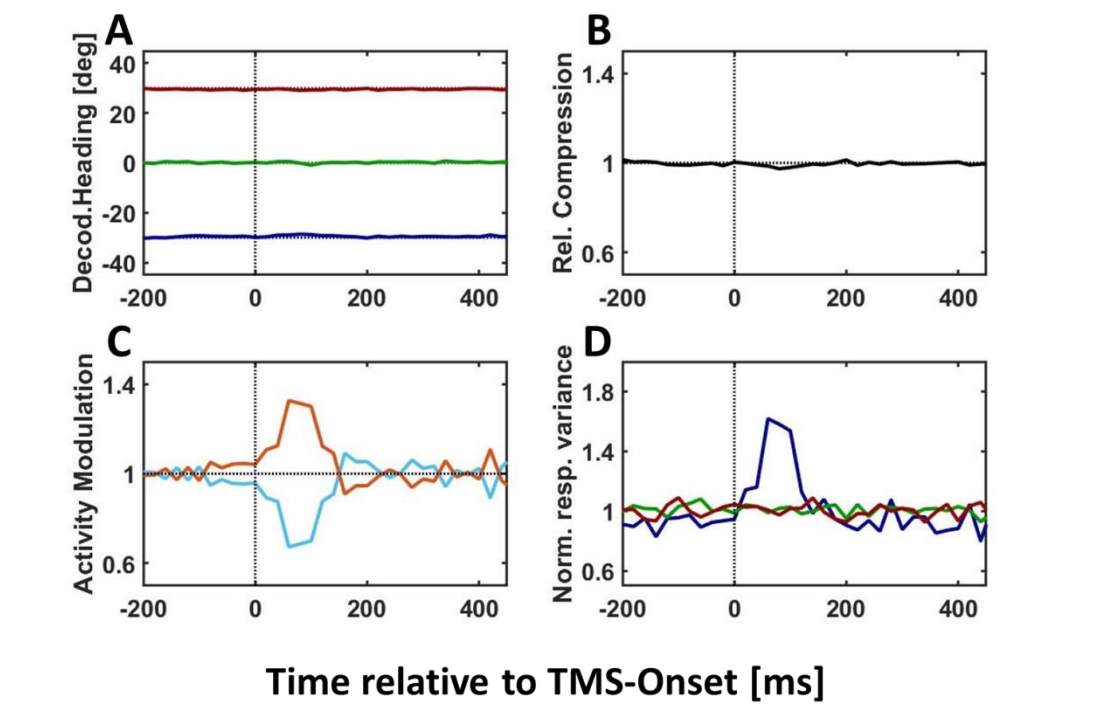

Figure S2-3: Time resolved model prediction for a virtual population of neurons. All four graphs depict a time window from 200 ms before to 450 ms after TMS onset at 0 ms. **A** shows the decoded heading in blue for self-motion 30° to the left, in green for self-motion straight forward and in red for self-motion 30° to the right. In **B** we plotted the relative compression. It was calculated as the normalized standard deviation of the three decoded headings. **C** shows the activity modulation. In light blue the suppression and in orange the enhancement modeled as the "mirror-image" of the suppression. **D** presents the effect of the TMS pulse as normalized variance of the decoded heading: in blue for heading 30° to the left, in green for straight forward and in red for the heading 30° to the right.

The enhancement was modeled as the "mirror-image" of the suppression. The result of this simulated TMS is shown in Figure S2-3D. It depicts the time courses of the normalized variance of decoded heading for the three simulated heading directions. While decoded heading was rather constant over time for simulated heading to the right and straight-ahead, it was clearly modulated resulting in a larger variance for heading to the left (i.e.

contraversive, assuming TMS over right hMST). Accordingly, for our behavioral experiment we predicted a disturbed heading perception only for contraversive heading, as indicated by a greater variance of the subjects' heading perception.

4.4.4.3 Behavioral and TMS data

In the behavioral part of our study we investigated the heading perception of our participants across TMS stimulation. In a given trial, subjects were presented optic flow stimuli simulating self-motion across a ground plane in one of three directions (30° to the left, straight-ahead or 30° to the right). At the end of each trial participants were presented a ruler stimulus and had to indicate the number which represented their self-motion direction via keyboard input. We excluded trials from further analysis in which a rightward self-motion was presented but the participants reported leftward self-motion and vice versa (approx. 1.2% of trials). We also excluded trials in which numbers were typed which were not shown in the ruler stimulus (approx. 0.3% of trials). In total for all participants we excluded 30 out of 2016 trials (1.5%). Single responses were also excluded from further analysis for each participant if the values differed from the mean of all the responses in the same condition for more than three times the standard deviation (about 3% of all trials). We assumed that in such case participants most likely made a typo error while typing in the response number.

Figure S2-4 shows the perceived heading data for one representative participant (participant 05). The three panels depict results from the three different stimulation conditions: A) TMS over hMST (targetTMS (T)), B) first control condition (C1): TMS over the control area, and C) second control condition (C2): no TMS. Due to the fact that the two stimulated sites (hMST and Control area) were so close together, the TMS-induced tactile sensations at the two sites did not feel different for the participants. Finally, we combined the data collected in all no TMS trials during which the coil was kept over the different stimulation sites for each presented heading direction. In the panels, each dot depicts the percept of the participant in a given trial. We calculated the mean of all responses separately for the three different self-

motion directions and plotted theses values as colored solid lines (data for rightward self-motion in red, for straight-ahead self-motion in green and for leftward self-motion in blue). In the condition “TMS over hMST”, the single trial responses varied the most from the calculated mean and, hence, showed the largest variance for self-motion to the left, less so for self-motion to the right and almost no variance for self-motion straight forward.

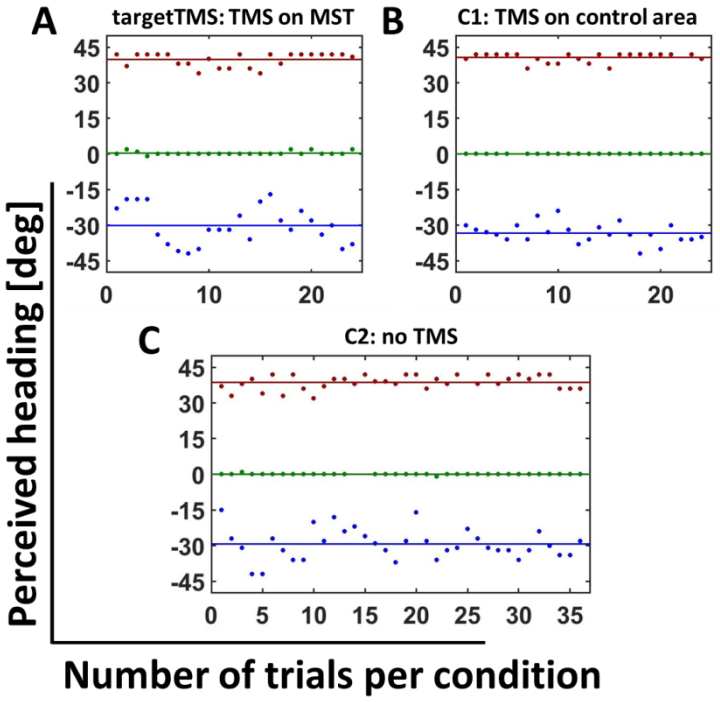

Figure S2-4: Perceived headings of one participant. In red data recorded in trials with a self-motion stimulus 30° to the right are presented, in green for self-motion straight forward (0°) and in blue for self-motion 30° to the left. The perceived headings are plotted in degrees with headings to the left with negative values and 0° as straight forward. We show the response data of one participant. Each dot represents the reply after one trial. The mean of all these single trial responses is plotted as a line for each direction and condition. **A** shows the data recorded after stimulation of area hMST (targetTMS (T)), **B** the data recorded in control condition 1 (stimulation of the control area) and **C** shows the data of control condition 2 (no TMS stimulation).

Importantly and in line with our model-based hypothesis, TMS over hMST did not shift the overall perception of heading. In other words, regardless of the simulated self-motion direction, average values of the responses for a given self-motion direction in the TMS condition were not significantly different from those in the two control conditions (participant 05: ANOVA with the responses of the participant; no significant main effect for stimulation

condition: F(2.0, 238)=0.23, p=0.8). Different from simulated self-motion to the left and straight-ahead, this participant overestimated heading to the right by about 12 degrees, irrespective of the stimulation condition. As in Bremmer et al. (2017), overall accuracy of heading perception varied across subjects and, as shown in the example above, sometimes even within subjects for the different heading directions. Accordingly, for our population analysis, we normalized data per subject and heading direction. Figure S2-5 shows the variance of the heading perception across all subjects and heading directions for the three different experimental conditions, i.e. (i) TMS over MST (targetTMS (T)), (ii) TMS over the control area (control condition 1, C1), and (iii) no TMS (C2). Darker colors indicate data from stimulation trials (hTMS and C1), while lighter colors indicate data from trials without TMS (C2). Consistent with the single participant data in Figure S2-4 the variance for simulated self-motion directed straight-ahead showed the smallest values. The variances for the self-motion direction to the right and to the left had larger values.

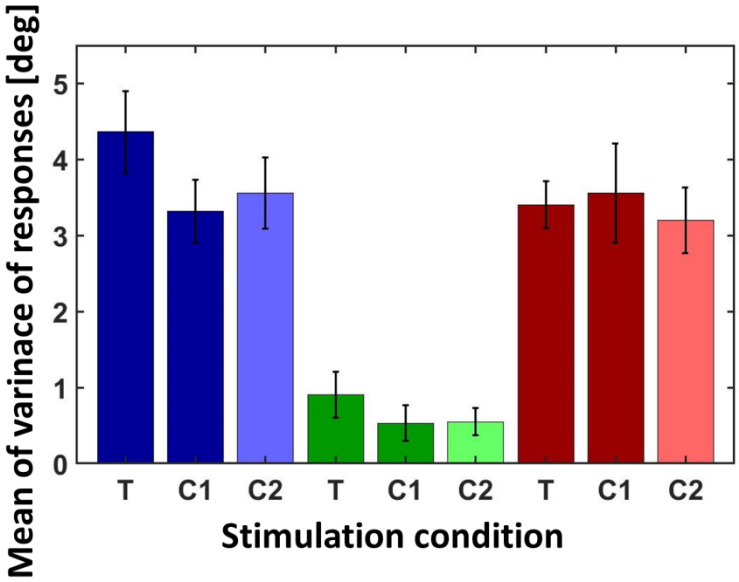

Figure S2-5: Mean variance for all participants. This plot shows the mean of variances with the standard errors of all eight participants' responses for the different stimulation conditions. For each self-motion direction the three stimulation conditions (TMS over area MST (T: targetTMS), control condition 1 (C1: stimulation of control condition) and control condition 2 (C2: no TMS)) are presented. In blue data of the self-motion direction to the left is shown, with light blue for no TMS trials. In green the self-motion direction straight forward is plotted, with light green for no TMS trials. In red the self-motion direction to the right is presented, with light red for no TMS trials.

We calculated two repeated measures ANOVAs. In the first one we used the stimulation of the control site as control condition and in the second we used as a control condition the no TMS data. In both we found a significant main effect for the heading direction (C1: $F(2.0, 6.0)=14.99$, $p=0.005$; C2: no TMS: $F(2.0, 6.0)=20.33$, $p=0.002$). For the comparison T vs. C2, our repeated measures ANOVA revealed also a significant main effect for stimulation condition ($F(1.0, 7.0)=6.2$, $p=0.042$). In order to test for our hypothesis that only TMS pulses over area hMST for heading to the left show an enhanced variance we calculated paired, one-tailed t-tests to compare conditions T and C2 for all three self-motion directions (heading: left: $t(7)=2.78$, $p=0.0136$; heading: straight ahead: $t(7)=1.51$, $p=0.0872$; heading: right: $t(7)=0.47$, $p=0.3263$). Accordingly, after a Bonferroni correction for multiple comparisons, only for heading to the left we found a significantly higher variance in responses for trials with TMS stimulation over hMST compared to noTMS data. This is in line with our hypothesis, i.e. a higher variance of the responses to self-motion to the left if area hMST in the right hemisphere was stimulated.

4.4.5 Discussion

A correct estimate of one's self-motion direction is a critical requirement for successful navigation in the world. We typically employ different sensory signals about our own movement which are integrated to a mostly accurate heading perception. In this study we focused only on visual information induced by self-motion, the optic flow (Gibson, 1950). Interestingly, pure visual information is often sufficient to judge heading veridically (Warren and Hannon, 1988; Royden et al. 1992; Lappe et al. 1999).

Numerous neurophysiological studies in the monkey and fMRI studies in the monkey and in humans have investigated the neural basis of the processing of visual self-motion information and especially the role of the medial superior temporal area (area MST) herein (monkey: e.g. Duffy and Wurtz, 1991; Lappe et al., 1996; Gu et al., 2006; humans: e.g. Huk et al., 2002; Morrone et al., 2000; Wall & Smith, 2008). These studies have documented a correlation

between neural activation patterns in specific regions of the brain, e.g. area MST, and self-motion stimuli. Yet, only an experimentally induced modification of neural processing accompanied by a modulation of perception can provide evidence for a *causal* role of this brain site for perception and/or behavior. Electrical microstimulation in the monkey has proven such an involvement of macaque area MST in heading perception (Britten and van Wezel, 1998; Gu et al., 2012).

TMS is an intensely-used, non-invasive approach to modulate neural processing. Here we used neuro-navigated TMS to modulate neural processing in human MST during concurrent perception of visually simulated self-motion across a ground plane. As predicted by an extended version of a linear decoder-model of heading perception (Bremmer et al., 2017), the variance in heading perception increased selectively for contraversive heading. This result not only provides further strong evidence for an involvement of hMST in the processing of self-motion information. Since the decoder-model was based on neurophysiological data from the macaque monkey, it also allows for a better understanding (and prediction) of effects of the modulation of neural activity in area MST on self-motion perception, as it might occur in very different contexts, e.g. during healthy aging (Lich and Bremmer, 2014) or in neurological or neuropsychiatric disorders (Mapstone and Duffy, 2010; van der Hoorn et al., 2014; Wang et al., 2017).

Localizer

A first and crucial step for our study was to localize area hMST at an individual subject level to be able to direct our TMS stimulation at area hMST and probe its role for heading perception. We used a functional localizer (as in Dukelow et al., 2001; Smith et al., 2006) and collected fMRI data from each of our participants. Different to human-MT, human MST (hMST) not only gets activated by contralateral, but also by ipsilateral visual stimuli. This approach allowed us to identify area hMST in both hemispheres in each participant. Talairach coordinates were well in line with published data (Dukelow et al., 2001; Cardin et al., 2012).

There are different strategies to choose a control area for TMS stimulation. One idea is to use sham stimulation as a control condition, other studies chose a central location, for example the location of the EEG electrode Cz from the well-established 10-20 system, in case this locations is not close to the region of interest. As a well-known fact, TMS induces tactile sensations. In the two control conditions described above, i.e. sham stimulation or stimulation at the Cz location, the TMS-induced tactile stimulation would have felt clearly different to the participants as compated to stimulation of hTMS (Dessing et al., 2013). This difference could have had an impact on our data. To avoid this potential problem, we followed the study of Dessing and colleagues (Dessing et al., 2013) in choosing our control area. In their study, the region of interest was area MT, which is just next to our target area hMST. Dessing and colleagues investigated the effect of stimulating different control sites and concluded that an area close to the region of interest is recommended because in such case participants can not differentiate between stimulation of the region of interest and the control area concerning TMS-induced tactile sensations. We decided to use a control area which was about 1.5 cm posterior to area hMST, similar to the study by Dessing and colleagues. Importantly, we made sure that this area didn't show any difference in fMRI-activation when comparing the BOLD response for presenting moving vs. stationary dots.

Heading discrimination: General aspects

Our behavioral data revealed a general larger variance in heading perception for peripheral as compared to straight-ahead self-motion. This is in line with previous studies showing that heading straight-ahead is perceived more accurate than self-motion directions towards a peripheral direction (Crane, 2012). The variances for peripheral headings were in the range of 3 to 4 degrees and hence expected based on what has been reported before (Warren et al., 1988). In addition, presentation time for our stimuli was only 50 ms and it has been shown before that performance in heading perception increases with presentation time for such ultra-short self-motion stimuli (Lich and Bremmer, 2014).

Heading discrimination: TMS-induced perturbation

In our study we stimulated always with three TMS pulses to maximize the influence of the stimulation. The timing of the pulses was always 100 ms before self-motion onset, right at motion onset and 100 ms after self-motion onset. There were two major reasons for choosing this time window: (i) a previous TMS study stimulating area hMT/V5+ documented an impairment in visual motion detection in time windows of 40-30 ms before and 130-150 ms after motion onset for the TMS pulse (Sack et al., 2006). These times are similar to the ones we used in our study. (ii) Our study was based on a previous study from our group showing an influence of saccades on self-motion perception (Bremmer et al., 2017). Similar to our current study, in the behavioral part of this previous work, we presented ultra-short self-motion sequences with varying visual-motion onset-times with respect to saccade onset. Results indicated an effect of saccades on heading perception from about 100ms before saccade onset until 100 ms thereafter. In our currently study, we mimicked the time-course of peri-saccadic response modulation by TMS-pulses. In future experiments it would be interesting to investigate the effect of the TMS pulses over time to determine the time-course of TMS-disturbance on visual processing similar to our previous work concerning saccades.

Heading discrimination: future directions

In the behavioral and TMS part of our study we presented optic flow stimuli simulating self-motion across a ground plane in one of three directions. Participants had to indicate their perceived heading via a ruler with random numbers and typing the number being closest to their perceived heading. In some of these trials we stimulated either hMST or the control site with TMS pulses. Our results, i.e. a greater variance in heading perception for contraversive self-motion confirmed our prediction. Our results are exciting for at least three reasons: first, a TMS-induced disturbance of neural processing of hMST induced a disturbance (larger variance) of heading perception in humans. Hence, our results provide further strong evidence for a critical role of hMST for the processing of (visual) self-motion information. Second, we hypothesized this outcome and this hypothesis was based on a model which

previously had already correctly predicted a hitherto unknown visual illusion, i.e. a peri-saccadic compression of perceived heading (Bremmer et al., 2017). Importantly, this model was based on neurophysiological recordings in the monkey. Accordingly, our results provide further and strong evidence for the macaque as animal model for human sensorimotor processing. Third and related to this previous point: invasive, neural recordings in the monkey allow investigating the processing of self-motion information at a spatial and temporal resolution which is not achievable in humans. At the same time, based on the similarity of self-motion processing in humans and non-human primates (NHPs), neural recordings and modulation of neural activity in NHPs are expected to contribute to a better understanding of the mal-processing of self-motion information as observed in cases of changes in the neural processing of self-motion information as occurring not only in healthy-aging (e.g. Lich and Bremmer, 2014) but also in neurological and neuropsychiatric disorders like Parkinson's or Alzheimer's disease (Mapstone and Duffy, 2010; van der Hoorn et al., 2014; Wang et al., 2017).

4.4.6 References

Angelaki, D. E., Gu, Y., DeAngelis, G. C. Visual and vestibular cue integration for heading perception in extrastriate visual cortex. *J Physiol*, **589.4**, 825-833 (2011).

Banks, M. S., Ehrlich, S. M., Backus, B. T., Crowell, J. A. Heading During Real and Simulated Eye Movements. *Vision Res*, **36:3**, 431-443 (1996).

Berthoz, A., Pavard, B., Young, L. R. Perception of Linear Horizontal Self-Motion Induced by Peripheral Vision (Linearvection) Basic Characteristics and Visual-Vestibular Interactions. *Exp. Brain Res.*, **23**, 471-489 (1975).

Binda, P., Morrone, M. C. Vision During Saccadic Eye Movements. *Annu Rev Vis Sci*. **4**, 193-213 (2018).

Bremmer, F., Schlack, A., Shah, N. J., Zafiris, O., Kubischik, M., Hoffmann, K., Zilles, K., Fink, G.R. Polymodal motion processing in posterior parietal and premotor cortex: a human fMRI study strongly implies equivalencies between humans and monkeys. *Neuron*. **29(1)**, 287-96 (2001).

Bremmer, F., Klam, F., Duhamel, J.-R., Hamed, S. B., Graf, W. Visual-vestibular interactive responses in the macaque ventral intraparietal area (VIP). *European Journal of Neuroscience*, **16**, 1569-1586 (2002).

Bremmer, F., Kubischik, M., Hoffmann, K. P., Krekelberg, B. Neural dynamics of saccadic suppression. *J Neurosci*. **29(40)**, 12374-83 (2009).

Bremmer, F., Kubischik, M., Pekel, M., Hoffmann, K.-P., Lappe, M. Visual selectivity for heading in monkey area MST. *Exp. Brain Res.*, **200**, 51-60 (2010).

Bremmer, F., Churan, J., Lappe, M. Heading representations in primates are compressed by saccades. *Nature Communications*, **8:920,** (2017).

Britten, K. H., van Wezel, R. J. A. Electrical microstimulation of cortical area MST biases heading perception in monkeys. *Nat Neurosci*., **1(1)**, 59-63 (1998).

Burr, D. C., Morrone, M. C., Ross, J. Selective suppression of the magnocellular visual pathway during saccadic eye movements. *Nature*. **371(6497)**, 511-3 (1994).

Cardin, V., Hemsworth, L., Smith, A. T. Adaptation to heading direction dissociates the roles of human MST and V6 in the processing of optic flow. *J Neurophysiol*, **108**, 794–801 (2012).

Chen, A., DeAngelis, G. C., Angelaki, D. E. Representation of Vestibular and Visual Cues to Self-Motion in Ventral Intraparietal Cortex. *The Journal of Neuroscience*, **31(33)**, 12036-12052 (2011).

Churan, J., von Hopffgarten, A., Bremmer, F. Eye movements during path integration. *Physiol Rep*, **6(22)**, e13921 (2018).

Crane, B. T. Direction Specific Biases in Human Visual and Vestibular Heading Perception. *PLoS ONE*, **7(12)**, e51383 (2012).

Dessing, J. C., Vesia, M., Crawford, J. D. The role of areas MT+/V5 and SPOC in spatial and temporal control of manual interception: an rTMS study. *Frontiers in Behavioral Neuroscience*, **7(15)** (2013).

Dokka, K., DeAngelis, G. C., Angelaki, D. E. Multisensory Integration of Visual and Vestibular Signals Improves Heading Discrimination in the Presence of a Moving Object. *The Journal of Neuroscience*, **35(40)**, 113599-13607 (2015).

Duffy, C., Wurtz, R. H. Sensitivity of MST Neurons to Optic Flow Stimuli. I. A Continuum of Response Selectivity to Large-Field Stimuli. *Journal of Neurophysiology*, **65:6** (1991).

Dukelow, S. P., DeSouza, J. F. X., Culham, J. C., van den Berg, A. V., Menon, R. S., Vilis, T. Distinguishing Subregions of the Human MT+ Complex Using Visual Fields and Pursuit Eye Movements. *J Neurophysiol.*, **86(4)**, 1991-2000 (2001

Gibson, J. J. The perception of the visual world. *The Riverside Press*, Cambridge, Massachusetts (1950).

Greenlee. M. W., Frank, S. M., Kaliuzhna, M., Blanke, O., Bremmer, F., Churan, J., Cuturi, L. F., MacNeilage, P. R., Smith, A. T. Multisensory integration in self-motion perception.*Multisensory Research*. **29**, 525-556 (2016).

Gu, Y., Watkins, P. V., Angelaki, D. E., DeAngelis, G. C. Visual and Nonvisual Contributions to Three-Dimensional Heading Selectivity in the Medial Superior Temporal Area. *The Journal of Neuroscience*, **26(1)**, 73-85 (2006).

Gu, Y., Fetsch, C. R., Adeyemo, B., DeAngelis, G. C., Angelaki, D. E. Decoding of MSTd Population Activity Accounts for Variations in the Precision of Heading Perception. *Neuron*, **66**, 596-609 (2010).

Gu, Y., DeAngelis, G. C., Angelaki, D. E. Causal Links between Dorsal Medial Superior Temporal Area Neurons and Multisensory Heading Perception. *The Journal of Neuroscience*, **32(7)**, 2299-2313 (2012).

Heuer, A., Schubö, A., Crawford, J. D. Different Cortical Mechanisms for Spatial vs. Feature-Based Attentional Selection in Visual Working Memory. *Front. Hum. Neurosci*., **10**:415 (2016).

Hlavacka, F., Mergner, T., Bolha, B. Human self-motion perception during translatory vestibular and proprioceptive stimulation. *Neuroscience Letters*, **210**, 83-86 (1996).

Huk, A. C., Dougherty, R. F., Heeger, D. J. Retinotopy and functional subdivision of human areas MT and MST. *J Neurosci*. 22(16), 7195-205 (2002

Kaminiarz, A., Krekelberg, B., Bremmer, F. Localization of visual targets during optokinetic eye movements. *Vision Research*, **47**, 869-878 (2007).

Kaminiarz, A., Schlack, A., Hoffmann, K.-P., Bremmer, F. Visual selectivity for heading in the macaque ventral intraparietal area. *J Neurophysiol*, **112**, 2470-2480 (2014).

Lappe, M., Rauschecker, J. P. An illusory transformation in a model of potic flow processing. *Vision Res*. **35:11**, 1619-1631 (1995).

Lappe, M., Bremmer, F., Pekel, M., Thiele, A., Hoffmann, K.-P. Optic Flow Processing in Monkey STS: A Theoretical and Experimental Approach. *The Journal of Neuroscience*, **16(19)**, 6265–6285 (1996).

Lappe, M., Bremmer, F., van den Berg, A.V. Perception of self-motion from visual flow. *Trends in Cognitive Sciences*, **3:9** (1999).

Lich, M., Bremmer, F. Self-motion perception in the elderly. *Frontiers in Human Neuroscience*, **8:681** (2014).

Mapstone, M., Duffy, C. J. Approaching objects cause confusion in patients with Alzheimer's disease regarding their direction of **self**-movement. *Brain*. 133(9), 2690-701 (2010).

Morrone, M. C., Tosetti, M., Montanaro, D., Fiorentini, A., Cioni, G., Burr, D. C. A cortical area that responds specifically to optic flow, revealed by fMRI. *Nat Neurosci*, **3(12)**, 1322-8 (2000).

Ross, J., Morrone, M. C., Goldberg, M. E., Burr, D. C. Changes in visual perception at the time of saccades. *Trends Neurosci*. **24(2)**, 113-21 (2001).

Rossi, S., Hallett, M., Rossini, P. M., Pascual-Leone, A. The safety of TMS Consensus Group. Safety, ethical considerations, and application guidelines for the use of transcranial magnetic stimulation in clinical practice and research. *Clinical Neurophysiology*, **120**, 2008-2039 (2009).

Rossini, P. M., Baker, A. T., Berardelli, A., Caramia, M. D., Caruso, G., Cracco, R. Q., Dimitrijevid, M. R., Hallett, M., Katayama, Y., Lücking C. H., Maertens de Noordhout, A. L., Marsden, C. D., Murray, N. M. F., Rothwell, J. D., Swash, M., Tomberg, C. Non-invasive electrical and magnetic stimulation of the brain, spinal cord and roots: basic principles and procedures for routine clinical application. Report of an IFCN committee. *Electroencephalography and clinical Neurophysiology*, **91**, 79-92 (1994).

Royden, C. S., Banks, M. S., Crowell, J. A. The perception of heading during eye movements. *Nature*, **360** (1992).

Saito, H., Yukie, M., Tanaka, K., Hikosaka, K., Fukada, Y., Iwai, E. Integration of direction signals of image motion in the superior temporal sulcus of the macaque monkey. *The Journal of Neuroscience*, **6(1)**, 145-157 (1986).

Sack, A. T., Kohler, A., Linden, D. E. J., Goebel, R., Muckli, L. The temporal characteristics of motion processing in hMT/V5+: Combining fMRI and neuronavigated TMS, *NeuroImage*, **29**, 1326 – 1335 (2006).

Schlack, A., Hoffmann, K.-P., Bremmer, F. Interaction of linear vestibular and visual stimulation in the macaque ventral intraparietal area (VIP). *European Journal of Neuroscience*, **16**, 1877-1886 (2002).

Shao, M., DeAngelis, G. C., Angelaki, D. E., Chen, A. Clustering of heading selectivity and perception-related activity in the ventral intraparietal area. *J Neurophysiol*, **119**, 1113-1126 (2018).

Smith, A. T., Wall, M., B., Williams, A. L., Singh, K. D. Sensitivity to optic flow in human cortical areas MT and MST. *Eur J Neurosci.*, **23(2)**, 561-9 (2006).

Taylor, P. C., Thut, G. Brain activity underlying visual perception and attention as inferred from TMS-EEG: a review. *Brain Stimul.* **5(2)**, 124-9 (2012).

Van den Berg, A. V., Beintema, J. A. Motion templates with eye velocity gain fields for transformation of retinal to head centric flow. *NeuroReport*, **8**, 835-840 (1997).

van der Hoorn, A., Renken, R. J., Leenders, K. L., de Jong, B. M. Parkinson-related changes of activation in visuomotor brain regions during perceived forward self-motion. *PLoS One*. **9(4)**, e95861 (2014).

von Hopffgarten, A., Bremmer, F. Self-motion reproduction can be affected by associated auditory cues. *Seeing Perceiving*, **24(3)**, 203-22 (2011).

Wall, M. B., Smith, A. T. The Representation of Egomotion in the Human Brain. *Current Biology*, **18**, 191–194 (2008).

Wang, J., Guo, X., Zhuang, X., Chen, T., Yan, W. Disrupted pursuit compensation during **self**-**motion** perception in early Alzheimer's disease. *Sci Rep*. 7(1), 4049 (2017).

Warren, W. H., Hannon, D. J. Direction of self-motion is perceived from optical flow. *Nature*, **336** (1988).

Study III:

A neural correlate of the subjective encoding of distance

Constanze Schmitt, Milosz Krala and Frank Bremmer

In preparation

4.5 Study III: A neural correlate of the subjective encoding of distance

4.5.1 Abstract

Navigating through an environment requires knowledge not only about one's direction of self-motion (heading), but also about traveled distance. Previous behavioral studies have shown that human participants are able to actively reproduce a previously observed travel distance purely based on visual information. Here, we employed EEG to determine the processing involved in actively controlled (simulated) self-motion as well as of distance reproduction.

We measured event-related potentials (ERPs) during visually simulated straight forward self-motion across a ground plane. The participants' task was to reproduce (active condition) double the distance of a previously seen self-displacement (passive condition) using a gamepad. We recorded the trajectories of self-motion during the active condition and played it back to the participants in another set of trials (replay condition). EEG data were aligned to the onset or to the offset of the simulated self-motion. Additionally, we aligned behavioral and EEG data also to half of the actively traveled distance, i.e. about the originally presented passive distance.

Response modulation of the evoked ERPs was stronger and several ERP-components had longer latencies in the passive as compared to the active condition. This result is in line with the idea of attenuated responses to self-induced vs. externally-induced sensory stimulation. Remarkably, wavelet based temporal-frequency analyses showed activation in the alpha band when passing the subjective (d_subjective) but not the objective single distance (d_objective) in about half of the participants. More generally, our approach of asking subjects to reproduce double instead of once the feature under study (here: distance) allows to investigate subjective perception in general without interfering neural signatures of the required response action.

4.5.2 Introduction

Navigating through and interacting with the environment is a complex behavioral task. Visual information as observed during self-motion (optic flow) does not only contain enough information to accurately judge heading, but also to estimate traveled distance (Gibson, 1950; Bremmer and Lappe, 1999). Behavioral studies have shown that human observers are able to actively reproduce a previously observed travel distance purely based on visual information (Bremmer and Lappe, 1999; von Hopffgarten and Bremmer, 2011; Churan et al., 2017). However, absolute information about the traveled distance cannot be revealed based on an abstract optic flow stimulus (Lee, 1980) unless information about the distance of visual objects to the observer or the general depth layout of the stimulus is provided. Comparing two distances presented with the same stimulus layout is not affected by this problem if one assumes the same spatial layout in both scenes. Nevertheless, in such a task, subjects often do not perform veridical but tend to overshoot short and undershoot long distances (Berthoz et al., 1995; Bremmer and Lappe, 1999; Glasauer et al., 2007; von Hopffgarten and Bremmer, 2011; Churan et al., 2017). Previous studies have revealed that participants base their active reproduction behavior on the velocity of the observed movement and try to reproduce the velocity profile in order to reproduce a previously observed displacement as accurately as possible (Bremmer et al., 1999; von Hopffgarten and Bremmer, 2011). Frenz & Lappe (2005) could show that subjects' performance is not only based on processing speed information concerning visual motion but also relies on an internal representation of the spatial layout of the scenery. A change of the height of a simulated observer above a ground plane, which went unnoticed by the subjects, induced predictable errors of their distance reproduction.

Although the visual self-motion stimulation might be exactly the same, active reproduction of a previously observed distance provides different sensory information compared to just passive viewing. It has been shown before that self-induced sensory stimuli are accompanied by attenuated neural activity as compared to passively experiencing the same

stimuli. Such findings have been reported in the visual (Erickson and Thier, 1991, Bremmer et al., 2009; Krock and Moore, 2014), somatosensory (Weiskrantz et al., 1971; Blakemore et al., 1999; Bays et al., 2005; Shergill et al., 2013;) and auditory domain (Bäß et al., 2008; Hughes et al., 2013; Wang et al., 2014). These results support the theory that an efference copy (von Holst and Mittelstaedt, 1950) or corollary discharge (Sperry, 1950) of the motor command is used to predict the sensory consequence of the resulting action (Miall and Wolpert, 1996; Shadmehr and Krakauer, 2008). An attenuated signal is found when the predicted sensory outcome matches the actual sensory event. In a recent Electroencephalography (EEG) study this attenuation effect was investigated on the early components of visual evoked potentials (VEP) (Benazet, et al., 2016). The authors reported an attenuation of the negative VEP-peak within a temporal window between 125 ms and 200 ms after stimulus onset.

EEG recordings easily allow to investigate perceptual and cognitive processes (Arnal and Giraud, 2012; Chakravarthi and VanRullen, 2012). Alpha band oscillations with frequencies around 10 Hz are the most dominant oscillations in the human brain (Klimesch, 2012). They occur in the auditory (Leske et al., 2014), sensorimotor (Haegens et al., 2015), and prefrontal areas (Supp et al., 2011), but also in visual areas being maximal over posterior brain regions and referred to processing in occipitoparietal cortex. Earlier studies had associated the occurrence of alpha power with attentional disengagement and reduced visual processing (Pfurtscheller et al., 1996; Lundqvist, et al., 2013). Recent studies have revealed a broader view on the involvement in cognition represented by changes in alpha band frequency (for a review see Clayton et al., 2018). Two main characteristics have been described: First, increased alpha power as indication of an inhibition of irrelevant visual processes (Jokisch and Jensen, 2007) for example when a distraction during a memory task has to be avoided. This alpha increase was documented to be related to improved memory performance (Lozano-Soldevilla et al., 2014). Second, alpha oscillations have been shown to represent feedback processes (Bastos et al., 2015; Jensen et al., 2015) combined with gamma oscillations reflecting bottom-up processes (Michalareas et al., 2016). These feedback

processes associated with alpha band activity (for a review see Clayton et al., 2018) are important in the context of predictive coding reflecting the top-down flow of predictions to the next lower level in order to be compared to incoming sensory information (Stefanics et al., 2014). The basis of this predictive coding theory is the idea of free energy minimization (Friston, 2005, 2010). In this framework, the brain constantly compares predictions about our environment formed by prior experiences about the upcoming events with the actual sensory stimulations. Differences resulting from these comparisons have to be kept as small as possible in order to optimize perception. The model of predictive coding is hierarchically structured and requires in addition to the above mentioned feedback of prediction signals a bottom-up information flow indicating prediction errors (Friston, 2005; Winkler and Czigler, 2012; Stefanics et al., 2014).

In this context, the goal of our current study was two-fold. First, we aimed to compare neural activation during externally induced and self-induced self-motion. We presented visually simulated forward self-motion across a ground plane in a distance reproduction task. Subjects had to reproduce double the distance of a previously seen passive self-displacement, while we recorded their EEG activity. We hypothesized attenuated neural activity during actively controlled as compared to passively observed self-motion. Second, we aimed to determine a neural correlate of the encoding of distance. We hypothesized to find increased alpha band activity, i.e. a feedback signal, when passing the single distance.

4.5.3 Materials and Methods

4.5.3.1 Participants

We invited 15 participants for this study (11 female, 4 male, mean age: 25.3 years, ranging from 20 to 34 years). All had normal or corrected to normal vision and except the author MK they were naïve about the purpose of this study. Our study was approved by the Ethics Committee of the Faculty of Psychology at Philipps-Universität Marburg and was in agreement with the Declaration of Helsinki. Prior to the experiment the participants provided

written informed consent. They were compensated with 8 € per hour for participation. We collected all data for each participant on a given day, except for three of the participants who came on two different days due to individual time restrictions on the first day of recordings.

4.5.3.2 Setup

The experiment was performed in a darkened, sound attenuated and electrically shielded room. The stimuli were presented on a monitor (*VPixx Technologies Inc.*, Saint-Bruno, QC, Canada), which was 42° wide and 24° high. Its resolution was set to 1920 × 1080 pixels and the refresh rate was 120 Hz. Participants sat in front of the monitor, whose center was positioned at eye level 68 cm in front of them. A chin rest stabilized their head while binocularly viewing the stimuli. Eye movements were recorded using an EyeLink 1000 system (*SR Research*, ON, Canada). A gamepad was positioned in comfortable reaching distance.

4.5.3.3 Stimulus and task

We presented an optic flow stimulus simulating forward self-motion across a ground plane depicted schematically in Figure S3-1. In addition, throughout the experiment a fixation target was presented above the ground plane at the center of the screen. The bull's eye fixation target with cross hair shape (target shape ABC in Thaler et al., 2013) had an inner radius of 0.08° and an outer radius of 0.32°. Throughout the whole experiment participants were asked to fixate the target. With each appearance the dots making up the ground plane stimulus were presented at new random locations. We presented trials of three different conditions: passive, active and replay (for serial order: see below). A red fixation target indicated the passive condition, a green target the active and a white target the replay condition. In the **passive** condition, first, the ground plane was presented stationary for 700 ms.

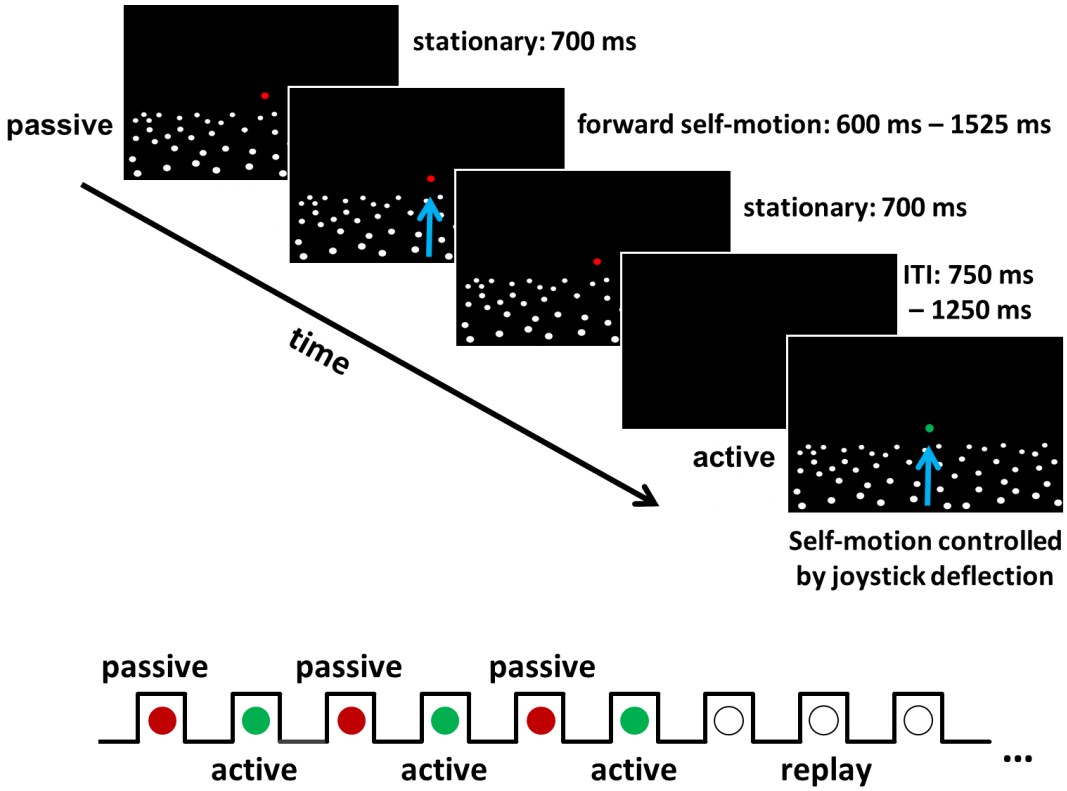

Figure S3-1: Stimulus and serial order of the trials from the different conditions. Each trial presented a forward displacement across a ground plane simulated by an optic flow stimulus. First, a passive trial was presented. In the passive condition the fixation target was red. The ground plane consisting of random white dots was presented stationary for 700 ms. Then the dots moved for 600 ms – 1525 ms depending on the speed (slow or fast) and distance (short, medium or long) simulating forward self-motion (represented by the blue arrow). After movement offset the ground plane was displayed stationary for another 700 ms before the screen turned black. This triggered an inter-trial-interval lasting between 750 and 1250 ms. Next, an active trial was presented, indicated by a green fixation target. Participants were asked to reproduce double the previously observed passive distance using a gamepad. Self-motion was controlled by deflecting a joystick. After movement offset the ground plane was again presented stationary for 700 ms. The movement was recorded and played back in the replay condition. Here the fixation target was white and participants were just asked to observe the self-motion stimulus. A passive and a following active trial were shown three times before the corresponding three replay movements were presented in pseudo-randomized order as demonstrated in the bottom row of the figure.

Second, a forward displacement of one of three different distances (28.4, 32.4 and 36.4 arbitrary units (a.u.)) at one of two different speeds (23.7 and 47.4 a.u./s) was simulated. This resulted in self-motion durations between 600 and 1525 ms. After movement offset, the

stationary ground plane was visible for another 700 ms before the screen turned black for 1000 ± 250 ms.

The participants' task was to reproduce in the following **active** condition double the distance of the previously presented self-motion. The ground plane and the fixation target were presented at the same time. The self-motion was initiated by deflecting the joystick on the gamepad with the left thumb. Participants were free to choose the speed of the self-motion by modulating the deflection angle of the joystick. Once the movement was stopped it was not possible for the participants to start it again in the same trial. After movement offset the stationary ground plane was visible for another 700 ms before the screen turned black. The exact speed profile of the self-motion in this active condition was recorded. In the **replay** condition, the exact velocity profile of a previously shown active condition was presented to the participants. In this condition, the subjects' task was simply to observe the optic flow stimulus.

4.5.3.4 Procedure

In total we presented 1080 trials (360 for each condition) to each participant: six sessions consisting of five blocks of 36 trials each. Prior to each session a calibration of the EyeLink was performed. The 36 trials in each block were presented in a specific order. A passive and the following active condition were presented three times right after each other. Thereafter, the resulting three replay conditions were displayed in pseudo-randomized order. Since replay trials presented exactly the same visual stimulus, the replay trials were not presented right after the corresponding active trial, to keep participants more engaged in the experiment. Before each passive trial as well as before each replay trail a drift correction with one fixation dot for the EyeLink was performed. After each session a short break was offered to the participants.

4.5.3.5 EEG recordings

The electroencephalogram (EEG) was recorded continuously throughout the experiment by an actiCHamp module (*Brain Products GmbH*, Gilching, Germany) and the software Brain Vision PyCorder (*Brain Vision LLC*, Morisville, NC, USA). We positioned 64 active Ag/AgCl electrodes according to the extended international 10-20 system on the participants' heads. Typically, the impedances of all electrodes were kept below 5 kΩ during the whole experiment. Data was recorded with Cz as reference electrode. The continuously recorded EEG signals were digitized at a sampling rate of 1000 Hz.

4.5.3.6 Analysis

EEG data were analyzed offline using the Brain Vision Analyzer software (*Brain Products*, Gilching, Germany) and Matlab (*MathWorks*, Natick, MA, USA). First, as the new reference signal the average signal of the mastoid electrodes TP9 and TP10 was applied. Second, data was filtered using a low pass filter with a cut-off frequency of 90 Hz, a high pass filter with a cut-off frequency of 0.5 Hz and a Notch filter at 50 Hz. Third, data containing blinks or eye movements in the relevant analysis time windows (see below) were excluded from further data analysis, separately for the different analysis steps. This resulted in different exclusion rates due to different analysis time windows (ERPs: motion onset: 16% (active), 17.1% (replay), 8% (passive); motion offset: 17.6% (active), 17.4% (replay), 9.9% (passive); Time-frequency analysis: 9.7% (active), 12.2% (replay); data from passive trials were not analyzed.

ERPs

Data were aligned to self-motion on- and offset and different time windows were used for baseline correction to avoid interference with ongoing ERP signals. For baseline correction, the average signal from -200 ms to 0 ms (0 ms representing motion onset) was used for alignment to motion onset. Likewise, average activity from -600 ms to -400 ms (0 ms

representing motion offset) was used for baseline correction at motion offset. In a last step, epochs starting 300 ms before motion on- and offset to 600 ms thereafter were extracted from the continuous EEG data. Epochs were averaged for subjects and conditions separately. Since we presented a visual stimulus covering the left and right visual field, we analyzed data collected at electrode Pz, a central electrode over parietal areas, because this electrode has been shown before to reveal a large motion-onset VEP (Kuba et al., 2007).

Time-frequency analysis

Data were first aligned to self-motion onset (0 ms representing motion onset) and a baseline correction was performed using the time window ranging from -700 ms to -400 ms. Next, data for each trial from the active and the respective replay condition were aligned to two different time points separately. The alignment times represented specific distances: 1) the subjective single distance (d_subjective), i.e. half of the traveled active distance; and 2) the objective single distance (d_objective), i.e. the travel distance of the passive displacement, which had to be reproduced. This resulted in four different data sets: alignment to d_subjective and d_objective for active and replay data, each. The following analysis steps were performed separately on these four data sets. Epochs ranging from 800 ms before the alignment time to 800 ms thereafter were extracted from the continuous EEG signal. The data was first averaged across all trials and then this data was converted separately for each participant with a continuous complex Morlet-wavelet transformation (with 10 voices per octave). This approach allows analyzing the evoked activity (Herrmann et al., 2014).

The time frequency data ranging from 2 to 25 Hz were divided into three time windows: One central window was defined to range from -250 ms to 250 ms, around either of the two alignment points (d_subjective vs. d_objective); one early window ranging from from -550 ms to -350 ms; and a late window ranging from 350 ms to 550 ms (Figure S3-7A). The early and late time windows were chosen to be as close as possible to the central window without creating overlap in the analyzed data. We expected to find differences in activation in the central time window as compared to the early and the late time window. We hypothesized

such activation to reflect a feedback signal indicating the subjective perception of passing the single distance (predictive coding). Participants revealing such an enhancement of power in the central time window for alignment to d_subjective were considered to show the hypothesized effect and their data were included in further time-frequency analyses. More specifically, we first aligned data from the active condition to d_subjective. The maximum power value in the central time window was identified. A region of interest around each of these maxima (of ±100 ms and ±2 Hz around the maximum power value) was defined resulting in 200 ms long and 4 Hz patches in time-frequency space (Central Patch, CP). Reference Patches (RPs) in the early as well as the late time window were defined for each participant. RPs were also 200 ms wide, the length of the early and late time window, respectively, and covered the same frequency range of 4 Hz. The power values in the CP and the RPs were averaged separately and compared to each other. We considered the data showing a distance related effect if this average value in the central region was at least 2.5 times larger than the average value of the RPs. For participants fulfilling this criterion, the averaged power values for the corresponding time-frequency patches were calculated for the other three conditions: the replay condition with data aligned to d_subjective and the active and replay conditions with data aligned to d_objective. One tailed paired t-tests were used to compare the results of the conditions separately for the three time windows.

4.5.4 Results

4.5.4.1 Distance reproduction

The similarity of the speed profiles in the passive and active condition of a representative participant shows that participants aimed to mimic the passive speed profile (Figure S3-2). In most of the trials the maximum possible joy stick deflection was chosen. In general, most of the participants traveled longer than double of the passive distance as can be seen in the mean across all trials per participant (Figure S3-3). When the short passive distance was presented the mean of the active distances across all participants was 27.67% longer than

the required distance, i.e. double the passive distance. After presentation of the medium distance, the overshoot was 20.12% and for the long distance trials the active distance was 10.64% longer. Participants whose distance reproduction performance is depicted in red in Figure S3-3 were included in the time-frequency analysis (for exclusion criteria see methods section).

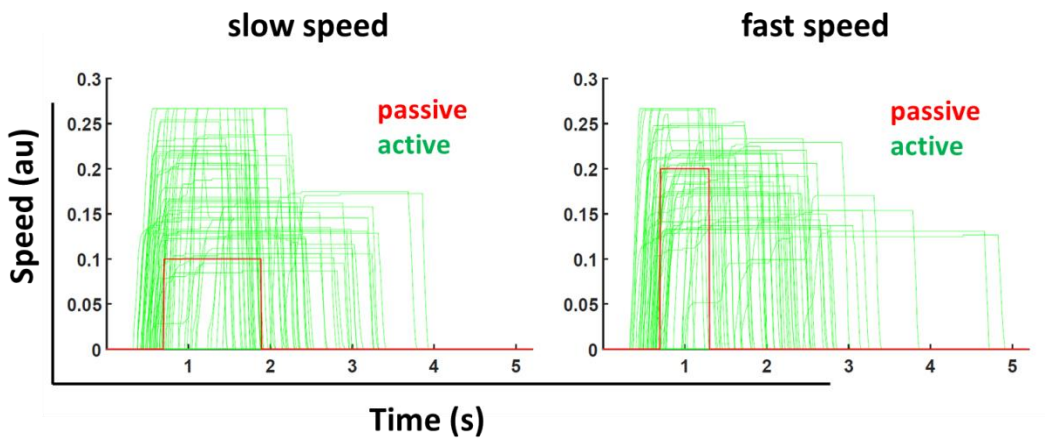

Figure S3-2: Velocity profiles generated by one participant for the short distance. The velocity profiles of the passive and all the active trials for one participant are presented. On the left we show data for the slow speed in the passive condition and on the right for the fast speed in the passive condition. Green lines represent the actively controlled velocity profiles of this participant. In red we present the passive velocity profile. The solid line shows the actual presented passive movement.

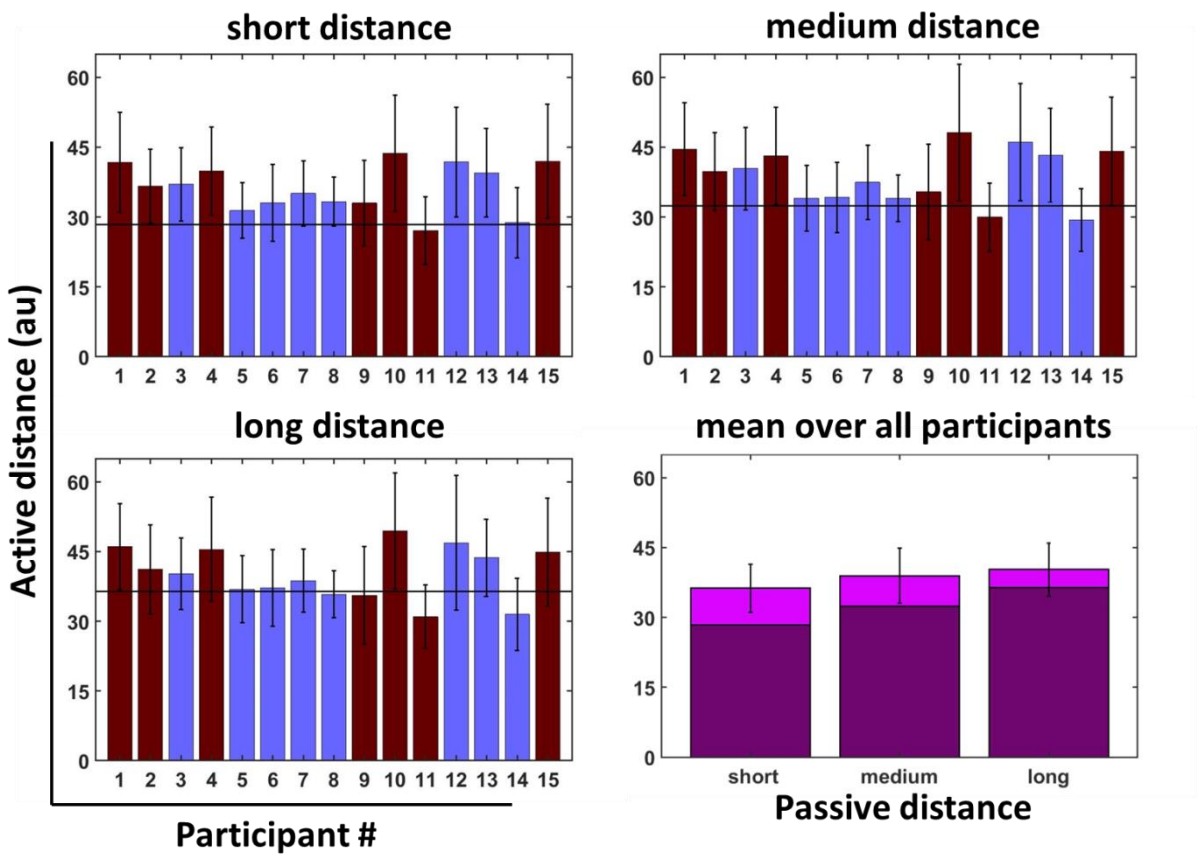

Figure S3-3: Distance reproduction performance. Bars show the reproduced distances in the active condition for all 15 participants separately. The mean distance over all trials is presented for each participant with the standard deviation as error bar. Data is shown for the three passive distances (short, medium and long). The black solid line in each plot represents double the passive distance. Participants whose data is presented in red were included in the time-frequency analysis (in-group participants). In the graph on the bottom right the average performance over all participants can be seen in light purple with double the passive distance in dark purple.

4.5.4.2 Visual processing of self-motion onset and offset

We investigated visual evoked potentials (VEPs) induced by motion onset and offset. Figure S3-4 shows data from electrode Pz averaged across all 15 participants as well as the different speeds and distances. Data were aligned to motion onset and motion offset separately and examined for the three different conditions, passive, active, and replay, respectively.

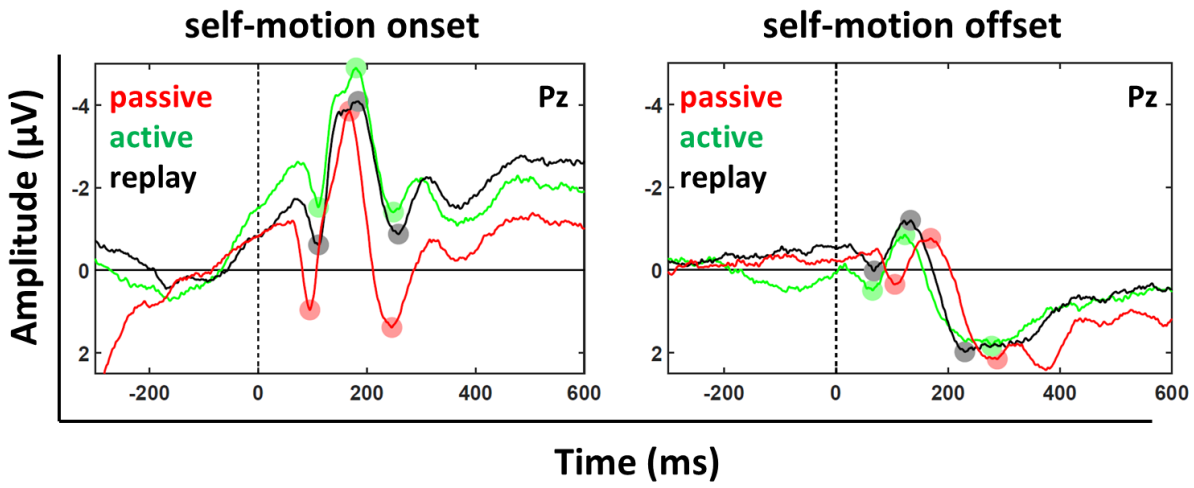

Figure S3-4: Visual evoked potentials (VEPs) elicited by self-motion onset and offset. We present data collected on electrode Pz for the three conditions: passive in red, active in green and replay in black**.** In the left panel, time 0 ms represents self-motion onset while in the right panel it represents self-motion offset.

We found the typical VEP-components N1, P1 and N2 after movement onset and offset with in general smaller values for the motion offset VEP-components. The latencies (peak times) for these three components as well as the amplitude values for the averaged data are depicted in Table S3-1.

	Self-motion onset			**Self-motion offset**		
	active	**replay**	**passive**	**active**	**replay**	**passive**
	latency	**latency**	**latency**	**latency**	**latency**	**latency**
P1	112 ms	112 ms	96 ms	66 ms	69 ms	106 ms
N2	181 ms	185 ms	169 ms	124 ms	134 ms	170 ms
P2	250 ms	259 ms	247 ms	280 ms	231 ms	289 ms
	amplitude	**amplitude**	**amplitude**	**amplitude**	**amplitude**	**amplitude**
|P1-N2|	3.33 µV	3.46 µV	4.78 µV	1.32 µV	1.2 µV	1.1 µV
|P2-N2|	3.47 µV	3.2 µV	5.21 µV	2.65 µV	3.17 µV	2.9 µV

Table S3-1: Amplitudes and latencies for the P1-, N2- and P2-components for the three conditions (active, replay and passive) for self-motion on- and offset.

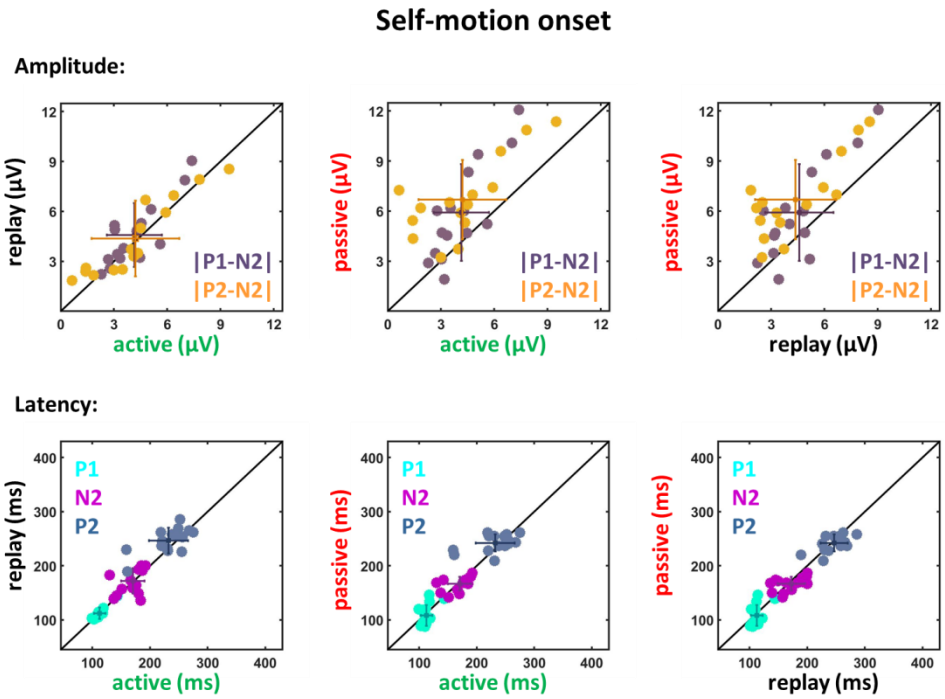

Figure S3-5: Amplitude differences and latencies of the components P1, N2 and P2 for self-motion onset VEPs. Panels depict data from the active and replay condition (left column), active and passive condition (middle column) and replay and passive condition (right column). In the top row we present the differences |P1-N2| (purple) and |P2-N2| (yellow) for the different conditions. In the bottom row the peak times for the three components P1 (cyan), N2 (magenta) and P2 (blue) are shown. In all 6 graphs in a darker color the mean values of each group of data with the corresponding standard deviations are presented.

In order to analyze the differences between the conditions (active, replay and passive) further, we quantified the scatter of the amplitudes and latencies for the 15 participants (Figures S3-5 and S3-6). In both figures, absolute differences between the peak amplitudes are shown in the top row (|P1-N2| and |P2-N2|), while latencies are depicted in the bottom row with each data point representing the results of one participant. We tested for differences of the amplitude values and the peak times between the three conditions. Here, we report only the p-values for the two cases which revealed significant differences: i) amplitude differences for motion onset (Table S3-2); ii) latency differences for motion offset (Table S3-3).

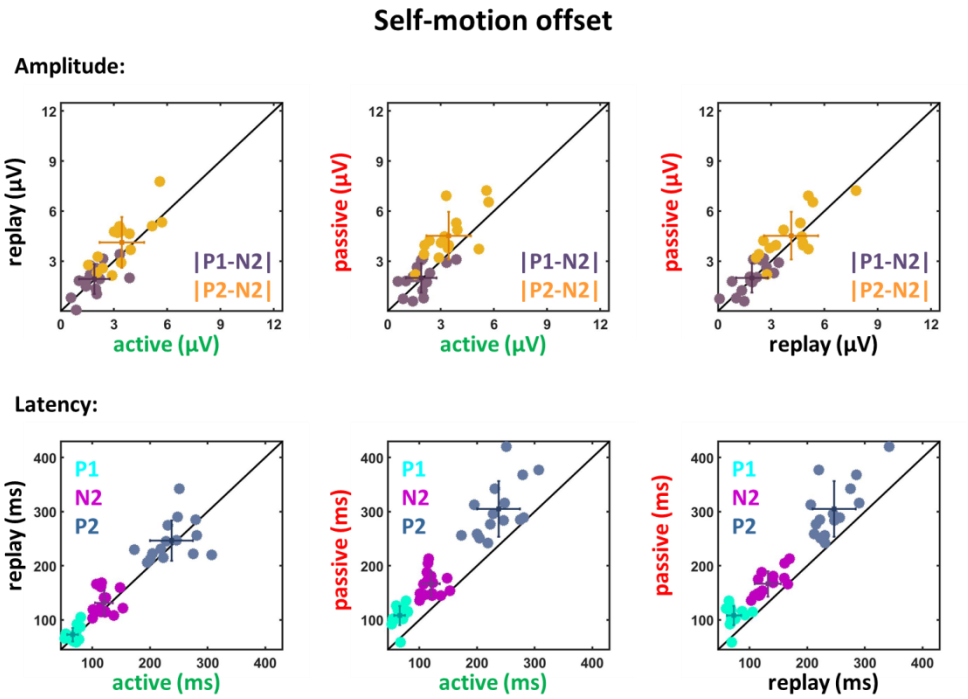

Figure S3-6: Amplitude differences and latencies of the components P1, N2 and P2 for self-motion offset VEPs. Conventions as in Figure S3-5.

We calculated paired two-tailed t-tests for each of the comparisons which resulted in a Bonferroni corrected significance level of $p<0.0083$ for the amplitude comparisons in the motion onset data and $p<0.0056$ for the latency comparisons in the motion offset data.

Self-motion onset: amplitudes				
	|P1-N2|		**|N2-P2|**	
	active	**replay**	**active**	**replay**
active		t(14)=-1.62, p=0.13		t(14)=-0.7, p=0.5
passive	t(14)=-3.78, p=0.002	t(14)=-3.06, p=0.0084	t(14)=-5.61, $p=6.4*10^{-5}$	t(14)=-6.09, $p=2.8*10^{-5}$

Table S3-2: Results of paired two-tailed t-tests for the comparisons between the amplitudes (|P1-N2|, |N2-P2|) of the different conditions.

Comparisons revealing significant differences without correction for multiple testing are colored in orange and non-significant comparisons in red. For self-motion onset, data from passive trials showed significantly larger amplitudes compared to the active and replay conditions.

Self-motion offset: latencies						
	P1		**N2**		**P2**	
	active	**replay**	**active**	**replay**	**active**	**replay**
active		t(14)= -2.45, p=0.028		t(14)=-1.7, p=0.11		t(14)=-0.83, p=0.42
passive	t(14)= -9.71, $p=1.3*10^{-7}$	t(14)=-6.2, $p=2.3*10^{-5}$	t(14)= -6.48, $p=1.4*10^{-5}$	t(14)= -8.48, $p=6.9*10^{-7}$	t(14)=-6.1, $p=2.7*10^{-5}$	t(14)=-6.02, p=0.000031

Table S3-3: Results of paired two-tailed t-tests for the comparisons between the latencies (P1, N2, P2) of the different conditions.

The latencies of the three components (P1, N2 and P2) did not show significant differences in data of self-motion onset between the three conditions (active, replay and passive). In the data for self-motion offset we found larger latencies for all three components in the passive condition compared to active and replay conditions. The amplitude differences of the VEP-components elicited by self-motion offset were not significantly different.

4.5.4.3 Time-Frequency data

A key goal of our study was to determine a neural correlate of distance estimation. Given that the subjects had to reproduce double the previously observed displacement, we hypothesized that they should develop a concept of when passing the single distance in the active condition. In the framework of predictive coding this should be indicated by a temporary increase in alpha band activity when aligning trials to the single distance.

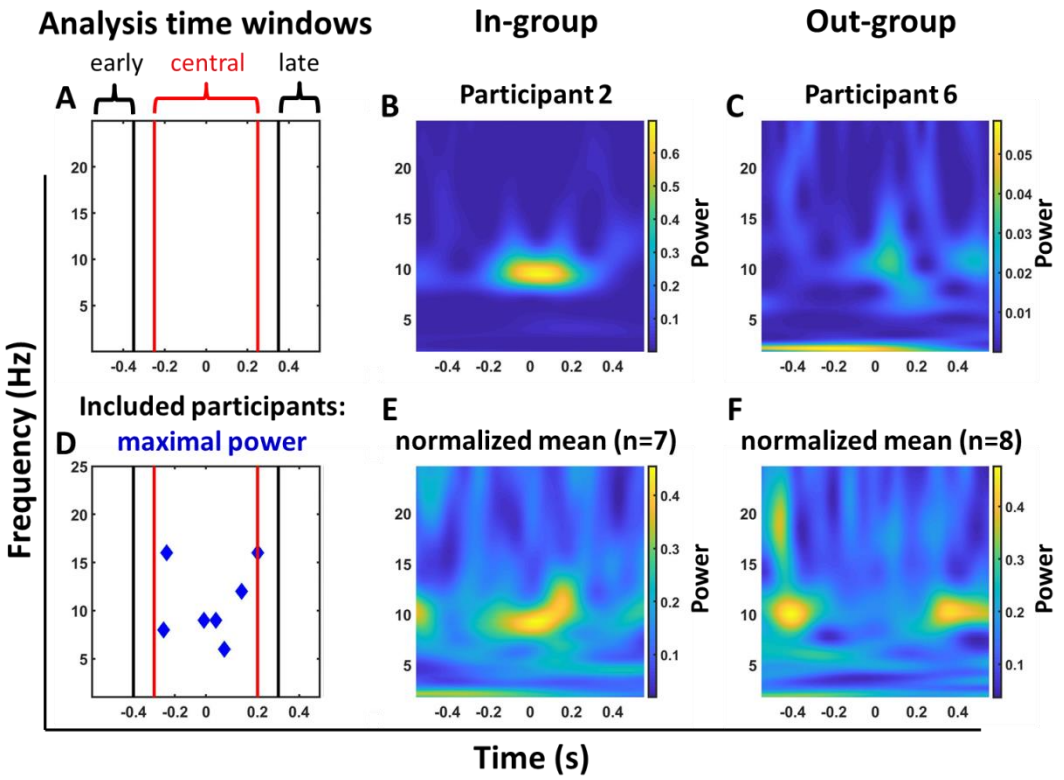

Figure S3-7: Time windows for analysis and corresponding time-frequency data from the active condition aligned to d_subjective of in-group and out-group participants. This plot shows in **A** and **D** the time windows used for the inclusion criterion. In addition, the times and frequencies of the maximum power values in the central window are presented in **D** for the in-group participants. Power spectra for the time window ±550 ms around d_subjective can be seen in **B**, **C**, **E** and **F**. In **B** data of a representative in-group participant is plotted in **B** and data of a representative out-group participant in **C**. The mean over the normalized power of all seven in-group participants is shown in **E** and the mean over the normalized power of the eight out-group participants in **F**.

Accordingly, we aligned EEG signals across trials to the moment when subjects had passed the objective single distance (d_objective) as well as the subjective single distance (d_subjective), i.e. half of the reproduced distance. Remarkably, seven out of fifteen of the participants showed an increase in power in the active condition time aligned to passing the subjective but not the objective single distance. In Figure S3-7B and S3-7C the time-frequency spectra for data from two representative participants can be seen, one of them representing an in-group (Figure S3-7B) and the other one an out-group (Figure S3-7C) participant (for inclusion criterion: see methods section). The in-group participant's data shows a power increase around 9 Hz for a short time window from about 150 ms before to 150 ms after the time for d_subjective. In the out-group participant's data the same effect can only be observed with a very small power increase. This temporary increase in power is also visible in the normalized mean data of the seven in-group participants (Figure S3-7E). It appears around 10 Hz defined as the alpha band frequency range. The normalized mean of the out-group participants' data (Figure S3-7F) does not show a short power increase around the time of alignment, i.e. the time when passing d_subjective. For each of the in-group participants the maximum power value of this alpha band power increase was determined. The corresponding time and frequency values can be seen in Table S3-4 and are plotted in the central time window in Figure S3-7D. We defined regions of ±100 ms and ±2 Hz around these values and averaged the power in these regions to compare them to the other conditions.

Participant #	**1**	**2**	**4**	**9**	**10**	**11**	**15**
Time (ms)	88	48	172	250	-190	-204	-9
Frequency (Hz)	6	9	12	16	16	8	9

Table S3-4: Times and Frequencies of the maximum alpha band power in the central time window for the seven in-group participants.

In a next step we compared these averaged power values with the power values in the same time-frequency window of corresponding replay condition also aligned to d_subjective, i.e. with data collected after the exact same visual stimulation (Figure S3-8A and S3-8B) separately for each of the time windows.

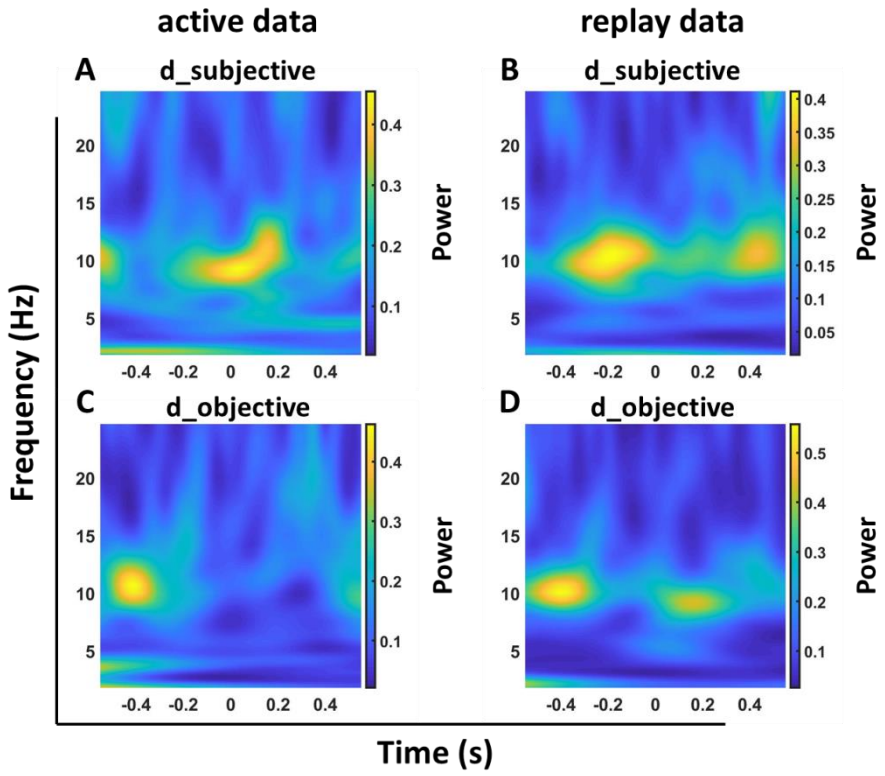

Figure S3-8: Time-frequency results from the active and replay condition for data aligned to d_subjective and for data aligned to d_objective. Power spectra for the time window ±550 ms around d_subjective can be seen in **A** and **B** and for the time window ±550 ms around d_objective are presented in **C** and **D**. In **A** and **D** data from the active condition is plotted and in **B** and **D** data from the replay condition. All four power spectra show the mean over data of all in-group participants. Before averaging the data was normalized to the maximum power value in the presented time windows for each participant separately.

The result showed a significant difference for the central time window, but not for the early and late time windows (Paired one-tailed t-test for the comparison active with replay: central: $t(6)=3.35$, $p=0.0077$; early: $t(6)=-2.07$, $p=0.96$; late: $t(6)=-0.82$, $p=0.78$, significance level for the total of 6 t-test after Bonferroni correction is 0.0083). This indicated the existence of a neural correlate of distance estimation around the alignment time. In order to test for this

effect being specific for the alignment to d_subjective, we compared the active and replay condition for data aligned to d_objective (Figure S3-8C and S3-8D) for the same time frequency regions per participant. For this new alignment the data did not show a significant difference for either of the time windows (Paired one-tailed t-test for the comparison active with replay: central: t(6)=-1.48, p=0.91; early: t(6)=-0.91, p=0.8; late: t(6)=0.85, p=0.21) supporting the idea that there is no distance effect for the alignment to the objective single distance.

We suggested that the increase of EEG activity in the alpha band as shown above is related to the subjects' concept of passing the distance to be reproduced. If this was the case, such increase in power in the alpha band should occur for multiples of this (perceived) distance. In order to test for this hypothesis, we invited one of the participants again. We presented the same stimuli, but now the participant's task was to the travel three times the distance perceived in the passive condition. We hypothesized to find an increase in alpha band activity when the subject passed the single and the double subjective distance.

We aligned single trial data to the subjective single distance (d_subjective_1/3), with d_subjective_1/3 being one third of the active distance, and to the corresponding double distance (d_subjective_2/3). The results can be seen in Figure S3-9 in the top row for the active and in the bottom row for the replay condition. Most remarkably, we observed a temporary increase in alpha band activity not only when this subject passed one third of its reproduced distance (B), i.e. d_subjective, but also when it passed two thirds, i.e. 2*d_subjective (C). No such power increase around the time of alignment was found for the replay condition. Taken together, we consider our results as further strong evidence for a neural correlate of subjective distance perception.

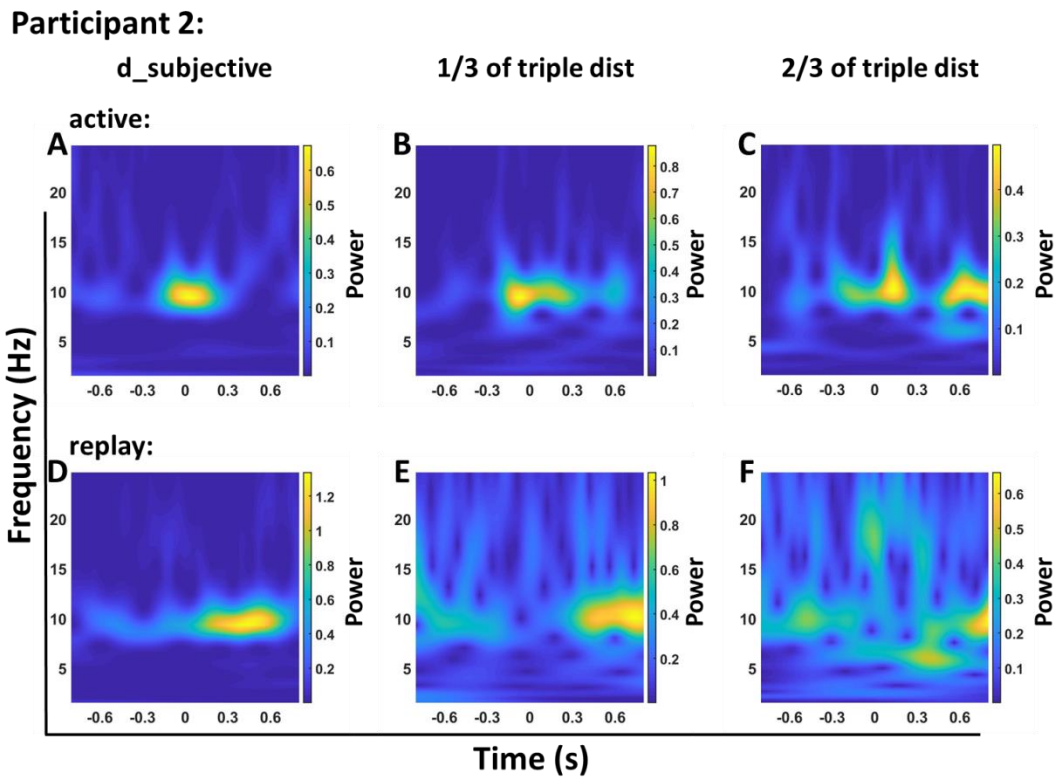

Figure S3-9: Time-frequency results for one participant from double and triple the passive distance experiments. We always present power spectra for the time window ±800 ms around the alignment time. In the top row (**A**, **B** and **C**) we show data from the active and in the bottom row (**D**, **E** and **F**) from the replay condition. For **A** and **D** data was collected in the experiment when the participant was asked to double the passive distance. Data was aligned to d_subjective, i.e. half of the traveled distance. For **B**, **C**, **D** and **F** results were calculated from data collected in the experiment when we asked the participant to triple the passive distance. In **B** and **E** data was aligned to one third of the traveled distance and in **C** and **F** to two thirds of the traveled distance.

4.5.5 Discussion

In this study we investigated neuronal correlates of the perception of traveled distance. A distance reproduction task was presented, with a passively observed displacement as a reference and the task to actively reproduce double of this perceived distance. A recording of the reproduced velocity profiles was played back to the participants later on in order to present trials with exactly the same visual information. This approach allowed us to compare the neural processing of self-induced vs. externally-induced visual stimulation. Participants showed an overshoot of reproduced distances, which decreased for larger distances, and a

velocity profile similar to the reference movement. EEG recordings revealed amplitude attenuation of VEP-components in response to self-motion onset and shorter latencies of VEP-components in response to self-motion offset – in the active as compared to the passive condition. Most remarkably, we were able to show an increase in alpha band activity corresponding to a subjective distance estimate. We suggest this increase in the alpha band activity to be indicative of a neural correlate of perceived travel distance.

It has been shown before that human participants are quite accurate in estimating traveled distances based solely on visual optic flow (Bremmer and Lappe, 1999). In this and related studies, participants typically overshot short and undershot long distances (Bremmer and Lappe, 1999; von Hopffgarten and Bremmer, 2011; Churan et al., 2017; Glasauer et al., 2007; Berthoz et al., 1995). Similar effects have also been documented with different response modalities and behaviors, like walking on a treadmill (Glasauer et al., 2007) or movement on a motorized robot while being blindfolded (Berthoz et al., 1995). In our study, we found an overshoot, which decreased for increasing travel distance. If we had tested even longer travel distances, this overshoot eventually might have turned in an undershoot.

Participants were explicitly asked to reproduce the previously observed distance rather than speed. Furthermore, across trials, displacements were presented at two different speeds, to avoid a too close link between velocity and distance. However, the most common strategy of our participants was trying to reproduce speed as observed in the passive displacement. When analyzing the velocity profiles of the active condition, we observed close similarities to the speed of self-motion stimulation in the passive condition. This reliance on the velocity profiles in distance discrimination tasks was reported before (Bremmer and Lappe, 1999; von Hopffgarten et al., 2011; Churan et al., 2017; Glasauer et al., 2007; Berthoz et al., 1995). Overall, our behavioral results were well in line with those from previous reports.

In addition to the behavioral performance of our participants, we also monitored the neural processing of visual self-motion information by means of EEG. Given that self-motion onset was not accompanied by a pattern onset, we were expecting to find a pronounced P1-N2-P2-complex with a N2 motion-specific peak dominance (Kuba et al., 2007; Heinrich,

2007). We found this response profile for all three experimental conditions (passive, active and replay). VEP data for motion offset also revealed the expected pattern, yet with amplitudes being on average lower than for motion onset. This differential effect is also in line with previous findings (Heinrich, 2007).

Continuous EEG activity preceding self-motion onset revealed some dynamics despite baseline correction. We consider this fluctuation to be not critical since we analyzed response modulation rather than absolute values. The response modulation, i.e. peak amplitude differences, for motion onset was larger in the passive as compared to the active and replay condition. In addition, for motion offset the P1-, N2- and P2-components appeared later, i.e. showed larger latencies, in the passive as compared to the active and replay conditions. These results are in line with the framework of predictive coding (Friston, 2005) and previous reports showing an attenuation of neural responses to self-induced sensory events (Shadmehr and Krakauer, 2008; Miall and Wolpert, 1996). The concept of predictive coding hypothesizes an efference copy (von Holst and Mittelstaedt, 1950) of the motor signal to help dissociating self-induced from externally induced sensory stimulation. In the passive condition, no such efference copy signal was available. Interestingly, active and replay conditions showed similar VEPs regarding to latency and response modulation although stimulation in the replay condition was not self-induced. This similarity could have occurred since participants might have been aware of the replay condition being a repetition of their own actively produced visual self-displacement. The difference of the passive and replay condition might also be due to the absence of a main task (besides fixation of the central target) in replay trials.

In the active condition participants deflected a joystick to control the self-motion stimulation. This deflection induced hand movement related signals in addition to the visual information. Remarkably, we could not find a significant difference between the VEPs of the active and replay condition evoked by the exact same visual stimulation. According to the general rule of “The absence of evidence is not evidence of absence”, this might simply be due to the large VEPs, which might have overruled smaller differences caused by the active as

compared to the replay condition. In addition, differential activation might have been found at other electrodes than Pz as studied here.

In order to analyze the subjective estimation of travel distance we investigated the EEG data in the time-frequency domain. We observe an enhancement in alpha band activity in the active condition time locked to when participants were passing d_subjective. We found such an enhancement for 7 out of 15 participants. These participants did neither show similar time locked activity increase in data from the replay condition nor in data aligned to d_objective. This suggests an internal representation of subjective distance perception. The design of the experiment allowed the participants to control the speed and duration of their movement. We conclude that the enhanced alpha band activity we found was most likely not related to their action, i.e. deflecting the joystick, because this would have been present throughout the whole movement. Interestingly, a similar increase in the alpha band could be observed when one participant was asked to triple the passively observed distance. So far, we only collected data from one participant in this task. We aligned the data to 1/3 and 2/3 of the traveled active distance and found an increase in alpha band activity time locked to these two alignment times. The finding of this effect for alignment to 1/3 of the active distance reproduces the results reported before, i.e. an increase in alpha band activity when passing d_subjective, for this participant. The occurrence of this effect also for the alignment to 2/3 of the traveled distance supports the idea of this alpha band increase showing a representation of the subjective single distance. Integration about the visual input and the resulting traveled distance could lead to an increase in activity as soon as the desired distance is reached. Our findings which report an increase in alpha band activity every time the single distance is completed suggest that this integration process starts again after passing the subjective single distance.

In contrast to the attenuated VEP signals in the active condition most likely being a consequence of the self-induced sensory stimulation, i.e. an efference copy signal (von Holst and Mittelstaedt, 1950), we found an increase in alpha activity in the active condition. However, we think also this enhanced activity could still be in line with the predictive coding

theory (Friston 2005, 2010). It describes loops of information flow. Predictions about upcoming events are processed as top-down signals to be compared to incoming sensory information. In order to optimize perception, the differences between the sensory signals and the predictions have to be kept as small as possible. Resulting prediction errors are processed as bottom-up signals to adjust the expectations about our environment. It has been shown that the different directions of information flow in the brain are associated with specific oscillatory activity. Gamma oscillations are suggested to facilitate bottom-up information flow, while alpha oscillations are indicative of top down feedback processes (Bastos et al., 2015; Jensen et al., 2015; Michalareas et al., 2016). The increase in alpha band activity around d_subjective could represent such a feedback process reporting to sensory cortex that the subjective single distance is reached and will be reproduced a second time.

In summary, we could confirm previous findings showing that human observers are capable of reproducing a traveled distance solely based on visually simulated self-motion. Active reproduction of a previously seen passive displacement was accompanied by an attenuation of the VEP-components in the self-generated stimulation as compared to the externally induced stimulation. These results are in line with the idea of an efference copy signal in the framework of predictive coding. Finally and most remarkably, using time-frequency analysis we found evidence for a neural signature of perceived distance.

4.5.6 References

Arnal, L. H., Giraud, A.-L. Cortical oscillations and sensory predictions. *Trends in Cognitive Sciences*, **16(7)**, 390-8 (2012).

Bastos, A. M., Vezoli, J., Bosman, C. A., Schoffelen, J.-M., Oostenveld, R., Dowdall, J. R., De Weerd, P., Kennedy, H., Fries, P. Visual areas exert feedforward and feedback influences through distinct frequency channels. *Neuron*, **85**, 390-401 (2015).

Bays, P. M., Wolpert, D. M., Flanagan, J., R. Perception of the consequences of self-action is temporally tuned and event driven. *Current Biology*, **15**, 1125-1128 (2005).

Bäß, P., Jacobsen, T., Schröger, E. Suppression of the auditory N1 event-related potential component with unpredictable self-initiated tones: Evidence for internal forward models with dynamic stimulation. *International Journal of Psychophysiology*, **70**, 137-143 (2008).

Benazet, M., Thénault, F., Whittingstall, K., Bernier, P.-M. Attenuation of visual reafferent signals in the parietal cortex during voluntary movement. *J Neurophysiol*, **116**, 1831-1839 (2016).

Berthoz, A., Israel, I., Georges-Francois, P., Grasso, R. and Tsuzuku, T. Spatial memory of body linear displacement: what is being stored? *Science,* **269**, 95–98 (1995).

Blakemore, S.-J., Wolpert, D. M., Frith, C. D. The cerebellum contributes to somatosensory cortical activity during self-produced tactile stimulation. *NeuroImage*, **10**, 448-459 (1999).

Bremmer, F., Lappe, M. The use of optical velocities for distance discrimination and reproduction during visually simulated self motion. *Exp Brain Res*, **127**, 33-42 (1999).

Bremmer, F., Kubischik, M., Hoffmann, K. P., Krekelberg, B. Neural dynamics of saccadic suppression. *J Neurosci*. **29(40)**, 12374-83 (2009).

Chakravarthi, R., VanRullen, R. Conscious updating is a rhythmic process. *PNAS*, **109(26)**, 10599-10604 (2012).

Churan, J., Paul, J., Klingenhoefer, S., Bremmer, F. Integration of visual and tactile information in reproduction of traveled distance. *J Neurophysiol*, **118**, 1650-1663 (2017).

Clayton, M, Yeung, N., Kadosh, R. C: The roles of cortical oscillations in sustained attention. *Trends in Cognitive Sciences*, **19(4)**, 188-195 (2015).

Clayton, M. S., Yeung, N., Kadosh, R. C. The many characters of visual alpha oscillations. *European Journal of Neuroscience*, **48**, 2498-2508 (2018).

Erikson, R. G., Thier, P. A neuronal correlate of spatial stability during periods of self-induced visual motion. *Exp Brain Res.*, **86(3)**, 608-16 (1991).

Frenz, H., Bremmer, F., Lappe, M., Discrimination of travel distances from 'situated' optic flow. *Vision Research*, **43**, 2173-2183 (2003).

Frenz, H., Lappe, M., Absolute travel distance from optic flow. *Vision Research*, **45**, 1679-1692 (2005).

Friston, K. A theory of cortical responses. *Philosophical Transactions of the Royal Society B*, **360(1456)**, 815-836 (2005).

Friston, K. Does predictive coding have a future? *Nature Neuroscience*, **21**, 1019-1021 (2018).

Gibson, J. J. The perception of the visual world. *The Riverside Press*, Cambridge, Massachusetts (1950).

Glasauer, S., Schneider, E., Grasso, R., Ivanenko, Y. P. Space–Time Relativity in Self-Motion Reproduction. *J Neurophysiol*, **97**, 451-461 (2007).

Haegens, A., Barczak, A., Musacchia, G., Lipton, M. L., Mehta, A. D., Lakatos, P., Schroeder, C. E. Laminar profile and physiology of the α rhythm in primary visual, auditory, and somatosensory regions in neocortex. *The Journal of Neuroscience*, **35(42)**, 14341-14352 (2015).

Heinrich, S. P. A primer on motion visual evoked potentials. *Doc Ophthalmol*, **114**, 83-105 (2007).

Herrmann, C. S., Rach, S., Vosskuhl, J., Strüber, D. Time-frequency analysis of event-related potentials: a brief tutorial. *Brain Topography*, **27**, 438-450 (2014).

Hughes, G., Desantis, A., Waszak, F., Attenuation of auditory N1 results from identity-specific action-effect prediction. *European Journal of Neuroscience*, **37**, 1152-1158 (2013).

Jensen, O., Bonnefond, M., Marshall, T. R., Tiesinga. P. Oscillatory mechanisms of feedforward and feedback visual processing. *Trends in Neurosciences*, **38(4)**, 192-194 (2015).

Jokisch, D., Jensen, O. Modulation of gamma and alpha activity during a working memory task engaging the dorsal or ventral stream. *The Journal of Neuroscience*, **27(12)**, 3244-3251 (2007).

Klimesch, W. Alpha-band oscillations, attention, and controlled access to stored information. *Trends in Congnitive Sciences*, **16(12)**, 606-617, (2012).

Krock, R. M., Moore, T. The influence of gaze control on visual perception: eye movements and visual stability. *Cold Spring Harb Symp Quant Biol*, **79**, 123-130 (2014).

Kuba, M., Kubová, Z., Kremlácek, J., Langrová, J. Motion-onset VEPs: characteristics, methods, and diagnostic use. *Vision Research*, **47(2)**, 189-202 (2007).

Leske, S., Tse, A., Oosterhof, N. N., Hartmann, T., Müller, N., Keil, J., Weisz, N. The strength of alpha and beta oscillations parametrically scale with the strength of an illusory auditory percept. *NeuroImage*, **88**, 69-78 (2014).

Lee, D. N. The optic flow field: the foundation of vision. *Philos Trans R Soc Lond (Biol)*, **290**, 169-179 (1980).

Lozano-Soldevilla, D., ter Huurne, N., Cools, R., Jensen, O. GABAergic modulation of visual gamma and alpha oscillations and its consequences for working memory performance. *Current Biology*, **24**, 2878-2887 (2014).

Lundqvist, M., Herman, P., Lansner, A. Effect of prestimulus alpha power, phase, and synchronization on stimulus detection rates in a biophysical attractor network model. *The Journal of Neuroscience*, **33(29)**, 11817-11824 (2013).

Miall, R. C., Wolpert, D. M. Forward models for physiological motor control. *Neural Networks*, **9(8)**, 1265-1279 (1996).

Michalareas, G., Vezoli, J., van Pelt, S., Schoffelen, J.-M., Kennedy, H., Fries, P. Alpha-beta and gamma rhythms subserve feedback and feedforward influences among human visual cortical areas. *Neuron*, **89**, 384-397 (2016).

Pfurtscheller, G., Stancák Jr, A., Neuper, C. Event-related synchronization (ERS) in the alpha band – an electrophysiological correlate of cortical idling; A review. *International Journal of Psychophysiology*, **24**, 39-46 (1996).

Shadmehr, R., Krakauer, J. W. A computational neuroanatomy for motor control. *Experimental Brain Research*, **185**, 359-381 (2008).

Shergill, S. S., White, T. P., Joyce, D. W., Bays, P. M., Wolpert, D. M., Frith, C. D. Modulation of somatosensory processing by action. *NeuroImage*, **70**, 356-362 (2013).

Stefanics, G., Kremlácek, J., Czigler, I. Visual mismatch negativity: a predictive coding view. *Frontiers in Human Neuroscience*, **8**, 666 (2014).

Sperry, R. W. Neural basis of the spontaneous optokinetic response produced by visual inversion. *J Comp Physiol Psychol.* **43(6)**, 482-9 (1950).

Supp, G. G., Siegel, M., Hipp, J. F., Engel, A. K. Cortical hypersynchrony predicts breakdown of sensory processing during loss of consciousness. *Current Biology*, **21**, 1988-1993 (2011).

Thaler, L., Schütz, A. C., Goodale, M. A., Gengenfurtner, K. R. What is the best fixation target? The effect of target shape on stability of fixational eye movements. *Vision research*, **76**, 31-42 (2013).

von Holst, E., Mittelstaedt, H. Das Reafferenzprinzip. *Naturwissenschaften*, **37(20)**, 464–476 (1950).

von Hopffgarten, A., Bremmer, F. Self-motion reproduction can be affected by associated auditory cues. *Seeing Perceiving*, **24(3)**, 203-22 (2011).

Wang, J., Mathalon, D. H., Roach, B. J., Reilly, J., Keedy, S. K., Sweeney, J. A., Ford, J. M. Action planning and predictive coding when speaking. *NeuroImage*, **91**, 91-98 (2014).

Weiskratz, L., Elliott, J., Darlington, C. Preliminary observations on tickling oneself. *Nature*, 230 (1971).

Winkler, I., Czigler, I. Evidence from auditory and visual event-related potential (ERP) studies of deviance detection (MMN and vMMN) linking predictive coding theories and perceptual object representations. *International Journal of Psychophysiology,* **83**, 132-143 (2012).

5 General discussion and outlook

In my thesis I used electroencephalogram (EEG) measurements and functional magnetic resonance imaging (fMRI)-guided transcranial magnetic stimulation (TMS) to investigate the processing of visually simulated self-motion, in particular, the perception of self-motion direction and traveled distance. The previously reported accurate performance of human participants in heading estimation and distance reproduction solely based on visual information was motivation to study the underlying neural processes. Of special interest was the role of predictions about the upcoming events for the processing of self-motion information. An additional main objective of my thesis was to compare self-motion processing in humans and the macaque monkey, i.e. the animal model for human sensorimotor processing.

5.1 Perception and neural correlates of visually simulated self-motion

Moving through our environment is an essential ability during everyday life. Under natural conditions an integration of signals from all the different senses provides the basis of accurate self-motion estimation (e.g. Hlavacka et al., 1996; Angelaki et al., 2011; von Hopffgarten, 2011; Churan et al. 2017). Interestingly, visual information only is sufficient for accurate judgement of one's direction of self-motion (heading) as well as distance estimation and distance reproduction (Heading: e.g. Gibson, 1950; Warren and Hannon, 1988; Lappe et al. 1999; Lich & Bremmer, 2014. Distance estimation and reproduction: Gibson, 1950; Bremmer and Lappe, 1999; Redlick et al., 2001; von Hopffgarten and Bremmer, 2011; Churan et al., 2017). Under static conditions, i.e. without object motion in the scene as well as without head or eye movements, the only visual information about self-motion is provided by a flow field of the surrounding environment, the optic flow (Gibson, 1950; Britten, 2008). The singularity of this flow field is correlated with the direction of self-motion.

In my thesis I presented optic flow stimulations to simulate forward self-motion. In addition to the above mentioned studies focusing on participants' behavior, I analyzed also the neuronal correlates of visual self-motion processing by means of EEG measurements and TMS. Using these methods I wanted to learn more about the information provided by optic flow and how it is processed to optimize self-motion perception. As a first important result I could show that the behavioral data of all three studies included in this thesis replicate the findings of previous studies and provide further evidence for the close-to-veridical perception of heading as well as the accurate estimation and reproduction of traveled distances based on information provided by optic flow.

One advantage of using EEG recordings is the very high time resolution of the data which allows to precisely analyze the responses to self-motion stimuli. In the data I found clear VEP-components showing the characteristics of EEG data recorded in response to visual motion-onset and -offset (Kuba, 2007; Heinrich, 2007). In addition, I investigated more complex EEG-components in response to the visual self-motion stimuli. In the first study of my thesis I could show that optic-flow stimuli presented in an oddball paradigm induce a visual Mismatch-Negativity (vMMN). The MMN is a component of the event related potentials as response to a deviant stimulus in a sequence of standard stimuli. An MMN has been reported for many visual features in previous studies, like orientation (Sulykos and Czigler, 2011), direction of motion (Kuldkepp et al., 2013), duration (Khodanovich et al., 2010), color (Müller et al., 2012), numerosity (Hesse et al., 2017), target trajectory (Schmitt et al., 2018), but also higher cognitive features such as object structure (Müller et al., 2013) and facial emotions (Wang et al., 2016). The occurrence of the vMMN in my results allowed some conclusions about the processing of visual self-motion information. First, a sequential rule concerning heading must have been extracted from the visual stimulus and predictions about the upcoming heading were formed. Previous studies have discussed that this building of an internal model based on the regularity of the stimulation is required for inducing a MMN-component (Stefanics et al. 2014). Second, violations to these predictions, i.e. a change in self-motion direction, were detected and led to the vMMN-component. The source for the

vMMN is the larger elicited N2-component in response to unexpected deviant stimuli compared to the response to standard stimuli. This result is well in line with previous studies on object-motion (Pazo-Álvarez, et al., 2004; Schmitt et al., 2018). Third, this MMN-component is considered to be a component indicating preattentive processing of the stimulus feature under study, here the heading. The idea of a preattentive nature of the MMN has been derived from studies in which participants had to pay attention to another feature of the visual scene not related to the standard and deviant stimulus (Pazo-Àlvarez et al., 2004; Stefanics, et al., 2012; Li et al., 2012; Kuldkepp et al., 2013). Along the same vein, my study also included a visual discrimination task unrelated to self-motion direction. Nevertheless, I found a vMMN-component in the EEG data. This MMN-component could be detected for both heading directions, but showed a lateralized effect. Despite the optic flow stimulus, the ground plane, covering the complete lower half of the monitor, the recorded vMMN-component was stronger, i.e. had more negative values, on electrodes contraversive to the self-motion direction. Based on this result I suggest as a fourth conclusion that predominantly brain regions contralateral with respect to the simulated heading are important for the extraction of self-motion direction information as early as around 150 ms after stimulus presentation. This idea is in line with results from a previous study employing single cell recordings in macaque monkeys in medial superior temporal area (MST) and the ventral intraparietal area (VIP) (Bremmer et al., 2010; Kaminiarz et al., 2014; Greenlee et al., 2016). In these studies, a bias towards contraversive heading was reported. More specific, most neurons in the right brain hemisphere showed maximum responses to optic flow stimuli with heading to the left and vice versa.

My second study, i.e. investigating self-motion processing in the human functional equivalent of macaque area MST (hMST), was based on this processing asymmetry. I used TMS pulses to stimulate area hMST, which has been shown to be important for self-motion processing (in macaque monkeys (MST): Saito et al., 1986; Duffy and Wurtz 1991; Lappe et al., 1996; Gu et al., 2006; Bremmer et al., 2010, in humans (hMST): Huk et al., 2002). I presented visually simulated forward self-motion with three different headings, but stimulated with TMS only the

right hemisphere hMST. The results revealed a significantly larger variance in heading estimation for self-motion to the left, i.e. heading contraversive with respect to the stimulation site. With this TMS study I could causally link the brain area hMST to the processing of heading and provide further strong evidence for a critical role of hMST in the processing of visually induced self-motion by optic flow stimulation.

Optic flow does not only reveal information concerning self-motion direction, but also accurate distance estimations can be performed based on optic flow stimulations (Bremmer & Lappe, 1999; Harris et al., 2000; Frenz et al., 2007; von Hopffgarten & Bremmer, 2011; Churan et al., 2017). This has e.g. been shown in a distance discrimination task in which two different visually simulated self-motion distances were presented to the participants (Frenz et al., 2003). The accurate performance of the participants was not influenced by displaying different environments for the two self-motions, nor by the simulated speed or the viewing angle. In following experiments it could be demonstrated that the estimation of a distance presented as an optic flow stimulus could be reproduced by actively walking this distance without visual feedback, by adjusting a static interval (Frenz and Lappe, 2005), or by indicating the distance estimation in a second visually simulated self-motion stimulus (Redlick et al., 2001). I could replicate these accurate behavioral results by asking participants to reproduce a traveled distance and additionally I could show differences in the VEPs measured after self-motion on- and offset. The potentials recorded in the different navigation conditions (passive, active or replay) revealed significant modulations. These results are in line with the attenuation of responses after self-induced sensory input reported by previous studies (e.g. Benazet et al., 2016). More generally, this result can be explained in the context of the predictive coding theory and will be discussed in the next chapter.

In addition, in the third and final study of my thesis I aimed to find a neural correlate of traveled distance. In this study, participants had to reproduce double the distance of a previously observed self-displacement. Interestingly, I found a neural correlate indicating the passing of a specific traveled distance in about half of the participants' data. Importantly, this result was found when aligning data to the participants' individual estimation of the previously

presented single distance. I found a short increase in alpha band activity of about 200 ms length time locked to passing this distance. Similar to the attenuated responses to expected sensory input this data can be interpreted with the predictive coding theory and will be discussed in the next chapter.

Taken together, with EEG measurements I was able to record the neuronal correlates of self-motion processing. Differences in the VEPs caused by changes in the self-motion stimulation showed an additional source of information for the understanding of the neural processing of visually simulated self-motion.

5.2 The role of prediction for self-motion processing

We are constantly busy with perceptual tasks and the processing of vast amounts of incoming sensory information. This context is at odds with our limited neural processing resources. One way of solving this conflict could be taking advantage of the knowledge about well-known processes in our environment. Based on our experiences and often based on repeating events we can form internal prediction models about upcoming events (prior). We expect to experience sensory events which have the highest probability in our internal models. This enables us to react fast and precise. Obviously the internal models have to be kept up to date and need to be adjusted to changes in the environment. The *predictive coding theory* describes the connection between perception and prediction (Friston, 2005, 2010). The underlying principle is the attempt of our brain to minimize the effort (or energy) required for any perceptual task. Predictions about the upcoming sensory event have the advantage that the system is already prepared for the predicted sensory input and does not need so much computational power if the prediction is fulfilled. In contrast, if something unexpected happens, which is usually critical for surviving, the prediction is violated and an error message, the prediction error, has to be reported in order to adjust the prediction model (Friston, 2005; Winkler and Czigler, 2012; Stefanics et al., 2014). This process and the underlying theory are important in almost every prediction task and it is crucial to explore the

neuronal processes. In the first and third study of my thesis I showed a fast processing of visual information using predictions about future events. In these studies I could show indications for the different steps of the predictive coding theory which is described as being organized in hierarchical loops (Friston, 2005; 2010; 2018; Stefanics et al., 2014).

The part of these loops describing the comparison of the predictions with the sensory input and the updating of the internal models caused by detected prediction errors could be revealed in the first study. I presented two different self-motion directions in an oddball paradigm and found a vMMN-component caused by smaller amplitudes of the N2 ERP-components after the predicted standard stimulation.

The vMMN-component is indicative of a prediction error (for reviews see Winkler and Czigler, 2012; Stefanics et al., 2014) and is visible in the data when a surprising deviant stimulus is presented. Importantly, in my study, standard and deviant stimuli were physically identical and their role (standard vs. deviant) was only defined through the context of presentation. According to the predictive coding model prediction errors have to be reported to a higher brain area in order to update the existing model about the upcoming sensory information. Most likely the MMN-component is a neuronal correlate of the updating process of these models (Winkler and Czigler, 2012; Stefanics et al., 2014).

In line with this finding, the VEP-components recorded in the third study showed a similar result. I compared data recorded in self-induced and externally-induced self-motion stimuli. Only during self-induced stimulation, the sensory event could be predicted. Indeed, I found an attenuation of the VEP-components' amplitude in self-induced stimuli for motion onset and a shorter latency for these components recorded after motion offset. These smaller and faster responses for self-induced stimuli can be explained with the concept of an efference copy (Benazet et al., 2016). An internal copy of every motor command is created which helps to anticipate the sensory consequences of the action. This internal representation is especially important for the sense of agency, the ability to differentiate between self-induced and externally-induced motions, and was termed efference copy (von Holst and Mittelstaedt, 1950) or corollary discharge (Sperry, 1950). Since the internal copy of the motor plan

provides information about the upcoming sensations before they occur in order to prepare our system, the whole model is based on predictions about future events. This concept, hence, is in line with the predictive coding theory and shows the minimization of energy used for the processing of expected events by the attenuated signals in response to self-induced motion (Wolpert, and Flanagan, 2001; Bays et al., 2006; Benazet et al., 2016). In contrast to the vMMN-component described earlier, in this case the predictions are not formed by the repetitive presentation of the same stimulus, but by an internal copy of a motor command. The concept of efference copy could represent one possibility to create the predictions necessary in the predictive coding theory. Violations to these predictions and the resulting errors have to be used to update the internal models. This updating of predictions in motor tasks based on violations of the expectations has been shown e.g. in studies which manipulated the outcome of motor actions (Cressman and Henriques, 2010). Participants learned over time that the predicted outcome of a motor action was modified in a specific way and they successfully adjusted their movement in order to reach the desired location.

So far, however, I have considered only parts of the predictive coding theory: The different ways of generating predictions, the comparison of them with the incoming sensory information and the updating of the internal models based on prediction errors. In order to complete the hierarchically structured loops of the predictive coding theory there is one more information flow which has to be considered. The predictions have to be reported in a feedback manner to lower levels to provide information for the comparisons e.g. with the sensory input (Friston, 2005; 2010; 2018; Stefanics et al., 2014). In order to study this part of the predictive coding theory I analyzed my data in the frequency domain. It has been shown that brain oscillations in different frequency bands are important for the communication between different brain areas and clusters of neurons (Clayton et al., 2015). Oscillations in the gamma range have been reported to carry bottom-up information while oscillations in the alpha range carry feedback information (Bastos et al., 2015; Jensen et al., 2015; Michalareas et al., 2016). This view is supported for example by a study using electrical stimulations in macaque monkeys (van Kerkoerle et al., 2014). The interaction of low-level and high-level

areas of the visual cortical system was investigated in order to distinguish between feedforward and feedback processes. It was demonstrated that stimulations of area V4 elicited alpha oscillations in the lower area V1 showing the propagation of alpha oscillations from V4 to V1. On the contrary, microstimulation of V1 elicited gamma oscillations in V4, suggesting gamma oscillations being a signature of feedforward processing.

In the third study of my thesis I found bursts of alpha activity in the data collected in the distance reproduction task in a specific condition. Data of the active trials were aligned to the subjective distance of a previously seen displacement (d_subjective) before a wavelet analysis was performed. An increase in alpha activity in about half of our participants around this time of alignment was revealed. No such alpha band activity occurred in the data from the replay trials which showed exactly the same visual input. Remarkably, when aligning the data to the objective (d_objective) time of passing this distance, i.e. to the exact distance independent of the single participants' performance, I also did not observe such an effect. I conclude that the data are showing the feedback process described in the predictive coding theory. In the active reproduction task, the incoming sensory information i.e. the traveled distance has to be continuously compared to the previously observed self-displacement. More specifically, travel distance constantly increased during self-motion and I expected a feedback signal to be induced when the required distance was reached. In a previous study it has been shown that participants used an integration process to estimate a traveled distance during optic flow (Lappe et al., 2007). It was reported that the task determined the integration variable. If a visually simulated forward self-motion with a specific distance was presented to the participants first and they had to adjust a target location to this distance in a second step, participants integrated over the remaining distance to the goal. In case of the static presentation of a target location first and the task to stop a visually simulated self-motion at the estimated target location, participants integrated over the cumulative distance starting from the origin. In my study, initially I had asked subjects to stop their actively controlled self-motion when the required distance was reached. Yet, this behavior induced (i) strong hand-action related artefacts and (ii) a dramatic change in ongoing visual stimulation. Hence,

participants' task was to reproduce double the length of the passively observed distance. At the subjective single distance (d_subjective) I expected participants to realize the completion of the remembered distance. In such case, they would have to start integrating the traveled distance again in order to reach the task criteria, i.e. to travel double the observed distance. In this scenario, I expected to find an increase in alpha band activity every time they would pass the remembered single distance. To test for this hypothesis I asked so far one participant to travel not only double but three times the previously observed self-displacement. I aligned the data to the passing of the single distance and to the passing of the double distance. When analyzing the data of this one participant I observed an increase in alpha activity at the time point when the single distance was passed, which means I could replicate the data from the previous experiment. I also observed as expected a similar effect when passing double the distance, which supports my hypothesis. Our results show indications for the feedback part of the loops described by the predictive coding theory important for the connections of the predictions to lower brain areas to be compared to the incoming signals.

Taken together, my thesis provides strong evidence for the importance of predictions for perceptual tasks in particular for the perception of optic flow stimuli simulating self-motion. In addition, my data supports the predictive coding theory in describing these prediction and perception processes.

5.3 Comparison between the processing of self-motion information in humans and non-human primates (NHP)

In my thesis I used different methods to learn more about the neuronal correlates of the perception of visually simulated self-motion. In the first study I recorded EEG data in an oddball-experiment presenting different self-motion directions and in the third study in a distance reproduction experiment. I used TMS in the second study to stimulate area hMST in order to disturb the heading discrimination abilities. These methods provided us with very

interesting results, but at the same time they are not as precise as single cell recordings. Especially the spatial resolution of the EEG recordings and TMS stimulation lack accuracy in comparison to recordings from single neurons. This shows the importance of an animal model for human sensorimotor processing. Studies combining human and non-human primate data are therefore essential in order to understand the similarities and potential differences in the neural processing of sensory information. In my thesis I applied the same experimental approach (oddball paradigm) in humans and macaque monkeys and used a model based on single cell recordings in monkeys to predict the modulation of heading perception due to TMS in humans.

In the first study of my thesis I recorded EEG data during an oddball experiment with two different self-motion directions as the difference between deviant and standard trials. In the results I found a vMMN-component with amplitude of about -2.8 µV around 140 ms after self-motion onset (Figure D-2, and in Figure S1-2 in the first study of this thesis). The same stimulus, without the attention task, was presented to a macaque monkey and data was collected by other members of our group with the same surface EEG-system. Due to spatial restrictions on the monkey's head we could only analyze one electrode which was placed over parietal areas (for exact location see Figure D-1). Interestingly, the data, which is presented in Figure D-2C and D-2D, revealed a structure similar to the human EEG data, presented in Figure D-2A and D-2B, and in Figure S1-2 in the first study of this thesis. The characteristic motion onset VEPs could be reported nicely in the human data for deviant as well as standard trials (Heinrich, 2007; Kuba, 2007). In the monkey data these components could be observed as well, although in a slightly different shape. In general, the characteristic components P1, N2 and P2 had shorter latencies of about 50 ms compared to the human data and showed larger amplitudes; the N2-component for example had a larger amplitude of about 5 µV. These differences between the human and monkey data are in line with previous studies (Reinhart et al., 2012, Woodman, 2012).

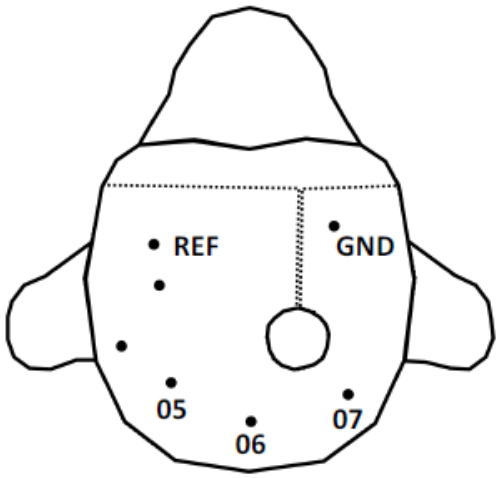

Figure D-1: Electrode arrangement on the macaque monkey. The figure shows the positions of the reference electrode (REF), the ground electrode (GND) and the five normal electrodes with the three posterior electrodes 05, 06, and 07.

Human as well as monkey data showed higher amplitudes for the N2-component in the deviant compared to the standard trials which resulted in the vMMN-components (deviant-standard). Accordingly, also in monkeys a sequential rule could be extracted from the standard stimuli, which was used to create a prediction about the upcoming stimulus according to the predictive coding theory. In case of a violation of this prediction, the presentation of a deviant stimulus, the resulting prediction error, has to be reported to the next higher brain area to update the internal prediction model (Stefanics et al. 2014). Additionally, the vMMN-component in the monkey data also suggests the preattentive processing of heading. We cannot exclude that the monkey might have payed attention to the self-motion direction, but the eye movements were controlled to ensure fixation to the presented target. In addition, the monkey was rewarded for fixating throughout the whole trial and had no motivation to perform another movement or attention task. Most important in this study was the finding of the similarity between the human and the monkey data which let us suggest that the underlying neuronal processes are very similar or the same for the perception of self-motion directions based solely on optic flow information. In a next step, EEG and single cell recordings shall be combined to further investigate the neuronal correlates of the processing of self-motion information.

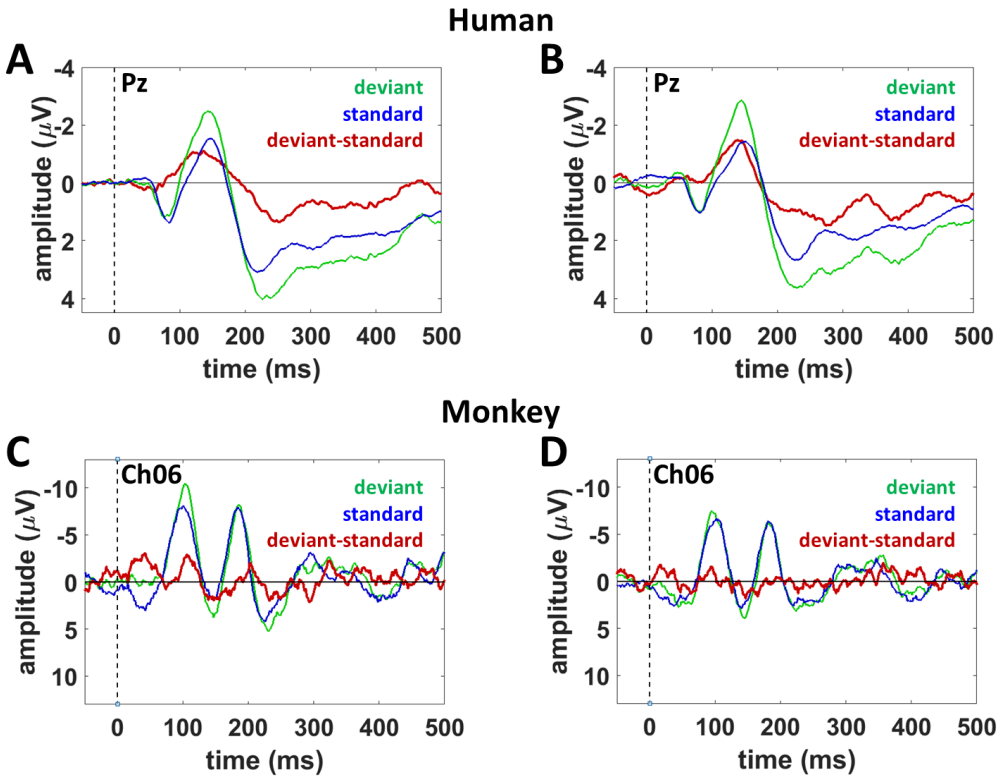

Figure D-2: Time course of a visual mismatch negativity (vMMN) component with data averaged over 12 human participants in the top row and one monkey in the bottom row. Human data was already presented and discussed in study I. The figure represents the EEG data recorded in an oddball experiment showing an optic flow stimulus simulating self-motion 10° to the right or 10° to the left across a ground plane of random dots on a monitor while the participants fixated the center of the screen. In one half of the trials heading to the left was presented as standard stimulus and heading to the right as deviant stimulus and vice versa in the other half of the trials. This made it possible to compare data for a given heading direction collected in oddball trials with data for the same heading direction collected in standard trials. The responses to deviant trials are plotted in green, the responses to standard trials in blue and the difference (deviant-standard) in red. The EEG data presented was aligned (t=0 ms) to the motion onset and recorded on electrode Pz for the human data and electrode 06 on the monkey head (see Figure D-1 for exact position).

In order to test if data from humans and non-human primates show similarities it is not always necessary to present exactly the same stimulus, instead data from an experiment with monkeys can be used to predict the outcome of a similar experiment in humans. In the second study in this thesis we used information provided from previous monkey studies to build a model which could predict the consequences of the TMS pulses on heading estimations. The model was based on neural activity from monkey areas MST and VIP. An

optic flow stimulus simulating self-motion was presented while reflexive slow and fast eye movements were measured (Bremmer, et al., 2017). The model developed in this study was trained to decode heading from neuronal discharges. For the second study included in this thesis a modification of this model was used to simulate the effect of TMS stimulations on area hMST. As predicted by the model we recorded a larger variance in heading estimations for self-motion to the left after TMS stimulation of right hemisphere hMST. These results showed that data recorded in macaque monkeys can be used to predict results measured with human participants.

More generally speaking, my thesis provided further strong evidence for the macaque monkey as animal model for human sensorimotor processing. This result should be taken into account for stimulus and experimental design in future studies. It might allow investigations of perceptual processes with a spatial and temporal resolution not achievable in humans. Especially advantages in a better understanding of mal-processing of self-motion information as observed in cases of changes in the neural processing of self-motion information as occurring not only in healthy-aging (e.g. Lich and Bremmer, 2014) but also in neurological and neuropsychiatric disorders like Parkinson's or Alzheimer's disease (Mapstone and Duffy, 2010; van der Hoorn et al., 2014; Wang et al., 2017) could be achieved.

5.4 References

Angelaki, D. E., Gu, Y., DeAngelis, G. C. Visual and vestibular cue integration for heading perception in extrastriate visual cortex. *J Physiol*, **589.4**, 825-833 (2011).

Bastos, A. M., Vezoli, J., Bosman, C. A., Schoffelen, J.-M., Oostenveld, R., Dowdall, J. R., De Weerd, P., Kennedy, H., Fries, P. Visual areas exert feedforward and feedback influences through distinct frequency channels. *Neuron*, **85**, 390-401 (2015).

Bays, P. M., Flanagan, J. R., Wolpert, D. M. Attenuation of self-generated tactile sensations is predictive, not postdictive. *PLoS Biol*, **4(2)**: e28

Benazet, M., Thénault, F., Whittingstall, K., Bernier, P.-M. Attenuation of visual reafferent signals in the parietal cortex during voluntary movement. J Neurophysiol, **116**, 1831-1839 (2016).

Bremmer, F., Lappe, M. The use of optical velocities for distance discrimination and reproduction during visually simulated self motion. *Exp Brain Res*, **127**, 33-42 (1999).

Bremmer, F., Kubischik, M., Pekel, M., Hoffmann, K.-P-, Lappe, M. Visual selectivity for heading in monkey area MST. *Exp. Brain Res.*, **200**, 51-60 (2010).

Bremmer, F., Churan, J., Lappe, M. Heading representations in primates are compressed by saccades. *Nature Communications*, **8:920,** (2017).

Britten, K. H. Mechanisms of self-motion perception. *Annu. Rev. Neurosci.*, **31**, 389–410 (2008).

Churan, J., Paul, J., Klingenhoefer, S., Bremmer, F. Integration of visual and tactile information in reproduction of traveled distance. *J Neurophysiol*, **118**, 1650-1663 (2017).

Clayton, M. S., Yeung, N., Kadosh, R. C. The roles of cortical oscillations in sustained attention. *Trends in Cognitive Sciences*, **19(4)**, 188-195 (2015).

Cressman, E. K., Henriques, D. Y. P. Reach adaptation and proprioceptive recalibration following exposure to misaligned sensory input. *J Neurophysiol*, **103**, 1888-1895 (2010).

Duffy, C., Wurtz, R. H. Sensitivity of MST Neurons to Optic Flow Stimuli. I. A Continuum of Response Selectivity to Large-Field Stimuli. *Journal of Neurophysiology*, **65:6** (1991).

Frenz, H., Bremmer, F., Lappe, M., Discrimination of travel distances from 'situated' optic flow. *Vision Research*, **43**, 2173-2183 (2003).

Frenz, H., Lappe, M., Absolute travel distance from optic flow. *Vision Research*, **45**, 1679-1692 (2005).

Frenz, H., Lappe, M., Kolesnik, M., Bührmann, T. Estimation of travel distance from visual motion in virtual environments. *ACM Trans. Appl. Percpt*., **4(1)**, Article 3 (2007).

Friston, K. A theory of cortical responses. *Philosophical Transactions of the Royal Society B*, **360(1456)**, 815-836 (2005).

Friston, K. The free-energy principle: a unified brain theory? *Nat Rev Neurosci.*, **11(2)**, 127-38 (2010).

Friston, K. Does predictive coding have a future? *Nature Neuroscience*, **21**, 1019-1021 (2018).

Gibson, J. J. The perception of the visual world. *The Riverside Press*, Cambridge, Massachusetts (1950).

Greenlee, M. W., Frank, S. M., Kaliuzhna, M., Blanke, O., Bremmer, F., Churan, J., Cuturi, L. F., MacNeilage, P. R., and Smith, A. T. Multisensory integration in self-motion perception. *Multisensory Research*, **29**, 525-556 (2016).

Gu, Y., Watkins, P. V., Angelaki, D. E., DeAngelis, G. C. Visual and Nonvisual Contributions to Three-Dimensional Heading Selectivity in the Medial Superior Temporal Area. *The Journal of Neuroscience*, **26(1)**, 73-85 (2006).

Harris, L. R., Jenkin, M., Zikovitz, D. C. Visual and non-visual cues in the perception of linear self motion. *Exp Brain Res*, **135**, 12–21 (2000).

Heinrich, S. P. A primer on motion visual evoked potentials. *Doc Ophthalmol*, **114**, 83-105 (2007).

Hesse, P. N., Schmitt, C., Klingenhoefer, S., Bremmer, F. Preattentive processing of numerical visual information. *Frontiers in human neuroscience*, **11**, 70 (2017).

Huk, A. C., Dougherty, R. F., Heeger, D. J. Retinotopy and functional subdivision of human areas MT and MST. *J Neurosci*. **22(16)**, 7195-205 (2002).

Hlavacka, F., Mergner, T., Bolha, B. Human self-motion perception during translatory vestibular and proprioceptive stimulation. *Neuroscience Letters*, **210**, 83-86 (1996).

Jensen, O., Bonnefond, M., Marshall, T. R., Tiesinga. P. Oscillatory mechanisms of feedforward and feedback visual processing. *Trends in Neurosciences*, **38(4)**, 192-194 (2015).

Kaminiarz, A., Schlack, A., Hoffmann, K.-P., Bremmer, F. Visual selectivity for heading in the macaque ventral intraparietal area. *J Neurophysiol*, **112**, 2470-2480 (2014).

Khodanovich, M. Y., Esipenko, E. A., Svetlik, M. V., Krutenkova, E. P. A Visual Analog of Mismatch Negativity When Stimuli Differ in Duration. *Neuroscience and Behavioral Physiology*, **40(6)**, 653-661 (2010).

Kuba, M., Kubová, Z., Kremlácek, J., Langrová, J. Motion-onset VEPs: characteristics, methods, and diagnostic use. *Vision Research*, **47(2)**, 189-202 (2007).

Kuldkepp, N., Kreegipuu, K., Raidvee, A., Näätänen, R., Allik, J. Unattended and attended visual change detection of motion as indexed by event-related potentials and its behavioral correlates. *Frontiers in Human Neuroscience*, **7**, 476 (2013).

Lappe, M., Bremmer, F., Pekel, M., Thiele, A., Hoffmann, K.-P. Optic Flow Processing in Monkey STS: A Theoretical and Experimental Approach. *The Journal of Neuroscience*, **16(19)**, 6265–6285 (1996).

Lappe, M., Bremmer, F., van den Berg, A.V. Perception of self-motion from visual flow. *Trends in Cognitive Sciences*, **3:9** (1999).

Lappe, M., Jenkin, M., Harris, L. R. Travel distance estimation from visual motion by leaky path integration. *Exp Brain Res*, **180**, 35-48 (2007).

Li, X., Lu, Y., Sun, G., Gao, L., Zhao, L. Visual mismatch negativity elicited by facial expressions: new evidence from the equiprobable paradigm. *Behavioral and Brain Functions*, **8**, 7 (2012).

Lich, M., Bremmer, F. Self-motion perception in the elderly. *Frontiers in Human Neuroscience*, **8:681** (2014).

Mapstone, M., Duffy, C. J. Approaching objects cause confusion in patients with Alzheimer's disease regarding their direction of self-movement. *Brain*. **133(9)**, 2690-701 (2010).

Michalareas, G., Vezoli, J., van Pelt, S., Schoffelen, J.-M., Kennedy, H., Fries, P. Alpha-beta and gamma rhythms subserve feedback and feedforward influences among human visual cortical areas. *Neuron*, **89**, 384-397 (2016).

Müller, D., et al. Impact of lower- vs. upper-hemifield presentation on automatic colour-deviance detection: a visual mismatch negativity study. *Brain Research*, **1472**, 89-98 (2012).

Müller, D., Widmann, A., Schröger, E. Object-related regularities are processed automatically: evidence from the visual mismatch negativity. *Frontier in Human Neuroscience*, **7**, 259 (2013).

Pazo-Álvarez, P., Amenedo, E., Lorenzo-López, L., Cadaveira, F. Effects of stimulus location on automatic detection of changes in motion direction in the human brain. *Neuroscience Letters*, **371(2-3)**, 111-116 (2004).

Reinhart, R. M. G., Heitz, R. P., Purcell, B. A., Weigand, P. K., Schall, J. D., Woodman, G. F. Homologous mechanisms of visuospatial working memory maintenance in macaque and human: Properties and sources. *J Neurosci.*, **32(22)**, 7711-7722 (2012).

Redlick, F. P., Jenkin, M., Harris, L. R. Humans can use optic flow to estimate distance of travel. *Vision Research*, **41**, 213-219 (2001).

Saito, H., Yukie, M., Tanaka, K., Hikosaka, K., Fukada, Y., Iwai, E. Integration of direction signals of image motion in the superior temporal sulcus of the macaque monkey. *The Journal of Neuroscience*, **6(1)**, 145-157 (1986).

Schmitt, C., Klingenhoefer, S., Bremmer, F. Preattentive and predictive processing of visual motion. *Sci Rep.*, **8(1)**:12399 (2018).

Sperry, R. W. Neural basis of the spontaneous optokinetic response produced by visual inversion. *Journal of Comparative and Physiological Psychology*, ***43*(6)**, 482–489 (1950).

Stefanics, G., Csukly, G., Komlósi, S., Czobor, P., Czigler, I. Processing of unattended facial emotions: A visual mismatch negativity study. *NeuroImage*, **59(3)**, 3042-3049 (2012).

Stefanics, G., Kremlácek, J., Czigler, I. Visual mismatch negativity: a predictive coding view. *Frontiers in Human Neuroscience*, 8, 666 (2014).

Sulykos, I., Czigler, I. One plus one is less than two: Visual features elicit non-additive mismatch-related brain activity. *Brain Research*, **1398**, 64-71 (2011).

van der Hoorn, A., Renken, R. J., Leenders, K. L., de Jong, B. M. Parkinson-related changes of activation in visuomotor brain regions during perceived forward self-motion. *PLoS One*. **9(4)**, e95861 (2014).

van Kerkoerle, T., Self, M. W., Dagnino, B., Gariel-Mathis, M.-A., Poort, J., van der Togt, C., Roelfsema, P. R. Alpha and gamma oscillations characterize feedback and feedforward processing in monkey visual cortex. *Proc. Natl. Acad. Sci. USA*, **111**, 14332–14341 (2014).

von Holst, E., Mittelstaedt, H. Das Reafferenzprinzip. *Naturwissenschaften*, **37(20)**, 464–476 (1950).

von Hopffgarten, A., Bremmer, F. Self-motion reproduction can be affected by associated auditory cues. *Seeing Perceiving*, **24(3)**, 203-22 (2011).

Wang, S. et al. ERP comparison study of face gender and expression processing in unattended condition. *Neuroscience Letters*, **618**, 39-44 (2016)

Wang, J., Guo, X., Zhuang, X., Chen, T., Yan, W. Disrupted pursuit compensation during self-motion perception in early Alzheimer's disease. *Sci Rep*. 7(1), 4049 (2017).

Warren, W. H., Hannon, D. J. Direction of self-motion is perceived from optical flow. *Nature*, **336** (1988).

Winkler, I., Czigler, I. Evidence from auditory and visual event-related potential (ERP) studies of deviance detection (MMN and vMMN) linking predictive coding theories and perceptual object representations. *International Journal of Psychophysiology,* 83, 132-143 (2012).

Wolpert, D. M., Flanagan, J. R. Motor prediction. *Current Biology*, **11(18)**, R729-R732 (2001).

Woodman, G. F. in The Oxford handbook of event-related potential components, Homologues of human event-related potential components in nonhuman primates, eds Luck, S. J., Kappenman, E. (Oxford UP, New York), 611-625 (2012).

6 Declaration of authors‘ contributions to the studies

This thesis consists of three studies I first authored, which are currently prepared for publication.

Study I:

Constanze Schmitt and Frank Bremmer (in preparation)

Predictive and preattentive processing of visually simulated self-motion

The study was planned by **Constanze Schmitt** and Prof. Dr. Frank Bremmer. The experiment was designed and programmed by **Constanze Schmitt**. Data were collected and analyzed by **Constanze Schmitt**. The chapter about study I was written by **Constanze Schmitt** and proofread by Prof. Dr. Frank Bremmer.

Study II:

Constanze Schmitt, Bianca R. Baltaretu, J. Douglas Crawford and Frank Bremmer (in preparation)

TMS-induced disturbance of self-motion perception in humans

The study was planned by **Constanze Schmitt**, Bianca R. Baltaretu, Prof. Dr. J. Douglas Crawford and Prof. Dr. Frank Bremmer. The experiment was designed and programmed by **Constanze Schmitt**. Data were collected by **Constanze Schmitt** and Bianca R. Baltaretu and analyzed by **Constanze Schmitt**. The chapter about study II was written by **Constanze Schmitt** and proofread by Bianca R. Baltaretu, Prof. Dr. J. Douglas Crawford and Prof. Dr. Frank Bremmer.

Study III:

Constanze Schmitt, Milosz Krala and Frank Bremmer (in preparation)

A neural correlate of the subjective encoding of distance

The study was planned by **Constanze Schmitt**, Milosz Krala and Prof. Dr. Frank Bremmer. The experiment was designed and programmed by **Constanze Schmitt** and Milosz Krala. Data were collected by student research assistant Nils Vorndran under supervision of **Constanze Schmitt** and by **Constanze Schmitt**. Data were analyzed by **Constanze Schmitt**. The chapter about study III was written by **Constanze Schmitt** and proofread by Prof. Dr. Frank Bremmer.

Danksagungen

Hervorheben möchte ich vor allem Prof. Frank Bremmer, der es mir ermöglicht hat, meine Promotion in seiner Arbeitsgruppe zu schreiben und mich während dieser Zeit hervorragend betreut hat. Vor allem bedanke ich mich für die ansteckende Begeisterung für die Wissenschaft und dafür, dass auftauchenden Fragen und Probleme immer zeitnah besprochen werden konnten. Außerdem bedanke mich für die Möglichkeit im Rahmen des IRTG zu promovieren, wodurch ich sehr viel lernen und viele andere tolle Wissenschaftler kennen lernen durfte.

Ich bedanke mich bei Prof. Anna Schubö, die sich bereit erklärt hat, die Zweitgutachterin für meine Arbeit zu sein, und mit der ich schon meine allerersten selbst gemessenen EEG-Daten während meiner Masterarbeit besprechen durfte.

Ich bedanke mich bei der gesamten AG Neurophysik, mit deren Mitgliedern ich eine tolle Zeit hatte und auf die ich mich jeden Morgen auf dem Weg ins Büro gefreut habe. Ich bedanke mich für das ganze Wissen, das an mich weiter gegeben wurde. Besonders bedanken möchte ich mich bei Frau Thomas für die immer schnelle und problemlose Unterstützung in Verwaltungsangelegenheiten. Außerdem bedanke ich mich bei Alexander Platzner für die technische Hilfe und die kreativen Lösungen bei allen Versuchsaufbauten.

Ich bedanke mich bei Prof. Doug Crawford, dessen Labor in Toronto ich im Rahmen des IRTG-Programms für ein halbes Jahr besuchen durfte, um eine meiner Studien durchzuführen. Ich bedanke mich bei allen Mitgliedern des *Crawford lab*, die mir bei allen meinen Problemen im Labor geholfen haben und durch die meine Zeit in Kanada ganz besonders schön war. Besonders bedanken möchte ich mich bei Bianca Baltaretu, die mich bei meinen fMRT und TMS Messungen unterstützt und mir die Auswertung von fMRT Daten beigebracht hat.

Ich bedanke mich bei André, Bianca, Uli und Cathi für das Korrekturlesen meiner Arbeit. Besonders bei André Kaminiarz, der sich viel Zeit genommen hat, Probleme mit mir zu besprechen und Lösungen zu finden.